Cathepsin D

Design and characterisation of new *in vitro* and *in vivo* substrates applied to biological samples

Cathepsin D

Entwicklung und Charakterisierung von neuen *in vitro* und *in vivo* Substraten und deren Anwendung in biologischen Proben

Dissertation

der Fakultät für Chemie und Pharmazie
der Eberhard-Karls-Universität Tübingen

zur Erlangung des Grades eines Doktors
der Naturwissenschaften

2005

vorgelegt von

Daniel Bächle

Tag der mündlichen Prüfung:	20.12.2005
Dekan:	Prof. Dr. S. Laufer
1. Berichterstatter:	Prof. Dr. U. Weser
2. Berichterstatter:	Prof. Dr. S. Stevanović

ACKNOWLEDGEMENTS

First of all I thank Hubert Kalbacher for making this work possible and for his outstanding engagement in leading young lives into the right direction. His comprehension for scientific as well as for everyday problems is remarkable. Thanks for all.

The friendly and inspiring atmosphere hand in hand with scientific knowledge at the medical and natural sciences research centre helped a lot to finish this thesis. Namely E. Malenke, J. Gogel, C. Luber, J. Brandenburg, T. Burster, J. Beck, J. Schnaut, K. Lehnert, M. Reich, A. Dittmar, T. Rückrich, F. Kramer A. Lautwein and T. Herrmann took part in solving practical and personal problems. I really appreciate your engagement.

For support during the run-up to this thesis I thank H.-G. Rammensee, G. Jung, H. Probst and C. A. Müller.

R. Fischer unselfishly helped me and showed me how *scientific work* happens in reality and therefore was the main motor for publishing parts of this work. For this reason I acknowledge the group of cellular signal transduction leaded by R. Brock and the members F. Duchardt, H. Hufnagel and M. Fotin-Mleczek.

Thanks to P. Hrstic and S. Stevanović for their never ending support in MALDI-MS analysis.

For the successful cooperation during the “sweat-project” I thank H. Steffen and B. Schittek from the Department of Dermatology, University of Tübingen.

Thanks to H. Dihazi for a good time during my visit at the University Hospital in Göttingen and for the help with SELDI-MS.

Personally I would like to acknowledge some persons who stood by my side throughout the years, independently of my work: J. Lottig and M. Brodt.

Furthermore I have enjoyed the following persons who have passed my way – scientifically and in private: W. Singer, H. Beck, G. Schwarz, M. Deeg and A. Beck.

Last but not least I appreciate the friendship of my band “From Beyond”. Making music and performing live will always be a part of my life. Living without making music I just can’t imagine and without… this work wouldn’t have been possible - “Up the Irons”: F. Allgaier, M. Baur and J. Schmierer.

For financial support I thank the “Bundesministerium für Bildung und Forschung” (BMBF, FKZ: 0312879A).

The newly founded biotechnology company PANATecs offered me a lot of promising opportunities. In particular A. Cansier and T. Flad accompanied me during my years of “learning and doing”.

My parents gave me everything they have – without regarding their own interests. Thanks for all the provided facilities and for a place I will always call my home.

(Meine Eltern haben mir alles gegeben, ohne auf ihre eigenen Interessen Rücksicht zu nehmen. Danke für alles was ihr mir ermöglicht habt und für einen Ort den ich immer *Mein Zuhause* nennen werde.)

They say that life's a carousel

spinning faster you've got to ride it well.

The world is full of kings and queens

who blind your eyes then steal your dreams

…It's heaven and hell

Black Sabbath (Butler, Dio, Iommi, Ward), 1980

CONTENT

1 A brief historical survey of cathepsin D (1929-2005)

The term “cathepsin” was introduced in 1929 [Willstätter & Bamann 1929] and the root of the word originates from the Greek, where it means “to digest”. In the beginning the term cathepsin was used to describe extracts of animal tissues containing a proteolytic system which showed proteolytic activity against hemoglobin at pH 3.5. Until that point, no further differentiation between the involved proteases had been made and so the first publication about isolation of this acidic proteolytic system from bovine spleen was entitled “The purification of cathepsin” [Anson 1940]. During these years, the term “cathepsin” was generally used to describe acidic intracellular proteases.

Great efforts have been made to characterise and specify proteases such as papain [Bergmann et al. 1935], papain peptidase I [Bergmann et al. 1936], pepsin [Fruton & Bergmann 1939], trypsin [Bergman et al. 1939] and chymotrypsin [Bergmann & Fruton 1937] in order to understand their physiological function. At the same time it has been shown that the enzymatic action of proteases is not only restricted to peptide bonds in proteins of high molecular weight but also to constructed peptides and peptide derivatives. First peptide substrates were designed, synthesised and used for the determination of enzyme specificity and characterisation [Bergmann et al. 1937].

The peptide substrates enabled the scientist for the first time to distinguish between similar protease activities in a fast and simple way. According to this, the proteolytic system so far known as cathepsin proved to consist of at least three types of cathepsins in bovine spleen [Fruton et al. 1941]. These enzymes of the cathepsin system were correspondingly named cathepsin A, B and C. Further investigations were made and in 1957 cathepsin B (CatB) was isolated from bovine spleen [Greenbaum & Fruton 1957]. At the end of 1959 a new member of the cathepsin family was detected in bovine spleen and was consequently named cathepsin D because it did not hydrolyse any of the typical substrates for cathepsin A, B and C [Press et al. 1960]. The new found cathepsin D differed not only in its specificity from the other cathepsins but also in its mechanism of action, since the protease inhibitors iodacetamide (inhibitor for cysteine proteases), ethylenediaminetetraacetic acid

(EDTA, inhibitor for metalloproteases) and diisopropylfluorophosphate (inhibitor for serine proteases) had no effect on its proteolytic activity. These finding showed, that CatD is an aspartate protease (also known as acid protease or aspartic protease) in contrast to CatA which is a serine protease and CatB and CatC [Tallan et al. 1952] which are cysteine proteases. CatD has a pH optimum of 3.0 and represents two-thirds of the proteolytic activity of crude spleen extract. The B chain of oxidized insulin [Sanger et al. 1949] was digested with pepsin and CatD and the generated peptides were identified, showing that the specificity of CatD, though more restricted, is similar to that of pepsin. CatD cleaved the B chain of oxidized insulin predominantly between leucine and tyrosine, phenylalanine and phenylalanine as well as between phenylalanine and tyrosine. Weak cleavage was observed between glutamic acid and alanine and between tyrosine and leucine [Press et al. 1960]. These newly introduced *in vitro* digestion experiments described for the first time the specificity of CatD to cleave peptide bonds preferably between hydrophobic and aromatic amino acids.

The subsequent enzymatic investigations and characterisations were all more or less based on peptide substrates. Therefore great amounts of synthetic peptides with high purities were required. At this time peptides were commonly synthesised in solution and expensive purification and recrystallisation procedures had to be made following each coupling step. The synthesis of a decapeptide, for example, took up to one month or even longer and this fact clearly limited investigations based on peptide substrates. In the early sixties a new, fast and effective method for peptide synthesis was introduced by Merrifield [Merrifield 1963]. Peptide synthesis was carried out on solid phase using a copolymer of styrene which was cross-linked with 1% divinylbenzene. The carboxyl group of the first amino acid was then coupled covalently to the resin and successively the peptide chain was elongated. The reason for this approach was that the growing peptide chain could easily be filtered and washed free of reagents and by-products. The combination of solid-phase peptide synthesis and *in vitro* digestion experiments smoothed the way for the characterisation of proteases.

In 1962 another cathepsin, differing from CatD in pH optimum and charge at pH 8.2 was isolated from rabbit bone marrow. The protease was also active against the synthetic substrates for CatA, CatB and CatC [Lapresle & Webb 1962] and was named CatE. The “enzyme brothers” CatD and CatE represented and still represent

the main aspartate proteases in mammalian cells and distinguishing between the two especially their involvement in cellular processes will become a biochemical problem, which will engage scientists for a long period of time [Arnold et al. 1997, Ostermann et al. 2004, Chain et al. 2005, Chou et al. 2005]. As recently as 2005 a specific substrate was described for CatE [Yasuda et al. 2005].

First assumptions were made to clarify the physiological function of CatD since cathepsins were known to be greatly elevated in muscular dystrophy [Tappel et al. 1962, Iodice et al. 1965] and therefore contribute to the increased protein catabolism [Iodice et al. 1966a]. CatD has also been implicated in the pathological breakdown of cartilage matrix in rheumathoid arthritis [Fell & Dingle 1963, Ali 1964], osteoarthritis [Weston et al. 1969], digestion of immunoprecipitates [Wasi et al. 1966] and with collagen loss in involution of the uterus post partum [Woessner 1965].

During the next years cathepsins were purified from various tissues such as CatA and CatD, which were isolated from skeletal chicken muscle [Iodice et al. 1966b], lysosomal acid proteases from rabbit liver [Barrett 1967] and CatD from human and chicken liver [Barrett 1970]. 12 distinct forms of CatD were found in bovine uterus [Sapolsky & Woessner 1972] and 6 CatD isozymes in porcine spleen [Huang et al. 1979]. For the first time Huang et al. showed, that CatD occurs as a single chain form with an apparent molecular weight of 50 kDa and a two-chain CatD form consisting of a light chain (15 kDa) and a heavy chain (35 kDa). Furthermore they showed that the N-terminus of CatD is homologous to other acid proteases such as pepsin and, that the N-terminal sequence of the single chain is apparently the same as the light chain sequence suggesting that these forms emerge from each other during biosynthesis. Further, the data of Huang et al. proved that CatD is a glycoprotein with at least four carbohydrate units, one in the light chain and three in the heavy chain. These preliminary results were studied in detail during the 1980s. Several purification methods and assays have been reviewed by Takahashi & Tang, 1981.

The knowledge of the biochemical properties of precursors and of their conversion to mature protein were well advanced in several systems, including secretory proteins [Campbell & Blobel 1976], membrane proteins [Toneguzzo & Ghosh 1978], viral proteins [Hershko & Frey 1975] and a few organellar proteins [Maccecchini et al. 1979, Cote et al. 1979]. The first results of the biosynthesis of lysosomal enzymes as precursors were published for β-galactosidase in macrophages of thioglycollate-

treated mice [Skudlarek & Swank 1979]. In the same year the group of Erickson and co-workers suggested a possible pathway for biosynthesis and proved the existence of two proforms of CatD, a 43 kDa and a 46 kDa form as well as the enzymatically active 30 kDa form of CatD [Erickson & Blobel 1979]. These initial findings were studied in more detail in the following years leading to the following pathway for the biosynthesis of CatD.

CatD (EC 3.4.23.5) is synthesized as non-glycosylated preprocathepsin D (MW 43000) at the rough endoplasmatic reticulum and represents the primary translation product which is then transported via the Golgi complex to the lysosomes [von Figura & Hasilik 1986, Kornfeld & Mellman 1989]. A sorting tag has been identified which distinguishes molecules destined for lysosomes. Phosphate attached to the 6 position of mannose residues on carbohydrate groups of soluble lysosomal enzymes is sufficient to target these molecules for lysosomal transport [Hasilik & Neufeld 1980]. The initial selection step for the pathway is carried out by a single phosphotransferase located in the *cis*-Golgi which distinguishes soluble lysosomal enzymes from the numerous other proteins passing through this compartment [Kornfeld & Mellman 1989].

The pre-sequence (20 residues), which resembles the sequences of secretory proteins, is then cleaved off to yield glycosylated procathespin D (MW 46000). The pre-sequence functions as a signal sequence for translocation across the endoplasmatic reticulum membrane. A part of procathepsin D is secreted and can be detected in the culture medium. The intracellular amount of procathepsin D is further converted to enzymatically active single chain CatD by removal of the pro sequence (44 residues) which shows sequence homology to the 44 residue activation peptide of pepsinogen. The pro-sequence serves as an activation peptide that keeps the enzyme inactive during intracellular transport to the lysosome [Erickson et al. 1981]. The cleavage of the pro sequence has been shown to be pH-dependent (pH 3.5) and pepstatin-inhibitable leading to an increase in enzyme activity [Hasilek et al. 1982]. During this processing step not only active single-chain CatD is generated but also three peptides which show inhibitory activity towards active CatD similar to the activation of pepsinogen [Puizdar & Turk 1981]. Activation of procathepsin D may occur via a unimolecular, autoproteolytic mechanism [Conner 1989]. Single chain cathepsin D undergoes further cleavage into a 15 kDa N-terminal domain (light chain) and a 30 kDa C-terminal domain (heavy chain). This cleavage results in the

removal of seven amino acid residues between the light chain and the heavy chain [Shewale & Tang 1984, Faust et al. 1985]. Finally, several amino acids are removed from the C-terminus of the heavy chain [Erickson & Blobel 1983].

In general all lysosomal enzymes are synthesized as inactive precursors which are processed either autocatalytically or by other enzymes to remove an N-terminal propeptide. The propeptide is thought to block the active site of the enzyme, thus preventing proteolytic activity. In addition to this inhibitory function, the propeptides of some aspartate proteases have been proposed to function in the folding of the nascent protein [Yonezawa et al. 1988] as proved to be the case for CatD [Conner 1992].

The current known structural properties of human preprocathepsin D concerning disulfide bonds, subdivisions, actice site residues and glycosylation sites [Zhang et al. 2003] are summarised in Figure 1 [reviewed by Fusek et al. 2005].

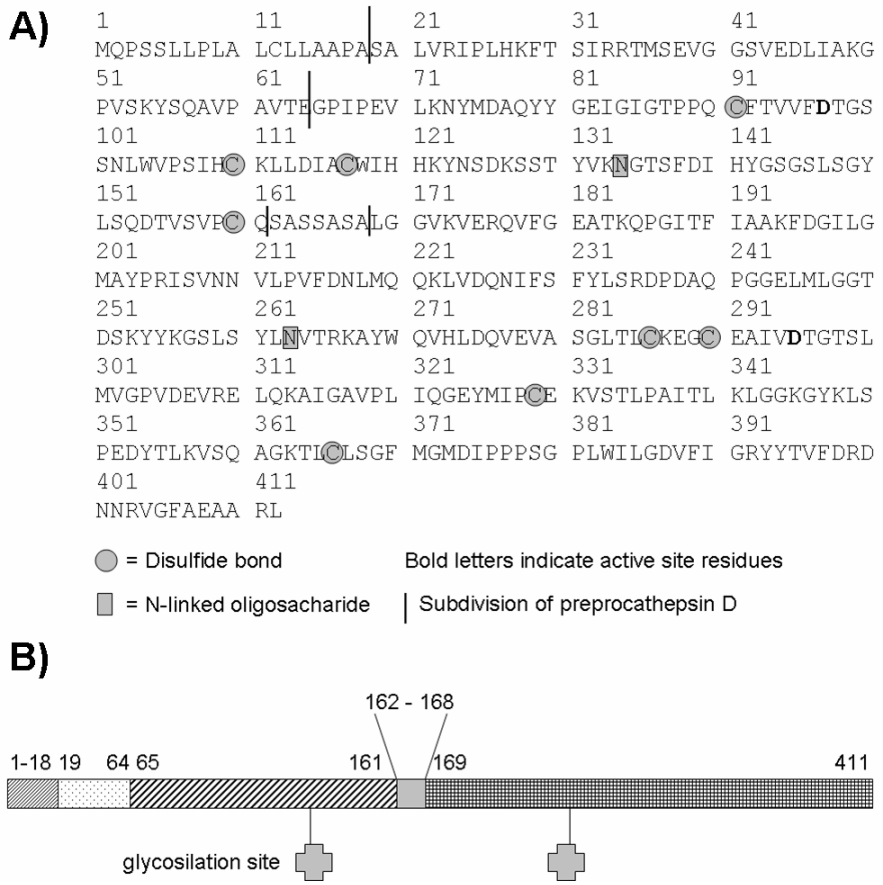

Figure 1 **(A)** Amino acid sequence of preprocathepsin D. Residues 1 to 18 are the signal peptide, residues 19 to 64 are the activation peptide, residues 65 to 161 represent the light chain and residues 169 to 412 represent the heavy chain. **(B)** Schematic representation of structural features of Preprocathepsin D

Lysosomal proenzymes, such as procathepsin D, have been shown to be associated with intracellular membranes in a mannose-6-phosphate-independent manner and therefore are sorted to the lysosome by another targeting system [Rijnboutt et al. 1991a, Rijnboutt et al. 1991b] differing from the common mannose-6-phosphate pathway. It is a fact that the propeptides of vacuolar enzymes also contain a signal that is necessary for targeting to the organelle [Rothman et al. 1989] but this sorting mechanism does not account for CatD [Conner 1989]. Recently published data show, that the cysteine protease CatL is involved in CatD processing in order to generate the light chain and heavy chain from single chain CatD [Wille et al. 2004].

Rapid affinity chromatography is the method of choice for the isolation of proteolytic enzymes, especially endoproteases. The commonly used ion-exchange methods or gel chromatography require large amounts of sample from which the recovery is rather small. Since 1970 the aspartate protease inhibitor pepstatin was discovered [Umezawa et al. 1970] and used as active site titrant [Workman & Burkitt 1979] and in immobilized form on sepharose for the isolation of CatD [Takahashi & Tang 1981, Kazakova et al. 1976] and CatE from rat spleen [Yamamoto et al. 1978].

The well established purification protocols permitted the isolation of CatD in large amounts and in high purity [Huang et al. 1979]. Isolation from porcine spleen was done by the group of Jordan Tang [Huang et al. 1979] as well as sequence analysis for the light [Takahashi & Tang 1983a] and heavy chain [Shewale & Tang 1983]. Further they showed that porcine spleen cathepsin D contains two glycosylation sites, one on each chain [Takahashi et al. 1983b]. Cloning and sequence analysis of cDNA for human CatD was done for the first time by Faust et al. 1985.

The aspartate protease inhibitor pepstatin was introduced by Morishima et al. 1970 and the interaction of human CatD with pepstatin was further investigated indicating that binding is strongly pH dependent so that in biological experiments near neutral pH, large molar excesses of pepstatin over CatD is required for efficient inhibition [Knight & Barrett 1976]. Presently the commonly used concentration of pepstatin for biological investigations is 10 µM and even 100 µM for cell cultur applications.

In the last decade of the 20th century the pepstatin inhibited crystal structure of CatD was determined [Baldwin et al. 1993] as well as mapping of the CatD subsite preferences [Majer et al. 1997].

Aspartate proteases represent a large family of enzymes that catalyze peptide bond hydrolysis through an acid-base mechanism mediated by two catalytic aspartic acid residues (^{97}Asp and ^{295}Asp) [Davies 1990, Tang & Wong 1987] from which only one carboxyl group is protonated due to the fact that the total charge of the active-site aspartic acids is -1 [Xie et al. 1997]. According to these properties aspartate proteases show an acidic pH optimum normally about pH 3-4. More recent results have also shown that pH dependent conformational switching of CatD modulates substrate specificity [Lee et al. 1998].

A set of inhibitory peptides had already been synthesized and tested for their inhibitory properties [Lin & Williams 1979] and new inhibitors based on the general structure 4-(morpholinosulfonyl)-L-Phe-P_2-(cyclohexyl)Ala-P_1'-P_2' [Rao et al. 1993]. The specificity of CatD was further investigated concluding the following preferences: a hydrophobic residue in P2 whereas residues capable of hydrogen bonding are also accepted but strongly positively charged amino acids are rejected; a preference of Ile in P3 over the smaller Ala was also observed [Scarborough et al. 1993]. Concerning the P2' position CatD prefers positively charged side-chains whereas Glu in P2' yielded a poor substrate and Asp in this position created a substrate that was not cleaved. Substrates bearing large hydrophobic side-chains at P3' were excellent substrates [Beyer & Dunn 1998].

In the human genome about 500-600 proteases have been identified [Lopez-Otin & Overall 2002] from which about 60 are lysosomal proteases [Mason 1995]. Lysosomal proteases include a group of about 12 papain-like cysteine proteases. These cysteine proteases are all named cathepsin. The sole lysosomal papain-like cysteine protease which is not named cathepsin is legumain or asparaginyl endopeptidase (AEP) [Chen et al. 1997, 1998] and was characterised within our group [Schwarz et al. 2002]. Among the cathepsins only CatE and CatG are not lysosomal [lysosomal cysteine proteases were reviewed by Turk et al. 2000, Turk et al. 2001, Turk & Guncar 2002]. In Table 1 all known cathepsins are listed.

Table 1 Nomenclature recommended by the IUBMB and properties of human cathepsins (www.branda.uni-koeln.de, www.merops.sanger.ac.uk)

	Recommended Name	EC number	Classification	Reference
Cysteine proteases	Cathepsin B	3.4.22.1	Carboxypeptidase, liberating C-terminal dipeptides	Bond et al. 1980, Barrett et al. 1981
	Cathepsin C	3.4.14.1	Aminopeptidase, release of a N-terminal dipeptide except when P1 is Arg or Lys, or P1' or P2' is Pro	Planta et al. 1964, Metrione et al. 1966
	Cathepsin L	3.4.22.15	Endoprotease, with preference for a residue bearing a large hydrophobic side chain at the P2 position and does not accept Val at P1', compared to CatB, CatL exhibits higher activity towards protein substrates, but has little activity on Z-Arg-Arg-NHMec and no peptidyl-dipeptidase activity	Kirschke et al. 1988; Barrett & Kirschke, 1981
	Cathepsin H	3.4.22.16	Aminopeptidase and endoprotease	Bromme et al. 1987
	Cathepsin K	3.4.22.38	Endoprotease, the major determinant of specificity is P2, which is preferably Leu, Met > Phe and not Arg	Inaoka et al. 1995, Bromme et al. 1996
	Cathepsin F	3.4.22.41	Endoprotease, cleaves synthetic substrates with Phe and Leu in P2 better than Val	Wang et al. 1998, Wex et al. 1999
	Cathepsin O	3.4.22.42	Endoprotease, hydrolyses Z-Phe-Arg-NHMec and Z-Arg-Arg-NHMec	Velasco et al. 1994
	Cathepsin S	3.4.22.27	Endoprotease, similar to CatL but with much less activity on Z-Phe-Arg-NHMec and more activity after the Z-Val-Val-Arg compound	Bromme et al. 1975, Kirschke et al. 1989
	Cathepsin V	3.4.22.43	endoprotease, hydrolyses proteins, Z-Phe-Arg NHMec > Z-Leu-Arg-NHMec > Z-Val-Arg-NHMec	Adachi et al. 1998, Bromme et al. 1999
	Cathepsin X	3.4.18.1	Carboxypeptidase which lacks action on C-terminal proline, weak endopeptidase activity	Nagler et al. 1999
Serine proteases	Cathepsin A	3.4.16.5	Carboxypeptidase (also known as carboxypeptidase C)	Miller et al. 1992
	Cathepsin G	3.4.21.20	Endoprotease which preferably cleaves after Leu, Tyr, Phe, Met, Trp, Gln and Asn	Tanaka et al. 1985
Aspartate proteases	Cathepsin D	3.4.23.5	Similar to pepsin A, between hydrophobic residues	Faust et al. 1985, Scarborough et al. 1993
	Cathepsin E	3.4.23.34	Similar to CatD	Azuma et al. 1989, Lapresle et al. 1986

Cathepsins which are not yet included in the IUBMB recommendations, e.g. CatP [Puzer et al. 2005] and CatW (P56202, EC number 3.4.22. - not yet assigned) [Dalton & Brindley 2004] are not considered. CatT (EC number 3.4.22.24) is a cysteine protease but was only detected in rattus norvegicus to date [Pitot et al. 1987] and therefore is not listed in table 1.

The intracellular distribution of CatD as well as the relative amount of CatD in several cell types such as B cells, monocytes, dendritic cells, HeLa cells etc. still needs to be determined and will be clarified in the following chapters.

In the early 1930s, proteases were typically determined using the trichloroacetic acid (TFA) method which uses denatured hemoglobin as substrate [Anson & Mirsky 1932]. After digestion the intact hemoglobin was precipitated with TFA and the digestion products in the supernatant were then estimated colorimetrically with a phenol reagent yielding a blue colour with tyrosine and tryptophane moieties [Folin & Looney 1922, Looney 1926]. The detection of tyrosine and tryptophane was improved using the Folin and Ciocalteu reagent [Folin & Ciocalteu 1927]. The method has then been applied to the four known types of proteases at that time which were pepsin [Anson & Mirsky 1932], trypsin [Anson & Mirsky 1933], papain [Anson 1936] and already cathepsin [Anson 1936]. About two years later these data were confirmed using a simplified and standardised protocol [Anson 1938] which became the standard method for determination of protease activity. Currently, CatD activity is still determined using the hemoglobin assay with slight modifications [Shibata et al. 2002, Williamson et al. 2002, Bidere et al. 2003, Skrzydlewska et al. 2005].

Recently, an enzyme-family assay based on microarrays was developed and used for determination of enzyme activities [Funeriu et al. 2005]. The new research results indicate, that the problem of specific and precise determination of enzyme activity is still ongoing. The presence and enzymatic function of CatD in various human cells and secrets such as sweat still needs to be investigated (see chapter 3 and 4).

Multicellular animals are obligated to eliminate cells that are in excess or potentially dangerous. Therefore a programmed cell death program is needed in order to control cell numbers, tissue sizes and to protect the organism itself from rogue cells that threaten homeostatis. The term finally adopted for programmed cell death was apoptosis [Kerr et al. 1972]. The apoptotic cell death differs from

pathological, necrotic cell death since only single cells are affected and not groups of neighbouring cells.

The mechanism of apoptosis is very complex and depends on various factors. In general, there are two major apoptotic pathways in mammalian cells known: the death-receptor pathway and the mitochondrial pathway [reviewed by Hengartner 2000, Boya et al. 2001, Kaufmann & Gores 2000]. Both pathways depend more or less on the activation of caspases (**C**ysteine **A**spartate **S**pecific **P**rote**ASE**s) [Alnemri et al. 1996]. Consequently apoptosis research has focused on caspases and their role in programmed cell death. The concept, that caspases are the sole executive proteases in apoptosis now seems to be outdated by a growing body of evidence that strongly points to a role of lysosomes, especially lysosomal proteases in apoptosis. This phenomenon is meanwhile widely recognized and the term "lysosomal pathway of apoptosis" is accepted [reviewed by Guicciardi 2004]. Lysosomal permeabilization [Erdal et al. 2005] induced by the synthetic lysosomotropic detergent O-methyl-serine dodecylamide hydrochloride causes apoptosis [Li et al. 2000]. Cells undergo either apoptotic or necrotic cell death dependent on the amount of lysosomal enzymes released into the cytosol: selective, partial permeabilization triggers apoptosis and complete lysosomal breakdown triggers necrosis [Bursch 2001, Turk et al. 2002]. Once in the cytosol, lysosomal proteases interfere with caspases in the signalling pathway which has been shown for CatB [Salvesen 2001] or by direct cleavage of key cellular substrates [Leist & Jaattela 2001]. It has been shown that lysosomal extracts cleaves proapoptotic Bcl-2-like proteins such as Bid or Bax and causes cytochrom c release followed by caspase activation [Stoka et al. 2001]. Detailed studies regarding CatD showed that it is rapidly translocated from lysosomes to the cytosol and increase the level of p53 protein. According to this finding the CatD activity is drastically increased during apoptosis induced by oxidative stress [Kagedal et al. 2001]. Pepstatin A prevented cytochrom C release [Roberg et al. 1999] producing evidence for the involvement of CatD in apoptosis. It has been reported that pharmacological inhibition of CatD block cell death induced by interferon-gamma [Deiss et al. 1996] or tumour-necrosis factor-α [Demoz et al. 2002]. Further investigations were made on the role of CatD in apoptosis and revealed, that CatD acts upstream of the caspase cascade i.e. before cytochrome c release and caspase activation at least in fibroblasts [Johansson et al. 2003]. However, in HeLa cells no influence on apoptosis concerning cleavage of Bid

by CatD has been observed but papain-like lysosomal cysteine proteases proved to be actively involved in apoptosis [Cirman et al. 2004]. Focusing on CatD, recently published results indicate that CatD triggers Bax activation and that early apoptotic events can be inhibited with pepstatin A causing a delayed cell death [Bidere et al. 2003].

At this time impressive results support the hypothesis that lysosomes and lysosomal proteases respectively may play a key role in apoptosis, but the mechanisms by which this occurs and the possible, functional relationship and/or cross-talks with other known apoptotic pathways remains largely unknown [Salvesen 2001]. However, it has been shown that catalytically inactive CatD did not affect apoptosis [Tardy et al. 2003].

For further investigations concerning the intracellular localization of active CatD new methods have to be developed for the visualization of enzyme activity within living cells (see chapter 5).

In the 1970s studies showed that coupling of poly-lysine to proteins enhances their cellular uptake [Ryser et al. 1978] which was the beginning of the area of so called cell-penetrating peptides (CPPs). A decade later it was shown that the HIV-1 Tat protein is internalized by tissue culture cells [Frankel & Pabo 1988] and further investigations revealed, that the basic domain containing amino acids 48 to 60 (Tat peptide) to be responsible for this [Vives et al. 1997]. In the 1990s other CPPs were described such as penetratin [Derrossi et al. 1994], transportan [Pooga et al. 1998] and poly-arginine (R_7 and R_9) [Suzuki et al. 2002] for which Futaki et al. demonstrated, that the optimal number of arginine residues for the most efficient translocation is approximately 9 [Futaki et al. 2003].

CPPs such as transportan [Pooga et al. 2001], Tat peptide [Silhol et al. 2002] and nona-arginine [Luedtke et al. 2003] were used as vehicles for the cellular delivery of substances such as oligonucleotide analogues [Turner et al. 2005], antigenic peptides [Shibagaki & Udey 2002], peptide nucleic acids [Pooga et al. 1998], full-lenghts proteins [Schwarze et al. 1999, Nagahara et al. 1998, Fawell et al. 1994] and drugs in general [reviewed by Trehin et al. 2004, Gupta et al. 2005]. A comparative study about protein cargo delivery by several CPPs was recently published [Säälik et al. 2004, see Graslund et al. 2004 and Lindgren et al. 2000 for reviews about CPPs in general]. The uptake of CPPs in cells can be accompanied by toxic effects

resulting from membrane perturbation at higher peptide concentration [Saar et al. 2005].

The mechanism of uptake is not completely understood and still discussed up to now. In the late 1990s a direct transport through the lipid bilayer has been proposed [Vives et al. 1997, Derossi et al. 1996] since internalization is not significantly inhibited by depletion of the cellular ATP or by inhibitors of endocytosis. Whereas more recentely it has been shown that endocytosis is involved in the cellular internalization of Tat peptide and nona-arginine [Richard et al. 2003]. Especially for the TAT peptide a clathrin-dependent endocytosis mechanism was shown [Richard et al. 2005].

New methods for the precise quantification of cellular uptake of CPPs and their proteolytic fate needs to be developed to learn more about the involved internalization mechanisms [reviewed by Liu et al. 2003]. This problem will be discussed in more detail in chapters 5 and 6 respectively whereas a new quantitative method for the detection of internalized fluorescent peptides will be described.

The functional linkage between apoptosis and cancer has been recently shown and reviewed by Kaufmann & Gores 2000, indicating that some oncogenes act by inhibiting cell turnover rather than enhancing proliferation e.g. *myc* [Evan et al. 1992, Vaux et al. 1998].

In general cysteine cathepsins [for review see Jedeszko & Sloane 2004] and in particular CatD [for review see Nomura & Katunuma 2005] are known to be involved in the pathology of various forms of cancer such as breast cancer [Foekens et al. 1999, Vetvicka et al. 2002], colorectal cancer [Skrzydlewska et al. 2005] or lung cancer [Vetvicka et al. 2004]. Recent studies could even show that defective acidification of intracellular organelles results in secretion of CatD in cancer cells [Kokkonen et al. 2005].

2 Materials and methods

2.1 Enzymes and chemicals

CatD (bovine spleen and human liver) was purchased from Sigma (Taufkirchen, Germany) and stored as a 32.3 µM stock solution in 0.1 M citric acid, pH 4.5 at -20 °C prior to use. Pepstatin A, Zwittergent 3-12 and Rink amide resin were purchased from Calbiochem-Novabiochem (Schwalbach, Germany). All other chemicals and solvents were from Merck (Darmstadt, Germany). Fmoc amino acids were purchased from MultiSynTech (Witten, Germany) for the synthesis of the CatD substrates I, II, III and for all DCD-1L derived peptides and LL-37.

Standard chemicals for the synthesis of R9-CatD-substrate were obtained from Fluka (Deisenhofen, Germany) and Merck (Darmstadt, Germany). All solvents were p. a. grade. Fmoc-amino acids were purchased from Novabiochem (Heidelberg, Germany), Senn Chemicals (Dielsdorf, Switzerland), and Orpegen Pharma (Heidelberg, Germany). Fmoc-Lys(Dde)-OH was purchased from Novabiochem (Läufelfingen, Switzerland). Rink amide resin was from Rapp Polymere (Tübingen, Germany). The isomeric mixtures of 5(6)-carboxyfluorescein (Fluo) and 5(6)-carboxytetramethylrhodamin (Tamra)-N-succinimidylester were from Fluka (Deisenhofen, Germany)**.**

Bafilomycin A1 was obtained from Tocris Biotrend, Bristol, UK and chloroquine diphosphate from Fluka [Bowman et al. 1988, Clague et al. 1994, de Duve et al. 1974, Kozak et al. 1999]. The bacterial metabolite lactacystin was purchased from Prof. Corey, Harvard University, Boston, USA) and Pepstatin A from Bachem, Bubendorf, Switzerland. The covalent cysteine protease inhibitor E-64d was purchased from Bachem.

2.2 Solid-phase peptide synthesis

Peptides were synthesized using standard Fmoc/tBu chemistry [Fields et al. 1991] and synthesis was performed on the multiple peptide synthesizer Syro II (MultiSynTech, Witten, Germany) on a 0.025 mmol scale using a six fold molar excess of Fmoc amino acids (MultiSynTech, Witten, Germany) on TCP-resin (PepChem, Reutlingen, Germany). All other reagents and solvents for peptide synthesis were purchased from Merck KGaA (Darmstadt, Germany). *In situ*

activation was performed using TBTU (6 eq.) and HOBt (1 eq.) followed by the addition of N-methylmorpholine (12 eq.) in DMF. After completion of the automated synthesis, the resin bound peptides were Fmoc-deprotected using 60% (v/v) piperidine in DMF twice for 15 min and washed subsequently with DMF, isopropanol and diethyl ether. To release the peptides from the resin and to remove the side chain protecting groups the following solution was used: 95% (v/v) TFA containing 3% (v/v) thioanisol, 3% (w/v) phenol and 2% (v/v) ethanedithiol. The peptides then were precipitated in diethyl ether, dried and dissolved in 80% (v/v) tert-Butanol in water followed by lyophilisation. Crude peptides were purified using preparative reversed-phase high-performance liquid chromatography (RP-HPLC) and identity of the peptides was confirmed using electrospray ionization mass spectrometry (ESI-MS). Peptide purities were determined via analytical RP-HPLC and proved to be higher than 97 %. The peptides were stored at 4 °C until use.

2.3 Synthesis of the CatD-substrates I, II and III

2.3.1 Synthesis of Fmoc-Lys(biotin)-Rink amide resin

Fmoc-Lys-OH (368.4 mg, 1.0 mmol) was dissolved in 8 ml DMF and reacted with biotin-OSu (341.4 mg, 1.0 mmol) and NMM (111 µl, 1.0 mmol) for 6 h. The reaction mixture was extracted with chloroform, washed twice with 4 M $KHSO_4$, water and finally evaporated to dryness. The obtained Fmoc-Lys(biotin)-OH derivative was coupled to Rink amide resin using the TBTU/HOBt coupling method. After this step the remaining free amino groups were blocked by acetylation with acetic anhydride/DIPEA/DMF (1:1:8, v/v/v) twice for 30 min. The degree of coupling was estimated to be 0.35 mmol/g.

2.3.2 Solid-phase peptide synthesis (SPPS)

The peptide substrates were synthesised by solid-phase synthesis using the standard Fmoc/tBu protocol [Fields et al. 1991] on the multiple peptide synthesizer Syro II (MultiSynTech, Witten, Germany) on a 0.025 mmol scale using a six fold molar excess of Fmoc amino acids. Side chain protecting groups were: tBu for Glu, Asp and Ser, Boc for Lys, 2,2,4,6,7-pentamethyl-dihydrobenzofuran-5-sulfonyl (Pbf) for Arg and Cys was Acm-protected.

In situ activation was performed using TBTU (6 eq) and HOBt (1 eq) followed by the addition of NMM (12 eq). After the completion of the coupling the resin bound peptides were Fmoc-deprotected using piperidine/DMF (2:3, v/v twice for 15 min) and washed subsequently with DMF, isopropyl alcohol and diethyl ether.

2.3.3 On-resin labelling of substrates with Amca

The fluorophore Amca (7-Amino-4-methylcoumarin-3-acetic acid) was coupled at a three fold excess directly to the α-amino group of the side chain-protected resin-bound peptide in DMF using the TBTU/HOBt activation method for 3 h in the dark. Subsequently the resin was washed with DMF, isopropyl alcohol, diethyl ether and then dried.

2.4 Kinetic characteristics of substrate I, II and III

To measure the initial rates of substrate proteolysis and to determine the kinetic parameters of the substrates, digestion was monitored using RP-HPLC. Hydrolysis of substrates was performed in 48 µl of 50 mM Gly/HCl buffer (pH 3.5) containing 1 µl of a 0.32 µM CatD solution. CatD dilutions were prepared in 0.1 M citric acid pH 5.0 containing 0.05% (v/v) Triton X-100. The reaction was started by adding 1 µl of the appropriate substrate solution so that the final substrate concentration was between 5 and 80 µM. The reaction was performed at 37 °C.

Every 2 min 2 µl of the reaction mixture were removed and added to 38 µl stop solution (H_2O/ACN/TFA/Zwittergent 3-12, (94:5:1:0.2, v/v/v/w)). The obtained solutions were applied to an analytical C8 column (Nucleosil 100, 125 $\times$ 2 mm, C8 column, 5 µm particle diameter, Wicom, Heppenheim, Germany) and eluted with a 0% to 80% gradient of solvent B for 40 min. The HPLC column eluent was analysed measuring fluorescence emission at 450 nm following excitation at 350 nm using a fluorescence HPLC monitor RF-535 (Shimadzu, Duisburg, Germany). The peak of fluorescently labelled digestion product and the peak of undigested substrate were integrated and the amount of converted substrate in µM was determined.

Then the initial velocity was calculated from the linear part of the cleavage curve which proved to be between 1 and 10 min. The K_m (µM) and V_{max} (µM $\times$ s^{-1}) values were determined using the Lineweaver-Burk method. The k_{cat} values (s^{-1}) were calculated from the equation:

$$k_{cat} = \frac{V_{\max}}{[CatD]_{total}} \qquad \text{(equation 1)}$$

where $[CatD]_{total}$ is the total enzyme concentration in µM and V_{max} is the maximal velocity in µM × s^{-1}.

2.5 Digest & pull down assay

The cleavage of the peptide amide substrates was performed in 48 µl 50 mM Gly/HCl buffer (pH 3.5) containing protease inhibitors (2 mM phenylmethanesulfonyl fluoride and 20 µM leupeptin for the inhibition of serine proteases, 10 mM EDTA for the inhibition of metalloproteases and 10 mM iodacetamide for the inhibition of cysteine proteases).

For the digest & pull down assay 1 µl of a 0.5 mM substrate solution in 50% (v/v) DMSO was used. The appropriate sample volume of the cell fractions containing 0.5 µg total protein determined according to Bradford [Bradford 1976] was then added. The calibration curve was determined using the appropriate sample volume of CatD.

After 10 min at 37 °C, 90 µl stop solution were added to 10 µl of the reaction mixture. The fluorescence of a 50 µl aliquot of the solution was then measured using the microplate reader Spectra Fluor (Nunc, Wiesbaden, Germany) at an emission wavelength of 465 nm with excitation at 360 nm, obtaining F_1 in fluorescence units (FU). This solution was then added to 5 µl of streptavidin-coated magnetic beads (MagPrep® Streptavidin Beads by Merck, 1 µm, 1.4 g/l, 10^{12} particles/g). Magnetic beads were rinsed twice for 2 min with 50 mM Gly/HCl buffer (pH 3.5) before application. We determined that 2 µl of the magnetic beads suspension captures up to 0.1 nmol biotinylated peptide. The mixture was stirred and kept at RT for at least 10 min but not longer than 30 min. Longer incubation leads to an increase of unspecific binding. The solution should be homogeneous for complete binding of the biotinylated molecules to the streptavidin-coated magnetic beads. After 10 min the magnetic beads were separated using a permanent magnet (after 1 min the supernatant should be clear). The fluorescence of 50 µl of the obtained supernatant was measured according to F_2. The concentration of generated digestion product (DP) in µmol/l per min is calculated using the equation

$$\frac{[DP]}{t} = [S_0] - \frac{F_1 - F_2}{F_1} \times [S_0] - [DP_0] \qquad \text{(equation 2)}$$

where $[S_0]$ is the initial substrate concentration (µM) and t is the digestion time in min. $[DP_0]$ is the value of biotinylated peptides not bound to the magnetic beads (µM) and has to be determined in parallel to each test series.

2.6 Synthesis of R9-CatD-substrate

The doubly-labeled peptide R9-CatD-substrate (Ac-RRRRRRRRR-Lys(Tamra)-APISFFELG-εLys(αFluo)-$CONH_2$) was synthesized using the previously developed N^{α}-carboxyfluorescein-labeled lysyl-Rink amide resin [Fischer et al. 2003]. The peptide RRRRRRRRR-Lys(Dde)-APISFFELG was assembled on this resin in a 15 µmol scale as described above. For analytical purposes a small fraction of the peptide was cleaved off and analyzed (RRRRRRRRR-Lys(Dde)-APISFFELG-εLys(Fluo)-$CONH_2$, purity 80 % as determined by RP-HPLC, 214 nm, calc. $[M+H]^+$ = 3164.7 Da, exp. $[M+H]^+$ = 3164.0 Da as determined by MALDI-MS).

Derivatizations of the peptide were performed manually in 2 ml syringes on a shaker at RT. Reactions were stopped by washing the resins 3 times each with DMF, MeOH, DCM and diethylether. The synthesis of the doubly-labeled peptide was performed in a 5 µmol scale. The amino terminus of the resin-bound and side-chain protected peptide was acetylated using 1 ml DMF/acetic anhydride/DIPEA (8:1:1, v/v/v). Deprotection of the Dde-protecting group was performed using 2 % (v/v) hydrazine monohydrate in DMF twice for 3 min. Then the free ε-amino group was reacted with 5(6)-carboxytetramethylrhodamine-N-succinimidyl ester (10 µmol, 5.3 mg) in DMF (200 µl) containing DIPEA (25 µmol, 4.3 µl). After 16 h, the resin was thoroughly washed followed by cleavage off the resin and deprotection of the doubly-labeled peptide amide. The peptide was dissolved in ACN/water (1:1, v/v), lyophilized and analyzed by RP-HPLC and MALDI-MS (see Figure 25). Afterwards the R9-CatD-substrate was purified by preparative RP-HPLC.

2.7 Cell culture

HeLa cells were grown in a 5 % CO_2 humidified atmosphere at 37 °C in RPMI 1640 medium with stabilized glutamine and 2.0 g/l $NaHCO_3$ (PAN Biotech, Aidenbach, Germany) supplemented with 10 % (v/v) fetal calf serum (PAN Biotech), 100 U/ml penicillin, and 100 µg/ml streptomycin (Biochrom, Berlin, Germany). Confluent cells were passaged by trypsinization with trypsin/ethylenediaminetetraacetic acid (EDTA) (0.05/0.02 % (w/v)) (Biochrom) in PBS every third to fourth day.

The EBV-transformed human B cell line Boleth (IMGT/HLA sequence database number: HC10329) and the human monocyte cell line U937 (ATTC number: CRL-2367) were grown at 37 °C in tissue culture flasks (Nunc, Wiesbaden, Germany) with RPMI 1640 medium (containing 10% (v/v) fetal calf serum; 2 mM L-glutamine; 25 mM Hepes; Invitrogen-Gibco, Karlsruhe, Germany) supplemented with 80 µg/ml gentamycin (Merck, Darmstadt, Germany) in a humidified atmosphere (5 % CO_2/air). 10^8 Cells were harvested (1000 rpm for 10 min, Heraeus-Christ Varifuge K) and subcellular fractionation was performed as previously described by Schröter et al. 1999. The obtained fractions were crude cell extract (CCE), endosomal fraction (E) and lysosomal fraction (L).

2.8 SDS-PAGE and western blot analysis

2.8.1 Western blot analysis of subcellular fractions

Subcellular fractions were separated by SDS-polyacrylamide gel electrophoresis (15 µg protein/lane) on a 15% separating gel and transferred to a PVDF-membrane (Amersham Biosciences, Freiburg, Germany) in a Novex mini-trans-blot-apparatus (Invitrogen, Karlsruhe, Germany). The membranes were blocked for 16 h at 4 °C in Tris buffered saline with Tween 20 (TBST, 0.15 M NaCl, 10 mM Trizma® Base, 0.05% Tween 20 (v/v), pH 8.0) containing 10% (v/v) Roti® Block (Roth, Karlsruhe, Germany). Rabbit anti-human CatD (Calbiochem, Schwalbach, Germany) was diluted 1:5000 in TBST containing 10% (v/v) Roti® Block and incubated for 2 h. Subsequently, filters were washed 3 times in TBST and incubated for 1 h with horseradish peroxidase-conjugated goat anti-rabbit IgG (Jackson Immuno Research, West Grove, USA) diluted 1:10000 in TBST containing 10% (v/v) Roti® Block. After

washing the filters 3 times with TBST, western blots were developed according to the ECL protocol by Amersham Biosciences (Freiburg, Germany).

2.8.2 Western blot analysis of HeLa cell lysate

10^6 HeLa cells were lysed in 200 µl phosphate buffered saline (PBS) containing 1 % (v/v) NP-40, 0.5 % (w/v) sodium desoxycholate and 0.1 % (w/v) sodium dodecyl sulfate (SDS) (all detergents were obtained from Sigma) complemented with protease inhibitors for tissue extracts (Sigma). The protein content of the lysate was determined using a commercially available Bradford protein assay kit (Bio-Rad Laboratories, München, Germany). Proteins were separated using SDS-polyacrylamide gel electrophoresis on a 10 % separating gel and then transferred to a PVDF-membrane in transfer buffer (195 mM glycine, 12.5 mM Tris/HCl, 0.01 % (w/v) SDS and 10 % (v/v) methanol) in a HEP-1 Panther Semi Dry Electroblotting System (OWL, Portsmouth, USA). The PVDF-membrane was first blocked for 1 h at RT with blocking solution (2 % (w/v) low-fat milk powder in PBST (PBS + 0.05 % (v/v) Tween) and subsequently incubated with rabbit anti-human CatD antibody at 4 °C for 16 h (Calbiochem-Novabiochem Corporation, San Diego, USA; diluted 1:5000 in blocking solution). Then the membrane was incubated with horseradish peroxidase-conjugated goat anti-rabbit IgG (DakoCytomation, Glostrup, Denmark; diluted 1:5000 in blocking solution) for 1 h at RT. After washing the membrane 3 times for 10 min with PBST, western blots were developed according to the ECL protocol by Amersham Biosciences (Freiburg, Germany).

2.8.3 Western blot analysis of sweat

Sweat samples were run on a 15% Bis-Tris (Bis-(2-hydroxyethyl)-glycin) separating gel with Tris-glycine running buffer (25 mM Tris-HCl, 192 mM glycine, 0.1% (w/v) SDS, pH 8.3) and stained with Simply Blue™ Safe Stain (Invitrogen, Karlsruhe, Germany). Gel bands were excised and stored at -18 °C until digestion with trypsin. Western blot analysis was performed using a 10% Bis-Tris gel (Invitrogen, Karlsruhe, Germany) with MES ((2-(N-morpholino)ethanesulfonic acid) running buffer according to the manufacturer's instructions. Proteins then were transferred to a PVDF (polyvinylidene difluoride) membrane (Amersham Biosciences, Freiburg, Germany) in a Novex mini-trans blot-apparatus (Invitrogen,

Karlsruhe, Germany). The membrane was blocked for 16 h at 4 °C in Tris buffered saline with Tween 20 (TBST, 0.15 M NaCl, 10 mM Trizma® Base, 0.05% (v/v) Tween 20, pH 8.0) containing 10% (v/v) Roti® Block (Roth, Karlsruhe, Germany). Rabbit anti-human CatD (Sigma, Taufkirchen, Germany) was diluted 1:10,000 in TBST containing 10% (v/v) Roti® Block. After 2 h incubation membranes were washed and incubated with horseradish peroxidase-conjugated goat anti-rabbit IgG (Jackson Immuno Research, West Grove, USA) (1:10,000) for 1 h. Western blots were then developed according to the ECL protocol of Amersham Biosciences.

2.9 Collection and preparation of sweat

Human sweat samples from several healthy donors were collected from the surface of the face, neck or chest during physical exercise or in a hot environment as previously described [Schittek et al. 2001]. For some experiments sweat samples were pooled (pooled sweat). SDS-PAGE analysis was performed with 100 µl sweat. Before gel electrophoresis sweat samples were dialyzed (48 h) using a 1 kDa membrane Tube-O-Dialyzer™ (Geno Technology, St. Louis, USA) to remove small interfering substances such as salts. The resulting 150 µl sample were concentrated to dryness using a centrifugal vacuum concentrator (Savant SpeedVac® SPD111, Thermo Quest, Egelsbach, Germany) and then resuspended in 20 µl water. Western blot analyses and *in vitro* digestion experiments were performed with pure sweat, centrifuged at 1500 g (Biofuge pico, Kendro, Osterode, Germany). The obtained supernatants were stored at -80 °C until use.

2.10 In-gel tryptic digestion and analysis of tryptic fingerprint

Excised gel bands were diced to approximately 1 mm^3 and washed once for 15 min with water before being resuspended in 40 µl 50% (v/v) acetonitrile (ACN)/water and incubating for further 15 min. Gel pieces were then subsequently shrunk with 40 µl 100% ACN and 40 µl of 100 mM $(NH_4)_2CO_3$. Afterwards gel pieces were incubated for 15 min with a 1:1 solution of ACN and 100 mM $(NH_4)_2CO_3$ and then vacuum-centrifuged to complete dryness. 40 µl of a trypsin solution (10 ng/ml) in digestion buffer (5 mM $CaCl_2$ and 50 mM $(NH_4)_2CO_3$) were added and incubated for 45 min. The trypsin solution was removed and gel pieces were incubated for 16 h at 37 °C in 50 µl digestion buffer. Tryptic peptides were eluted from the gel pieces by

covering them with 0.1% (v/v) TFA in water and sonicated for 30 min. The extraction step was repeated successively with 30% (v/v) ACN/water and with 60% (v/v) ACN/water. The obtained supernatants were pooled and vacuum centrifuged to 50% of the original volume to remove TFA and ACN. After adding 10 µl formic acid, samples were measured by MALDI-Re-TOF (time of flight) MS on a Voyager DE-STR (Applied Biosystems, Foster City, CA, USA). Peptide fingerprints were exported for database matching, and subsequently identified using the Mascot program [Perkins et al. 1999] available through www.matrixscience.com. In certain cases the results of tryptic fingerprint analysis were not definite, thus the samples were additionally analyzed by automated LC-ESI-MS/MS using an Esquire 3000 plus ion-trap mass spectrometer (Bruker-Daltonics, Bremen, Germany). The obtained MS/MS data were also analyzed using Mascot sequence query for probability based peptide identification.

2.11 In vitro digestion of LL-37 and DCD-1L with CatD

In vitro digestions of synthetic LL-37 and DCD-1L with CatD (Sigma, Taufkirchen, Germany) were performed in 50 mM Glycine/HCl buffer pH 3.5 and in sweat buffer pH 5.5 (40 mM NaCl, 10 mM KCl, 1 mM $CaCl_2$, 1 mM $MgCl_2$ and 1 mM NaH_2PO_4) (14). DCD-1L (24.9 µM) and LL-37 (26.7 µM) were incubated with 0.6 µM CatD for 8 h at 37 °C. The reaction was stopped by addition of 25 µl stop solution (95% (v/v) ACN, 1% (v/v) TFA in water).

Peptide fragments were separated via analytical RP-HPLC using a 125 × 2 mm Nucleosil 100 C 8 column (Wicom, Heppenheim, Germany) with the following solvent system: (A) 0.055% (v/v) TFA (trifluoroacetic acid) in H_2O and (B) 0.05% (v/v) TFA in ACN/H_2O (4:1, (v/v)). The column was eluted with a 5% to 80% gradient of solvent B for 40 min. UV-detection was carried out at 214 nm (UV detector SPD-10AV, Shimadzu, Duisburg, Germany). Manually collected fractions were subsequently analyzed by matrix-assisted laser desorption/ionization mass spectrometry (MALDI-MS) and Edman degradation on an automated 494A Procise peptide sequencer (Applied Biosystems, Darmstadt, Germany). The *in vitro* inhibition experiments were analyzed in the same way using a RF-10AXL fluorescence detector (Shimadzu, Duisburg, Germany) by measuring the emission at 450 nm following excitation at 350 nm.

2.12 Determination of aminopeptidase activity

Aminopeptidase activity was measured using the substrate H-Leu-AMC (Bachem AG, Bubendorf, Switzerland) (15 µM) according to the manufacturer's protocol and 25 µl pooled sweat to a final volume of 200 µl in PBS. Fluorescence signal was continuously measured using the microplate reader Spectra Fluor (Nunc, Wiesbaden, Germany) at an emission wavelength of 465 nm with excitation at 360 nm.

2.13 SELDI Protein Chip® Technology

Sweat samples were analyzed by surface-enhanced laser desorption/ionization (SELDI) mass spectrometry [Wright 2002] on reversed-phase (H4) chips (Ciphergen Biosystems, Fremont, USA) which were equilibrated three times for 5 min in ACN/water (1:1, (v/v)). 1 µl human sweat was diluted into 2 µl binding buffer (50 mM sodium phosphate pH 6.5) and the chromatographic arrays were incubated in a humid chamber for 30 min. Then chips were washed three times for 5 min with binding buffer followed by a final water wash to remove interfering substances such as salts. After drying a saturated solution of sinapinic acid in ACN/H_2O (1:1, (v/v)) supplemented with 0.5% (v/v) TFA was added and peptide masses were read from the array surface using a ProteinChip Reader (Ciphergen Biosystems, Fremont, USA). The instrument was externally calibrated using two different synthetic peptides (DCD-1L and DCD-1) and bovine insulin. Internal calibration was performed by adding 100 fmol of porcine dynorphin A, adrenocorticotropic hormone (1-24) and bovine insulin. The data obtained were analyzed using the ProteinChip Software (Version 3.0).

2.14 Antimicrobial assays

Antimicrobial activities of synthetic peptides were tested by the Department of Dermatology, University of Tübingen, using the colony-forming units (CFU) assay as previously described [Valore et al. 1998]. *Escherichia coli* (ATCC 25922) or *Staphylococcus aureus* (ATCC 25923) single cell colonies were cultured overnight, subcultured and grown to mid-exponential growth phase prior to the antimicrobial assay. Cells were washed twice with 10 mM Na-phosphate buffer pH 7.0 containing

10 mM NaCl. Bacterial concentration was estimated photometrical at 600 nm. Absorbance of 1.0 corresponded to $8.56*10^8$ cells of E. coli and to $1.97*10^8$ cells of *S. aureus* per ml. After dilution to a concentration of 10^6 CFU/ml in 30 mM Na-phosphate buffer pH 7.0 containing 30 mM NaCl, 10µl of the dilutions were incubated at 37°C for 2h with 20µl various peptide concentrations in water. After incubation cells were diluted 1:100 in 10 mM Na-phosphate buffer pH 7.0 containing 10 mM NaCl. Then 90 µl of the diluted bacterial suspension were plated in triplicates on blood agar. The plates were incubated overnight at 37 °C and the number of colonies were counted. Antimicrobial activity is expressed as percentage of cell death (PCD):

$$PCD = \left[1 - \left(\frac{CFU_{sample}}{CFU_{control}}\right)\right] \times 100$$

where $CFU_{control}$ is the number of colony-forming units without peptide incubation and CFU_{sample} is the number of colony-forming units of the appropriate sample.

2.15 RP-HPLC for the R9-CatD-substrate

The peptide was analyzed by analytical RP-HPLC using a H_2O (0.1 % TFA) (solvent A)/ACN (0.1 % TFA) (solvent B) gradient on a Waters 600 System (Eschborn, Germany) with detection at 214 nm. The sample was analyzed on an analytical column (Nucleosil 100, 250 x 2 mm, C18 column, 5 µm particle diameter; Grom, Herrenberg, Germany) using a linear gradient from 10 % B to 100 % B within 30 min (flow rate: 0.3 ml/min). The R9-CatD-substrate was purified by preparative RP-HPLC (Nucleosil 300, 250 x 20 mm, C18 column, 10 µm particle diameter; Grom, Herrenberg, Germany) on a Gilson (Bad Camberg, Germany) preparative system, equipped with a 321 Pump and a 156 UV/Vis Detector, flow rate: 10 mL/min.

The purified R9-CatD-substrate was dissolved in DMSO at a concentration of 10 mM. This stock solution was further diluted 1:20 in H_2O. The peptide concentration was determined by UV/VIS-spectroscopy of a further 1:100 dilution in methanol. Absorptions of these solutions were then measured at 540 nm (ε = 95.000 L/(mol·cm).

2.16 MALDI-MS

1 µl of 2,5-dihydroxyacetophenone (DHAP) matrix (20 mg of DHAP, 5 mg of ammonium citrate in 1 ml of isopropyl alcohol/H_2O (4:1, v/v)) was mixed with 1 µl of each sample (dissolved in ACN/water (1:1, v/v) at a concentration of 1 mg/ml) on a gold target. Measurements were performed using a MALDI-TOF (time-of-flight) system (G2025A, Hewlett-Packard, Waldbronn, Germany). For signal generation 20-50 laser shots were added up in the single shot mode.

2.17 Digestion of the R9-CatD-substrate with proteinase K for ratiometric measurements

Fluorescence emission spectra were recorded at RT using an LS50B spectrofluorometer (Perkin-Elmer, Norwalk, USA). The spectra were corrected for the sensitivity of the detection system. The excitation and emission bandwidths were set to 10 nm. Purified R9-CatD-substrate (100 nM) was digested at 37°C with proteinase K (20 µg/ml, Sigma, Taufkirchen, Germany) in NP-40 lysis buffer (0.5 % (v/v) NP-40, 150 mM NaCl, 5 mM EDTA, 50 mM TRIS, pH 7.0). After 3 h the reaction was stopped by adding PMSF (final concentration 500 µM). Definite amounts of digested and undigested R9-CatD-substrate diluted in 100 nM in NP-40 lysis buffer, including 500 µM PMSF were mixed and fluorescence emission spectra of the solutions were recorded (excitation 492 nm). All digests and measurements were performed as duplicates.

2.18 Fluorescence emission measurements in cell lysates

HeLa cells were seeded in 12-well plates (Becton-Dickinson, Heidelberg, Germany) in serum-containing medium and grown to 90% confluency (300,000 cells per well). The cell layer was first washed with serum-free medium and incubated with 250 µl serum-free medium (containing the indicated inhibitors) for 30 min. Then the R9-CatD-substrate was added at the indicated concentration. Following the peptide incubation for 1 h cells were washed twice with PBS, detached using 5 mM EDTA in PBS (15 min at 37 °C), transferred into a tube and spun down. The cell pellet was then lysed in 200 µl NP-40 lysis buffer containing a protease inhibitor cocktail (Roche Diagnostics, Mannheim, Germany). These lysates were sonicated and centrifuged for 10 min at 4 °C and 14,000 rpm. Fluorescence emission spectra of the

supernatants were recorded immediately (excitation at 492 nm) and fluorescence emission ratios (520nm/585 nm) were calculated.

In the cases of the digestion of the lysate with proteinase K (Figure 3A), four wells of a 12 well plate were incubated with the R9-CatD-substrate as indicated. Two of four obtained cell pellets were lysed in protease inhibitor containing NP-40 lysis buffer as indicated above and fluorescence emission spectra of the two lysates were recorded (excitation at 492 nm). The other two cell pellets were lysed in NP-40 lysis buffer without protease inhibitors and lysates were prepared. Those lysates were subsequently digested with 0.1 mg/ml proteinase K for 16 h.

2.19 Confocal laser scanning microscopy (CLSM)

CLSM was performed on an inverted LSM510 laser scanning microscope (Carl Zeiss, Göttingen, Germany) fitted with a Plan-Apochromat 63x 1.4 N.A. lens. All measurements were performed with living, non-fixed cells.

HeLa cells were seeded at a density of 50,000/well in eight-well chambered cover glasses (Nunc, Wiesbaden, Germany). One day later cells were washed once with serum-free medium. AlexaFluor 633-Transferrin (Molecular Probes, Eugene, USA) and R9-CatD-substrate were added as indicated in serum-free medium. After 30 min incubation with the R9-CatD-substrate and AlexaFluor 633-Transferrin, images were acquired immediately at RT with peptide and transferrin in the medium.

For triple detection of fluorescein, Tamra and AlexaFluor 633, a 488 nm Argon-ion laser, a 543 nm Helium/Neon and a 633 nm Helium/Neon laser were used for excitation in combination with a filter set containing an HFT UV/488/543/633 beam splitter. For fluorescein detection a BP 505-530 detection filter was applied, for Tamra detection a BP 560-615 detection filter, and a LP650 long pass filter for AlexaFluor 633 detection. To avoid cross-talk detection, the multi-track modality of the LSM was employed for image acquisition. The AlexaFluor 633 channel was virtually free of cross-talk from the other two fluorophores as determined from control samples loaded with the R9-CatD-substrate.

3 New substrates for the detection of CatD activity

3.1 Intention

For cellbiological investigations, for the discovery of specific inhibitors or for clinical diagnostics it is necessary to have a fast and reproducible assay for the parallel testing of the proteolytic activity of CatD. Previously, several methods have been described for measuring the activity of aspartic proteases [Folin & Ciocalteau 1927, Anson 1938, Dunn et al. 1986, Filippova et al. 1996, Gulnik et al. 1997, Yasuda et al. 1999]. A very common method using natural protein substrates like bovine hemoglobin is rather time consuming and lacks of specificity [Anson 1939]. The generated trichloroacetic acid soluble cleavage products of hemoglobin are measured at 280 nm or the tyrosine and tryptophane content is determined using the phenol reagent of Folin and Ciocalteau [Folin & Ciocalteau 1927]. A faster method uses substrates containing a chromophore, such as a nitrophenylalanine residue, at position P1'. Product formation can be measured by monitoring the increase of absorbance at 300-310 nm by UV spectroscopy [Dunn et al. 1986]. Recently, fluorogenic substrates containing fluorophore and quencher groups like o-aminobenzoic acid and p-nitroanilide [Filippova et al. 1996] or 5-[(2-aminomethyl)amino]naphthalene-1-sulfonic acid) (EDANS) and 4'-dimethylaminoazobenzene-4-carboxylic acid (DABCYL) [Gulnik et al. 1997, Matayoshi et al. 1990] within the same molecule have been developed. Upon cleavage of the peptide the fluorescence signal is no longer quenched and its increase can be measured continuously [Yaron et al. 1979].

Here we describe the synthesis of simultaneously fluorophore and biotin labelled decapeptide amide substrates and their application to a novel heterogeneous bead-assay for the determination of CatD activitiy. This method is applied to biological samples to analyse CatD activity in endosomal and lysosomal compartments as well as in cell lysates of human EBV-transformed B cells and human monocytes.

3.2 Results

3.2.1 Synthesis of biotinylated and fluorescent CatD substrates

The substrate I was designed based on the published CatD peptide substrate KPILF↓FRL. Within this substrate the Phe-Phe bond is predominantly cleaved by CatD as previously described by Scarborough et al. 1993. We modified this substrate for our digest & pull down assay system by including the two charged amino acids glutamic acid and aspartic acid (Table 2) at the N-terminus in order to increase solubility. At the C-terminus a glycine residue was introduced as a spacer and a lysine residue for the conjugation of the biotin moiety via its ε-amino-group. This was achieved by using a Rink amide resin carrying an ε-biotinylated lysine residue (Fig. 2). The peptide substrate then was synthesised by elongation via SPPS on the lysine's α-amino-group. After SPPS the substrate was then N-terminally labelled with the pH-insensitive fluorophore Amca due to the fact that the assay will be performed in an acidic buffer system because CatD has a pH optimum at 3.5 – 4.0 [Yasuda et al. 1999]. After deprotection and cleavage from the resin the peptide amides were purified by preparative RP-HPLC and checked for their correct masses using ESI-MS. Peptide purities were determined via analytical RP-HPLC and proved to be higher than 97 %.

Table 2 Proteolytic fragments obtained after digesting substrate I, II and III with CatD as determined with mass spectrometry. P1 and P1' residues are shown in bold.

#	substrates and digestion products	expected mass [M + H]$^+$	[M + H]$^+$	ΔDa
I	Amca-EDKPILFFRLGK(biotin)-$CONH_2$	1904.3	1904.3	0.0
	Amca-EDKPILF-OH	1077.2	1077.4	0.2
	NH_2-FRLGK(biotin)-$CONH_2$	846,1	845,5	0.6
	Amca-EDKPIL-OH	930.1	930.0	0.1
	NH_2-FFRLGK(biotin)-$CONH_2$	993.3	993.3	0.0
	Amca-EDKPI-OH	816,9	817.1	0.2
	NH_2-LFFRLGK(biotin)-$CONH_2$	1106.4	n.f.$^+$	-
II	Amca-EEKPIC(Acm)FFRLGK(biotin)-$CONH_2$	1979.4	1981.3	1.9
	Amca-EEKPIC(Acm)F-OH	1152.3	1151.2	1.1
	NH_2-FRLGK(biotin)-$CONH_2$	846.1	845.2	0.9
III	Amca-EEKPISFFRLGK(biotin)-$CONH_2$	1892.3	1890.9	1.4
	Amca-EEKPISF-OH	1065.2	1063.7	1.5
	NH_2-FRLGK(biotin)-$CONH_2$	846.1	845.0	1.1

$^+$n.f. = not found

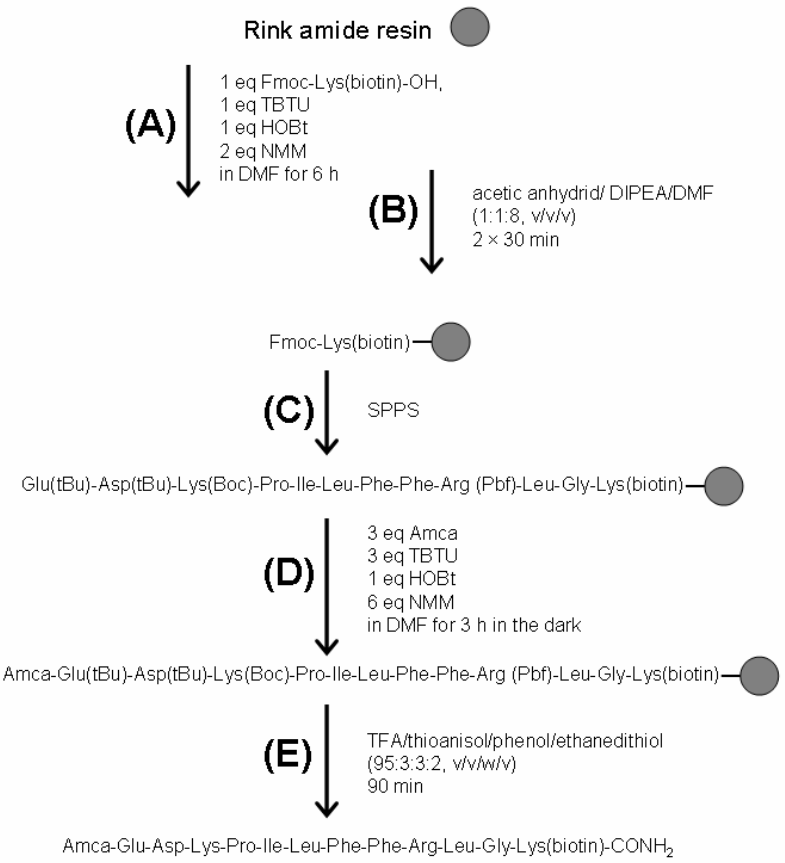

Figure 2 Synthesis of the biotinylated and fluorescent peptide amide Amca-EDKPILFFRLGK(biotin)-$CONH_2$. **(A)** Coupling of Fmoc-Lys(biotin)-OH to Rink amide resine. **(B)** Capping of the remaining amino-groups by acetylation. **(C)** Solid-phase peptide synthesis. **(D)** Introduction of the fluorophor Amca at the N-terminus. **(E)** Cleavage of the peptide from the resin and side chain deprotection

3.2.2 In vitro digestion and optimisation of the peptide substrate

Substrate I was digested *in vitro* with CatD and the generated peptide fragments were separated using RP-HPLC (Fig. 3, panel A) and identified by MALDI-MS (Table 2). Substrate I did not posses just one single cleavage site for CatD and was cleaved between I↓L, L↓F and F↓F (Table 2, entry I). However, the development of a specific CatD assay preferably requires a substrate possessing one single cleavage site. Therefore we replaced the hydrophobic amino acid residue leucine in P2 position with the Acm-protected cysteine derivative Cys(Acm) (substrate II) or the hydrophilic amino acid serine (substrate III), respectively. The peptide amide substrates II and III were synthesised as described in the experimental section and peptide purities were determined using analytical RP-HPLC and proved to be higher than 97 %. Substrate II and III were also digested with CatD and the generated

peptide fragments were separated by RP-HPLC and identified by MALDI-MS. Both substrates were only cleaved between the two phenylalanine residues yielding 2 peptide fragments (Table 2, entries II and III). No further digestion products were observed.

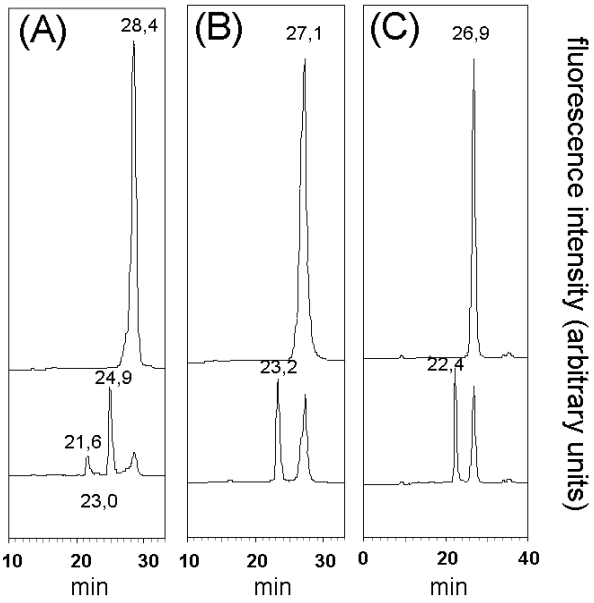

Figure 3 RP-HPLC profiles of substrates I-III after incubation with CatD at pH 3.5 in 50 mM Glycin-HCl buffer with (upper line) or without (lower line) 10 µM Pepstatin using fluorescence detection ($\lambda_{Ex.}$ = 350 nm, $\lambda_{Em.}$ = 450 nm). **(A)** Digestion of substrate I with CatD leads to at least 6 determined cleavage products. Substrate II **(B)** and III **(C)** show only one cleavage site for CatD.

These results suggest that CatD preferable cleaves peptide substrates between uncharged and hydrophobic amino acids according to previous published data [Scarborough et al. 1993]. Replacement of the uncharged hydrophobic amino acid leucine at P2 position renders the substrates II and III to more specific substrates which make them attractive tools for the development of a specific CatD assay.

3.2.3 Kinetic characteristics of the developed CatD substrates

Next we characterised substrates I, II and III with respect to their kinetic properties by measuring the initial velocities at various substrate concentrations using analytical RP-HPLC with fluorescence detection for the quantification of proteolytic activity. In order to obtain data that can be used for kinetic analysis, we tested in which time frame the initial velocity is linear (Fig. 4). Within the first 10 min the initial velocity is linear and the obtained parameters could be used for Lineweaver-Burk analysis as

described in the experimental section. The obtained K_m, k_{cat} and k_{cat}/ K_m values of the substrates I, II and III are listed in Table 3.

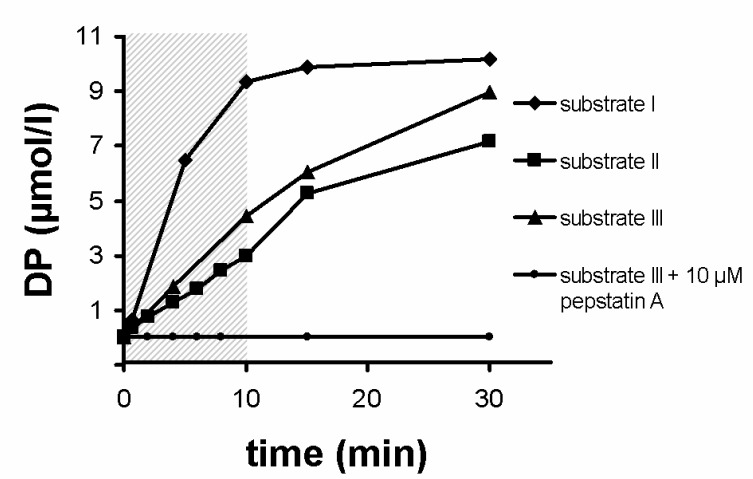

Figure 4 Time courses of the hydrolysis of 10.5 µM substrate I, II and III with 6.5 nM CatD in 50 mM Gly/HCl buffer (pH 3.5). The amount of digestion product (DP) was determined using RP-HPLC with fluorescence detection as described in the experimental section. The hatched area indicates the linear phase of the hydrolysis (0 - 10 min). In the presence of 10 µM pepstatin A CatD was completely inhibited.

The determined kinetic parameters for the substrates are slightly higher than described for previously published substrates [Scarborough et al. 1993, Gulnik et al. 1997, Yasuda et al. 1999]. Conjugation with biotin and Amca as well as the replacement of the hydrophobic amino acid leucine in P2 position leads to a small increase of the K_m values. As expected substrate I exhibits the lowest K_m value due to the fact that it possesses several cleavage sites for CatD. Substrate III is more specific than substrate I and has a smaller K_m value than substrate II and therefore proved to be the most suitable substrate for a rapid and specific substrate-based CatD assay. Therefore substrate III was used for further experiments.

Table 3 Kinetic parameters for the hydrolysis of the synthesised fluorescent substrates I, II and III by CatD. P1 and P1'residues are shown in bold.

#	Sequence	K_m (µM)	k_{cat} (s^{-1})	k_{cat} / K_m ($\mu M^{-1} \times s^{-1}$)	Ref.
I	Amca-EDKPIL**FF**RLGK(biotin)-$CONH_2$	12.2	0.41	0.03	
II	Amca-EEKPIC(Acm)**FF**RLGK(biotin)-$CONH_2$	72.5	6.34	0.09	
III	Amca-EEKPIS**FF**RLGK(biotin)-$CONH_2$	53.0	7.28	0.14	
	Ac-EE(Edans)KPIC(Et)**FF**RLGK(Dabcyl)E-NH_2	27.5	196.0	7.10	[Gulnik et al. 1997]
	MOCAc-GKPIL**FF**RRLK(Dnp)γ-NH_2	3.7	57.8	15.60	[Yasuda et al. 1999]
	KPIR**FNph**RL-NH_2	72.0	6.0	0.08	[Scarborough et al. 1993]

MOCAc, (7-methoxycoumarin-4-yl)acetyl; Dnp, N-2,4-dinitrophenyl; Nph, p-nitrophenylalanine

3.2.4 Application of the substrates for the determination of CatD activity

Figure 6 shows the principle of our novel digestion & pull down assay. After incomplete digestion of the substrate III the following peptides are in solution: intact substrate and both, fluorescent and biotinylated digestion products. First total fluorescence of the reaction solution is measured at an emission wavelength of 465 nm with excitation at 360 nm immediately after digestion. The obtained value is called F_1 and represents the total amount of fluorescent peptides in solution i.e. digested and undigested fluorescent substrate. In the next step all biotinylated peptides are removed using streptavidin-coated magnetic beads, leaving only fluorescent digestion products in solution. Then the remaining fluorescence is measured yielding the value F_2.

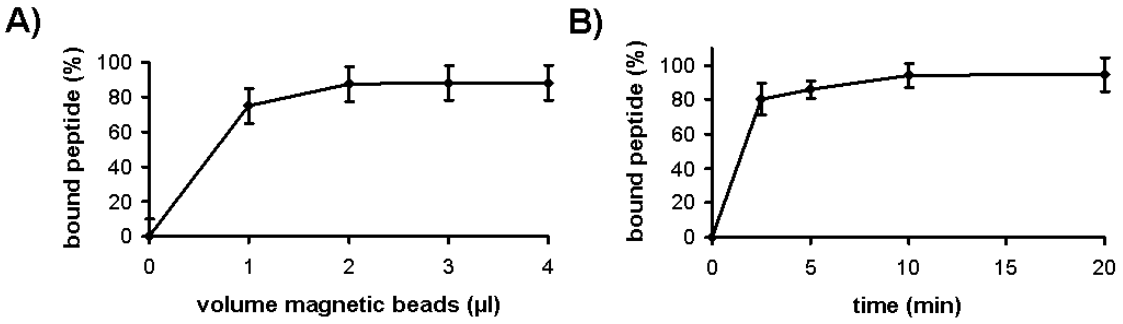

Figure 5 Characterisation of the streptavidin-coated magnetic beads. **(A)** Binding capacity of the streptavidin-coated magnetic beads. **(B)** Time course of the conjugation of biotinylated peptide substrate III to 2 µl of the streptavidin-coated magnetic beads.

Under the conditions described in the experimental section about 95 % of all biotinylated molecules are bound and removed (Fig. 5A) from the solution within 10 min (Fig. 5B). Longer incubation times or the application of more magnetic beads do not improve the efficiency of the removal of the biotinylated peptides. The difference between the values F_1 and F_2 coincides proportionally with the amount of digested substrate. Using equation 2 shown in the experimental section, the concentration of the digestion product (DP) after the appropriate time can be calculated.

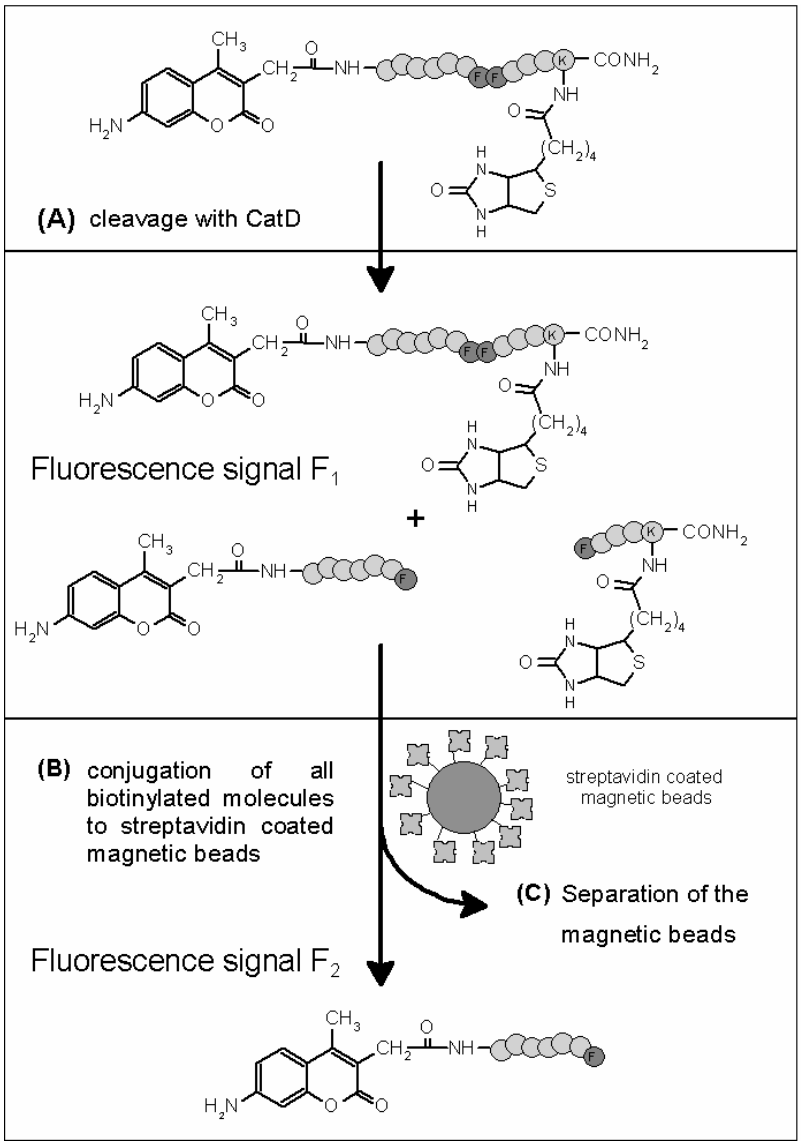

Figure 6 Principle of the digest & pull down assay: **(A)** Incomplete digestion of peptide substrate and fluorescence measurement (F_1). **(B)** Capturing of biotinylated digestion products with streptavidin-coated magnetic beads. **(C)** Measurement of fluorescence (F_2) after separation of magnetic beads with a permanent magnet

Determination of absolute CatD activity in biological samples requires a calibration curve. For this purpose substrate III was incubated with different amounts of CatD in the range from 15 mU/ml to 45 mU/ml (Fig. 7). The obtained values were interpolated leading to the following equation

$$CatD = \frac{[DP]}{t \times 0.1656} \qquad \text{(equation 3)}$$

where [DP] is the concentration of the digestion product in µmol/l, t is the digestion time in min and CatD is the enzyme activity in mU/ml. The constant factor 0.1656

represents the slope of the calibration curve. One unit is defined as the increase in the absorbance at 280 nm of 1.0 in 30 min at pH 3.3 and at 37 °C measured as trichloroacetic acid soluble products using acid-denaturated hemoglobin as substrate (Sigma-Aldrich, Taufkirchen, Germany).

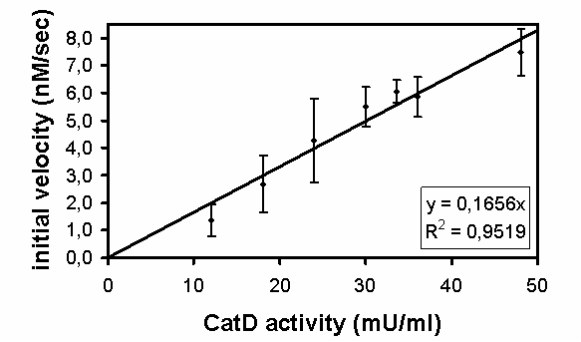

Figure 7 Calibration curve for the determination of CatD activity using the bead-assay. Varying concentrations of CatD were incubated with substrate III (10.6 µM) in 50 µl 50 mM Gly/HCl buffer (pH 3.5) at 37 °C for 10 min. Values represent the mean of at least three independent experiments

3.2.5 Determination of CatD activity in subcellular compartments of human B cells and monocytes

To demonstrate the applicability of the digest & pull down assay for biological samples the distribution of CatD in different subcellular fractions of the human EBV-transformed B cell line Boleth and the human monocyte cell line U937 was analysed. The two cell lines were selected because of their different CatD expression levels. The cell line U937 exhibits a very high level of CatD compared to the Boleth cell line where no CatD was detectable in cell lysates using western blot analysis [Greiner et al. 2003].

In order to validate the versatility of our novel digest & pull down assay for cellular CatD activity measurements we compared it with standard western blot analysis. Therefore the two cell lines were homogenized and fractionated as previously described [Schröter et al. 1999] yielding the following subcellular fractions: crude cell extract (CCE), endosomal fraction (E) and lysosomal fraction (L). The total amount of protein of each fraction was determined using the method of Bradford [Bradford 1976]. 15 µg total protein of the subcellular fractions were applied to a 15 % SDS-polyacrylamide gel and the proteins then were transferred to a PVDF-membrane followed by western blot analysis using a rabbit anti-CatD (human) antibody (Fig.

8A). Lanes 1, 2 and 3 and 5, 6, 7 represent lysosomal fraction, endosomal fraction or crude cell extract of the Boleth cell line and U937 cell line, respectively. Human CatD was used as a positive control and is shown in lane 4. The band migrating at 31 kDa represents the active mature form of CatD. Two weaker bands at 44 kDa and 51-55 kDa stand for the intermediate single chain form of CatD and for glycosylated proforms of CatD respectively [Rijnboutt et al. 1992]. The control human CatD shows a major band at 31 kDa and a small amount of the intermediate single chain form and the proform of CatD due to the fact that it has been isolated from human liver.

In the endosomal fraction and in crude cell extracts of the Boleth cell line no CatD could be detected. The band visible in crude cell extract and in the lysosomal fraction of the Boleth cell line migrating at 33 kDa is not mature CatD due to the fact that it migrates above the mature CatD band. This CatD form has not been identified by anyone until now. Only in the lysosomal fraction of the Boleth cell line a small amount of mature CatD as well as the intermediate single chain CatD and the proform of CatD could be detected.

In contrast to this intracellular CatD distribution in the Boleth cell line, in all fractions of the U937 cell line almost the same amount of mature CatD was detected. The single chain intermediate form of CatD is predominantly found in endosomal fraction and to a smaller amount in lysosomal fraction and crude cell extract.

Now the two cell lines were analysed for their CatD activity using substrate III and our novel digest & pull down assay. The digest & pull down assay was performed with 0.5 µg total protein of the subcellular fraction. The digestion products were then separated by RP-HPLC and identified by MALDI-MS. Substrate III was only cleaved between the two phenylalanine residues and no further cleavage sites were observed when using the inhibitor mix described in the experimental section (data not shown). These findings proved that substrate III can be used for specific determination of CatD in subcellular fractions of human B cells and human monocytes respectively.

Substrate III was also incubated for 10 min with the subcellular fractions and analysed using a microplate reader at an emission wavelengths of 465 nm with excitation at 360 nm obtaining F_1 and F_2 respectively. The amount of digestion product in µmol/l was calculated using equation 2. For the determination of the absolute CatD activity in the subcellular fractions the obtained amount of digestion product was inserted in equation 3 yielding the absolute CatD activity in mU/ml

sample volume. The results are shown in Figure 8B and represent the mean of at least 3 different experiments.

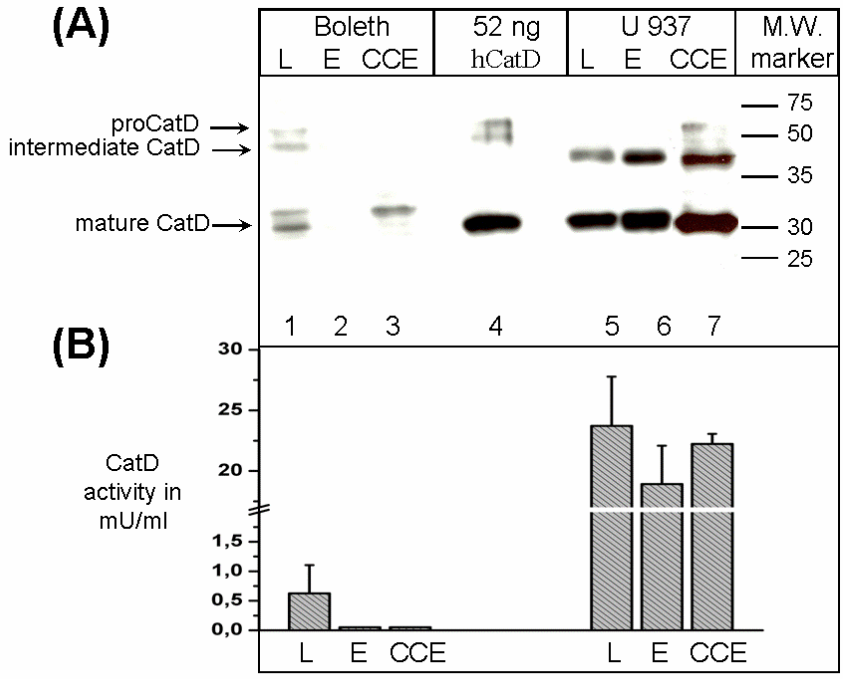

Figure 8 **(A)** Distribution of CatD in subcellular fractions of human EBV-transformed B cells and human monocytes (U937) detected by western blot analysis: 52 ng of hCatD was used as a positive control and shows a signal at 31 kDa (mature CatD) and at 51-55 kDa (proCatD). In all fractions of U937 and in the lysosomal fraction of Boleth cells the 31 kDa-mature CatD band is visible. The intermediate single chain form of CatD migrating at 44 kDa could only be detected in U937. **(B)** CatD activity in mU/ml as determined by the bead-assay using the calibration curve shown in figure 6 (L, lysosomal fraction; E, endosomal fraction; CCE, crude cell extract)

In the endosomal fraction and in the crude cell extract of the Boleth cell line no CatD activity could be detected. Only weak CatD activity was measured in the lysosomal fraction. These results concerning the distribution of CatD in subcellular compartments agree well with those obtained by western blot analysis.

As previously described the U937 cell line exhibits a higher CatD expression level [Greiner et al. 2003] corresponding to the results obtained with the digest & pull down CatD assay. We found an about 40-fold higher CatD activity in the fractions of the U937 cell line compared to the Boleth cell line. Another difference between these two cell lines is the intracellular distribution of CatD. The lysosomal fraction of U937 shows an about 20 % higher CatD activity than the endosomal fraction whereas CatD in the Boleth cell line could only be detected in the lysosomal fraction and not in endosomal fractions. Furthermore the crude cell extract of the U937 cell line

exhibits almost the same CatD activity as the lysosomal fraction of U937. These results suggest that CatD maybe only slightly enriched in lysosomal fractions and otherwise more ubiquitary distributed in the human monocyte cell line U937.

The developed digest & pull down assay proved to be suitable for determination of CatD activity in biological samples. The measured activity using substrate III is specific for CatD under the described conditions since there was no other cleavage site observed.

3.3 Discussion

This contribution describes a robust and specific method for the determination of CatD activity in biological samples. We present the solid-phase synthesis and *in vitro* digestion of biotinylated fluorescent CatD substrates and their application to a novel digest & pull down assay. The CatD digest & pull down assay presented here is based on the CatD-mediated cleavage of peptidic substrates bearing a fluorophore at their N-terminus and a biotin moiety at their C-terminus. The biotin tag and the fluorophore are separated upon digestion with CatD. Subsequent removal of all biotin-carrying peptides from the assay solution using streptavidin-coated magnetic beads leaves only digested fluorescent substrate in solution. From this amount of fluorescent peptide the enzymatic activity of CatD can easily be determined.

The digest & pull down assay offers several advantages over other state-of-the-art protease assays. Commercially available sensitive assays (Amersham Biosciences, Freiburg, Germany) are based on the application of substrates bearing two different fluorophores. The synthesis of such doubly-labelled fluorescent peptides goes beyond standard SPPS [Hoogerhout et al. 1999, Fischer et al. 2003]. Moreover many fluorescent dyes used for these substrates are reasonable expensive in milligram quantities which clearly limits their broad applicability in straightforward solid-phase synthesis, which routinely requires high molar excesses. The choice of the two fluorescent dyes for these substrates needs to be evaluated carefully since the two different fluorophores can either undergo FRET or quench each other significantly [Wei et al. 1994].

Another commercially available CatD assay (Molecular Probes, EnzChek™ protease assay kit, Leiden, the Netherlands) is based on casein derivatives that are labelled with many fluorescent dyes, resulting in almost total quenching of the

conjugate's fluorescence because of the high density of fluorophores within the casein protein. After cleavage of the fluorescent casein the quenching of the dyes is abolished and the net fluorescence increases significantly [Jones et al. 1997]. However, this system lacks specificity since there are lot of potential cleavage sites in casein for other proteases.

The presented digest & pull down assay proved to be more specific for CatD since substrate III was only cleaved between the two phenylalanine residues by reaction with the subcellular fractions. Another advantage of the digest & pull down assay over the assays using quenched peptide substrates is, that a change of the fluorescence signal can only result from cleavage of the substrate and not from conformational changes of the peptide backbone e.g. caused by binding to another protein contained in the sample.

In the digest & pull down assay described here, short incubation times were selected for a fast assay performance. In order to increase the assay's sensitivity longer incubation times may also be applied. The described synthesis of fluorescent peptide substrates is simple and can easily be transferred to peptide substrates of other proteases and would clearly extend the applicability of this digest & pull down assay. Moreover other pH-stable fluorescent dyes, such as rhodamine derivatives, may be used for N-terminal labelling of the protease substrates and thus increase the sensitivity of the digest & pull down assay due to higher quantum yields.

For technical applications and high-throughput screening the digest & pull down assay can be performed in 96-well plates. All steps including enzymatic hydrolysis, removal of biotinylated peptides using the streptavidin-coated magnetic beads and fluorescence measurements can be realised in parallel and performed in the 96-well plate format. This option underlines that the digest & pull down assay offers a fast alternative to other commercially available assays.

3.4 Supplemental data

3.4.1 Distribution of Cathepsin D in different human cells

The described digest and pull down assay was additionally applied to determine CatD activity in different human PBMCs (peripheral blood monocyte cells). Therefore human PBMCs were isolated from buffy coats of donor blood. Subpopulations of B-lymphocytes, monocytes, granulocytes, and T-cells were positively selected by

MACS technique (Miltenyi Biotec, Bergisch Gladbach, Germany) using CD 19, CD 14, CD 15 and CD 3 antibodies, respectively. Immature dendritic cells were generated from CD 14 positiv monocytes which have been isolated using Miltenyi Beads after culturing them in IL-4 and GM-CSF containing medium. The CD1c positive subform of dendritic cells was directly isolated from human blood. Dendritic cells were stimulated for 24 h with lipopolysacharid (LPS), interferon γ (IFNγ) and tumor necrosis factor α (TNF-α).

Table 4 CatD Activities in endocytic compartments of different human blood cells.

subpopulation	turnover in pmol per minute
CD 19	1.75
CD 14	3.02
CD 15	0.44 ± 0.03
CD3	3.32 ± 0.28
DC unstimulated	0.99 ± 1.63
DC + LPS	2.80 ± 0.90
DC + TNFα	2.83 ± 0.47
DC + IFN	1.64 ± 0.33

[a] CatD activities were determined using 0.01 µg substrate III using 1 µg total protein per cell lysat. The reaction was carried out in 50 mM glycine/HCl buffer pH 3.5 supplemented with 500 mM EDTA, 100 µg/µl leupeptin and 2 mM PMSF (phenylmethylsulfonylfluoride) for 15 min.

To determine cathepsin D activity in samples where only a very low amount of material is available we analyzed the hydrolysis products by using microbore RP-HPLC with fluorescence detection. We have been able to measure cathepsin D in endocytotic compartments of different human blood cell subpopulations (table 2). Endocytic compartments of granulocytes (CD 15) show the smallest amount of cathepsin D compared to B-lymphocytes (CD 19), monocytes (CD 14), T-cells (CD 3) and dendritic cells (DC). The highest cathepsin D activities were measured in monocytes and T-cells and are comparable to each other. As previously described [Fiebiger et al. 2001] cathepsin D is important for processing of antigens in professional antigen-presenting cells (APC) such as DCs. Thus the amount of cathepsin D in endocytic compartments of dendritic cells was determined.

We stimulated dendritic cells with LPS, TNF-α and IFN-γ and determined the cathepsin D activities. Stimulated (mature) DCs showed the same cathepsin D activity as unstimulated (immature) DCs. These results are in good agreement with published data from Trombetta et al. 2003.

Further the activity of CatD in lysosomes from resting vs. IFN-γ-stimulated microglia as well as astrocytes as a control was tested. CatD showed little variability in the presence/absence of IFN-γ both in microglia and astrocytes (Fig. 9).

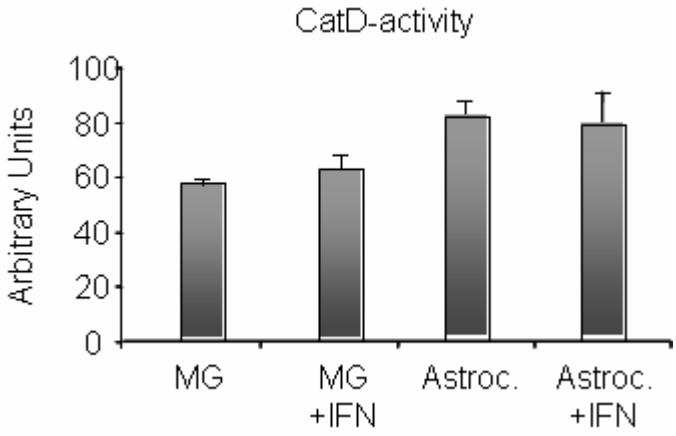

Figure 9 Lysosomal extracts from resting vs. IFN-γ-stimulated microglia (MG) was assessed for CatD activity. Astrocytes (Astroc.) served as controls and CatD activities are expressed in arbitrary units. Mean values and standard deviation of triplicate samples are presented (from: Burster et al., 2005).

4 Cathepsin D in human eccrine sweat

4.1 Intention

The protein pattern of healthy human eccrine sweat was investigated and 10 major proteins were detected from which apolipoprotein D, lipophilin B and cathepsin D (CatD) were identified for the first time in human eccrine sweat. We focused in our studies on the function of the aspartate protease CatD in sweat. *In vitro* digestion experiments using a specific fluorescent CatD substrate showed that CatD is enzymatically active in human sweat. To identify potential substrates of CatD in human eccrine sweat, LL-37 and DCD-1L, two antimicrobial peptides present in sweat, were digested *in vitro* with purified CatD. LL-37 was not significantly digested by CatD whereas DCD-1L was cleaved between ^{44}L and ^{45}D and between ^{29}L and ^{30}E almost completely. The DCD-1L derived peptides generated *in vitro* by CatD were also found *in vivo* in human sweat as determined by surface-enhanced laser desorption/ionization (SELDI) mass spectrometry. Furthermore, besides the CatD processed peptides we identified additionally DCD-1L derived peptides which are generated upon cleavage with a 1,10-phenanthroline sensitive carboxypeptidase and an endoprotease. Taken together proteolytic processing generates 12 DCD-1L derived peptides. To elucidate the functional significance of postsecretory processing the antimicrobial activity of three CatD processed DCD-1L peptides was tested. Whereas two of these peptides showed no activity against gram-positive and gram-negative bacteria, one DCD-1L derived peptide showed an even higher activity against these microorganisms than DCD-1L. Functional analysis indicated that proteolytic processing of DCD-1L by CatD in human sweat modulates the innate immune defense of human skin.

Human skin serves as a first line of defense against potential pathogens by building a mechanical barrier. In addition to physical mechanisms, the epithelia of mammalian skin produce antimicrobial peptides such as cathelicidins [Zanetti et al. 1995, Nizet et al. 2001] and β-defensins [Harder et al. 1997, Ali et al. 2001] or small proteins, such as the recently described 11 kDa S100 protein psoriasin [Glaser et al. 2005]. Cathelicidins and β-defensins share properties concerning their biosynthesis as proforms, which are subsequently processed into mature peptides [Zanetti et al. 1995, Daher et al. 1988, Valore & Ganz 1992]. During inflammatory conditions such

as wound healing [Frohm et al. 1997] or psoriasis [Ong et al. 2002] the expression, processing and secretion of the antimicrobial peptides LL-37 [Murakami et al. 2002] and β-defensin 1 and 2 [Ali et al. 2001] are increased. As part of the innate defense of human skin the antimicrobial peptide dermcidin (DCD) is constitutively expressed in eccrine sweat glands, secreted into sweat [Rieg et al. 2004] and present on the skin surface at an average concentration of 1 to 10 µg/ml [Schittek et al. 2001]. In human sweat the 110 amino acid dermcidin-proform is first processed to the 48 amino acid peptide DCD-1L. Subsequently DCD-1L is further C-terminally processed by a yet unidentified carboxypeptidase [Flad et al. 2002, Rieg et al. 2005].

The sole human cathelicidin hCAP-18 is extracellularly processed by proteinase 3 [Sorensen et al. 2001] to an active 37 amino acid peptide named LL-37 which is found in sweat at an average concentration of 0.013 µM [Lopez-Garcia et al. 2005]. After secretion LL-37 undergoes further enzymatic processing by an unidentified serine protease yielding 3 peptides which enhances the antimicrobial activity of LL-37 itself [Murakami et al. 2004].

Beside these antimicrobial peptides and proteins the surface of human skin provides other proteins such as human serum albumin [Nakayashiki 1990], cytokeratin I [Langbein et al. 2005], Zn-α-2-glycoprotein [Tada et al. 1991], prolactin-inducible protein [Myal et al. 1991] and cystatin A [Zeeuwen et al. 2001, Zeeuwen et al. 2002]. Additionally certain proteases have been described in human sweat such as gelatinolytic and caseinolytic proteases [Horie et al. 1986], cathepsin B- and H-like cysteine proteases [Yokozeki et al. 1987], human stratum corneum chymotryptic enzyme [Kishi et al. 2004] and tissue kallikrein and kininase II [Hibino et al. 1994]. In general, the physiological function of these proteins and proteases as well as their significance for the immunity of the skin and their interaction with other sweat components, especially with antimicrobial peptides, still remains to be determined.

This contribution presents an overview of the major proteins in human eccrine sweat involving 10 dominant proteins. 7 out of these proteins have already been described in sweat glands, in sweat or to be secreted by keratinocytes. For the first time apolipoprotein D, lipophilin B and CatD (EC 3.4.23.5) were detected and identified in human eccrine sweat.

Furthermore our data show, that CatD takes part in the postsecretory processing of the antimicrobial peptide DCD-1L. During these *in vitro* and *in vivo* studies we

observed two other yet unidentified protease avtivities: a 1,10-phenanthroline sensitive carboxypeptidase and an endoprotease which in combination with CatD are responsible for the degradation of DCD-1L in sweat yielding 12 DCD-1L derived peptides. The antimicrobial activity of three CatD processed DCD-1L peptides was tested. Whereas two of these peptides showed no activity against gram-positive and gram-negative bacteria, one DCD-peptide showed a higher activity against these microorganisms. These data indicate that by postsecretory proteolytic processing the antimicrobial activity of DCD-1L is modulated and therefore the immune defense on the skin surface.

4.2 Results

4.2.1 Identification of dominant proteins in human eccrine sweat

In order to identify dominant proteins in human eccrine sweat standard proteomic techniques were applied. In a first step female and male human eccrine sweat samples were separated by SDS-PAGE and proteins were stained using Simply Blue™ Safe Stain (Fig. 10A). Major protein bands were then excised and digested in-gel with trypsin. Resulting tryptic peptides were analyzed by MALDI-Re-TOF-MS and LC-ESI-MS/MS, respectively. Altogether 10 dominant proteins were identified by peptide mass fingerprinting and are listed in Figure 10B.

We identified human serum albumin (band at 65 kDa) and the antimicrobial peptide DCD-1L (bands at 4 kDa) which both have already been described in sweat [Nakayashiki 1990, Schittek et al. 2001]. Cytokeratin I (19; 53 kDa) as well as Zn-α-2-glycoprotein [Tada et al. 1991](38 kDa) and cystatin A [Zeeuwen et al. 2001, Zeeuwen 2002](12 kDa) have been described to be present in the duct and secretory coil of sweat glands. Myal *et al.* showed that the prolactin-inducible protein (15 kDa) is present in sweat glands [Myal et al. 1991]. Psoriasin has been recently identified in keratinocytes [Glaser et al. 2005]. Since psoriasin is secreted by keratinocytes in large amounts onto the skin surface it is not surprising that we identified this protein also in human sweat. Besides these proteins already described to be present in sweat glands or sweat we identified for the first time in eccrine sweat apolipoprotein D, lipophilin B and CatD.

A)

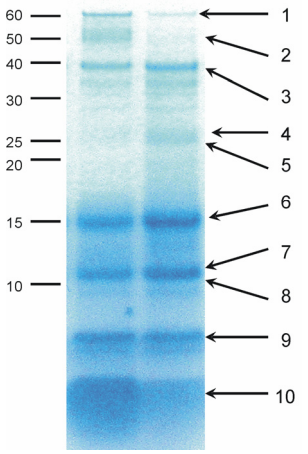

B)

No.	identified protein	primary accession number	probability based mowse score+	aa lenghth	M.W. (Da)	origin	reference
1	human serum albumin	P02768	81	609	69366	sweat	Nakayashiki, 1990 (18)
2	cytokeratin I	P04264	54	643	65886	duct and secretory coil of sweat glands	Langbein *et al*, 2005 (19)
3	Zn-α-2-glycoprotein	P25311	71	295	33872	secretory potion of sweat glands	Tada *et al*, 1991 (20)
4	apolipoprotein D	P05090	61	189	21275	various human tissues	-
5	cathepsin D β-chain	P07339 E.C. 3.4.23.5	82	241	26229	-	-
6	prolactin-inducible protein	P12273	77	146	16572	sweat glands	Myal *et al*, 1991 (21)
7	psoriasin S100 calcium-binding protein A7	P31151	132*	100	11326	keratinocytes	Glaser *et al*, 2004 (5)
8	cystatin A	P01040	157*	98	11006	secretory coil of sweat glands	Zeeuwen *et al*, 2001 (22) Zeeuwen *et al*, 2002 (23)
9	lipophilin B	O95969	109*	90	9925	Endocrine-responsive tissues	-
10	DCD-1L and DCD-1L derived peptides	P81605	70*	48	4819	sweat glands and sweat	Schittek *et al*, 2001 (12)

+protein scores greater than 63 are significant ($p<0.05$)

Figure 10 **A)** 15% SDS-PAGE of 100 µl desalted and concentrated female and male sweat samples. Proteins were stained using Simply Blue™ Safe Stain. **B)** Proteins identified in human eccrine sweat as determined by in-gel tryptic digestion followed by mass spectrometry analysis. In certain cases (*) data were additionally obtained by automated LC-ESI-MS/MS analysis. All MS data were analyzed using Mascot Sequence Query at www.matrixscience.de for probability based peptide identification.

4.2.2 The active β-chain of cathepsin D is present in human eccrine sweat

We identified for the first time the β-chain of the aspartate protease CatD in human eccrine sweat. The results obtained with tryptic fingerprint analysis were proven by Western blot analysis of male (two individuals), female (two individuals) and pooled human eccrine sweat. Purified human CatD was used as a positive control. Both forms, the active β-chain of CatD (31 kDa) as well as the proform (56 kDa) could be detected in eccrine sweat, the latter in lower amounts (Fig. 11). We did not observe any significant differences between male and female sweat.

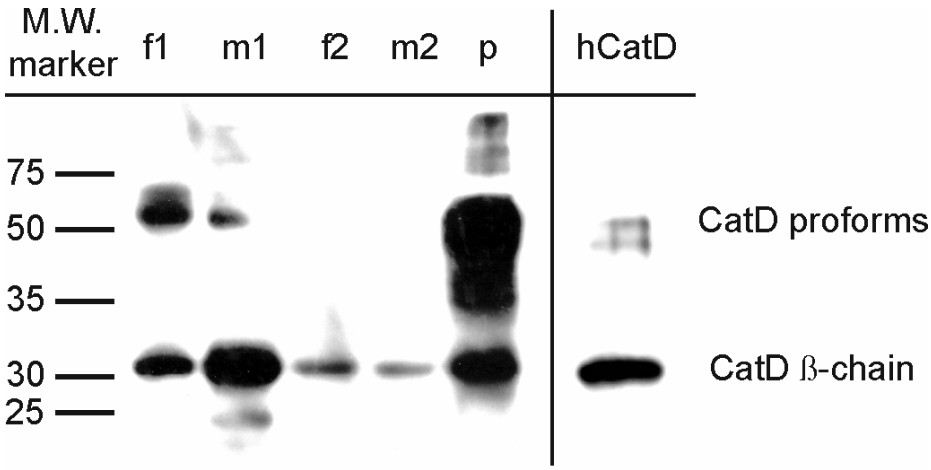

Figure 11 Western blot analysis of 16 µl female (f1 and f2), male (m1 and m2) and pooled (p) human eccrine sweat. Polyclonal rabbit anti-human CatD was used as primary antibody and horseradish peroxidase-conjugated goat anti-rabbit IgG as secondary antibody. Purified human cathepsin D (human liver) served as control and shows a major band at 31 kDa (enzymatically active β-chain) and weaker bands at 50 kDa representing several proforms.

Next, we investigated if the β-chain of CatD is enzymatically active in sweat by performing *in vitro* digestion experiments using a specific fluorescent CatD substrate as we reported previously [Baechle et al. 2005]. The substrate was incubated for 30 min with purified CatD or pooled sweat, respectively. Digestion products were then separated using analytical RP-HPLC with fluorescence detection (Fig. 12). CatD cleaves the substrate Amca-EEKPISFFRLGK specifically between the two phenylalanine residues yielding the two peptides Amca-EEKPISF and FRLGK. Only the first peptide can be detected using fluorescence detection. The amount of generated fluorescent Amca-EEKPISF is proportional to the CatD activity. Figure 12A shows the undigested CatD substrate with a retention time of 21.7 min. Figure 12B shows the digestion product Amca-EEKPISF eluting at 20.6 min after digestion with purified CatD. In Figure 12C the same sample was measured in presence of the metalloprotease inhibitor 1,10-phenanthroline (peak at 11.6 min). The peak areas of Amca-EEKPISF in chromatogram B and C are comparable indicating that the inhibitor 1,10-phenanthroline has no influence on CatD activity.

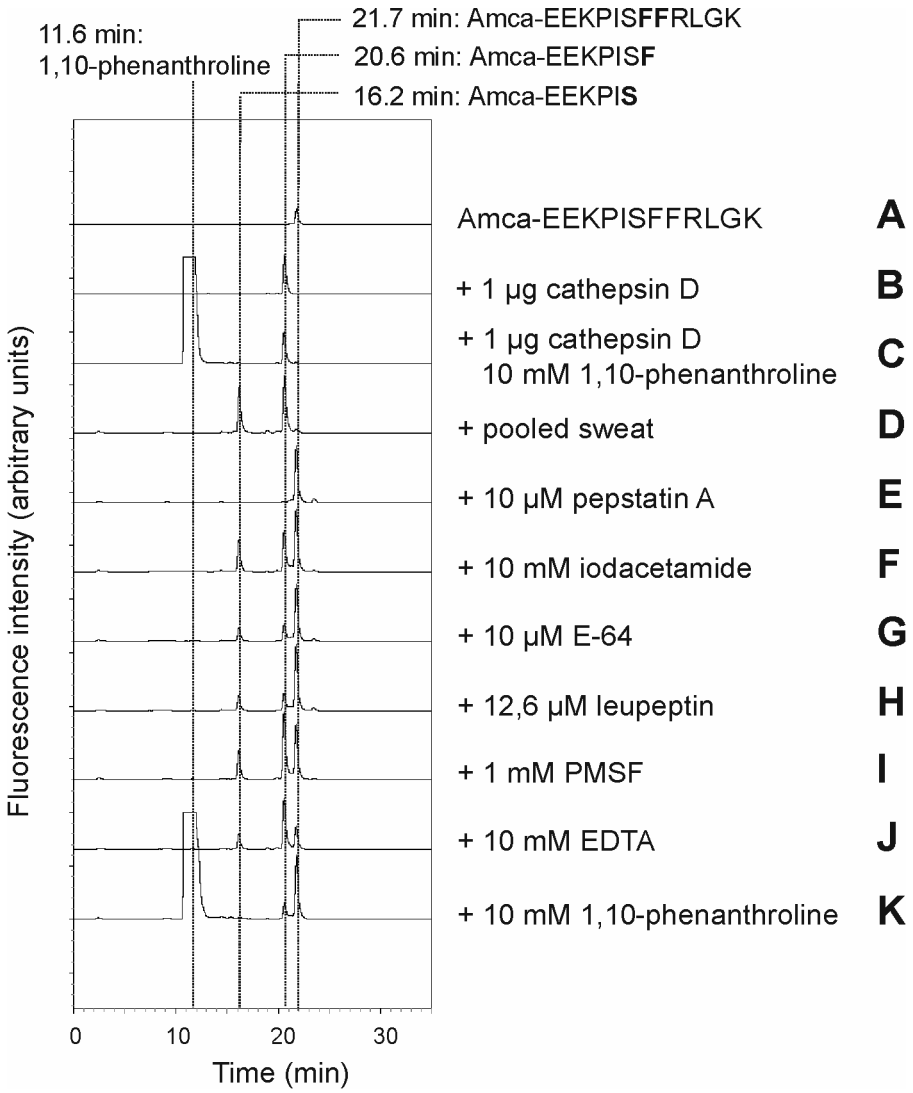

Figure 12 The CatD substrate Amca-EEKPISFFRLGK was incubated with CatD (B), without CatD (A), with CatD and the aspartate protease inhibitor pepstain A (C) and with CatD and 1,10-phenanthroline. The substrate further was incubated with pooled sweat (D) and with pooled sweat in the presence of pepstatin A (E), iodacetamide (F), E-64 (G), leupeptin (H), PMSF (I), EDTA (J) and 1,10-phenanthroline (K). Digestion products were then separated using RP-HPLC with fluorescence detection (λ_{ex}=350 nm; λ_{em}=450 nm).

After incubation of the substrate with pooled human eccrine sweat Amca-EEKPISF was generated according to the specificity of CatD (Fig. 12D). This cleavage site could be completely inhibited with the aspartate protease inhibitor pepstatin A (Fig. 12E), but not with iodacetamide and E-64 (inhibitors for cysteine proteases, Fig. 12F and Fig. 12G), leupeptin and PMSF (inhibitors for serine proteases, Fig. 12H and Fig. 12I) or EDTA and 1,10-phenanthroline (inhibitors for metalloproteases, Fig. 12J and Fig. 12K). These data show, that digestion between

the phenylalanine residues is caused by CatD and consequentially that CatD is present in its enzymatically active form in human eccrine sweat.

4.2.3 A 1,10-phenanthroline sensitive carboxypeptidase is present in human eccrine sweat

The CatD-substrate is additionally cleaved between serine and phenylalanine when incubated with sweat yielding Amca-EEKPIS which has a retention time of 16.2 min. This finding indicates that another protease is present in sweat. Its activity could be completely and specifically inhibited with 1,10-phenanthroline (Fig. 12K) showing that the protease is presumably a Zn^{2+}-metalloprotease as the common metalloprotease inhibitor EDTA had no effect on the activity (Fig. 12J). Surprisingly pepstatin A inhibited both, CatD and the observed cleavage between serine and phenylalanine (Fig. 12E). This finding show, that the 1,10-phenanthroline sensitive protease cannot cleave the intact substrate until CatD has digested the substrate. This suggests that the carboxypeptidase could not cleave the basic amino acid lysine but the hydrophobic amino acid phenylalanine.

To verify this hypothesis the substrate was incubated longer in order to achieve additional digestion products which are not generated within 30 min. After 1 h over 95% of the substrate was cleaved and digestion products were then identified using UV-detection and MALDI-MS (data not shown). The peptides Amca-EEKPISF and the corresponding peptide FRLGK are initially generated by CatD. Subsequently the C-terminally trimmed peptides Amca-EEKPIS, Amca-EEKPI and Amca-EEKP are generated but not the corresponding peptides FFRLGK, SFFRLGK and ISFFRLGK as would be required for the cleavage by an endopeptidase. These findings show that the responsible protease is a carboxypeptidase.

The intact CatD substrate (lysine at its C-terminus) and Amca-EEKP are not C-terminally trimmed showing that the 1,10-phenanthroline sensitive protease is a carboxypeptidase which releases C-terminal amino acids such as phenylalanine, serine and isoleucine but not lysine and proline.

Our results show that the β-chain of CatD as well as a 1,10-phenanthroline sensitive metalloprotease with carboxypeptidase activity are present in their active forms in human eccrine sweat.

4.2.4 In vitro digestion of the antimicrobial peptides LL-37 and DCD-1L with cathepsin D

Next we investigated whether CatD is able to cleave peptides present in sweat. Therefore we incubated the antimicrobial peptides DCD-1L and LL-37 with purified CatD and digestion products were then analyzed using RP-HPLC (Fig. 13) followed by MALDI-MS of the single fractions (Table 5). These *in vitro* digestion experiments were performed in CatD-buffer (Fig. 13A) and in sweat buffer (Fig. 13B). There were no differences for CatD activity detectable between these buffer systems. In both buffer systems CatD could be completely inhibited with pepstatin A showing that the detected digestion products are exclusively generated by CatD.

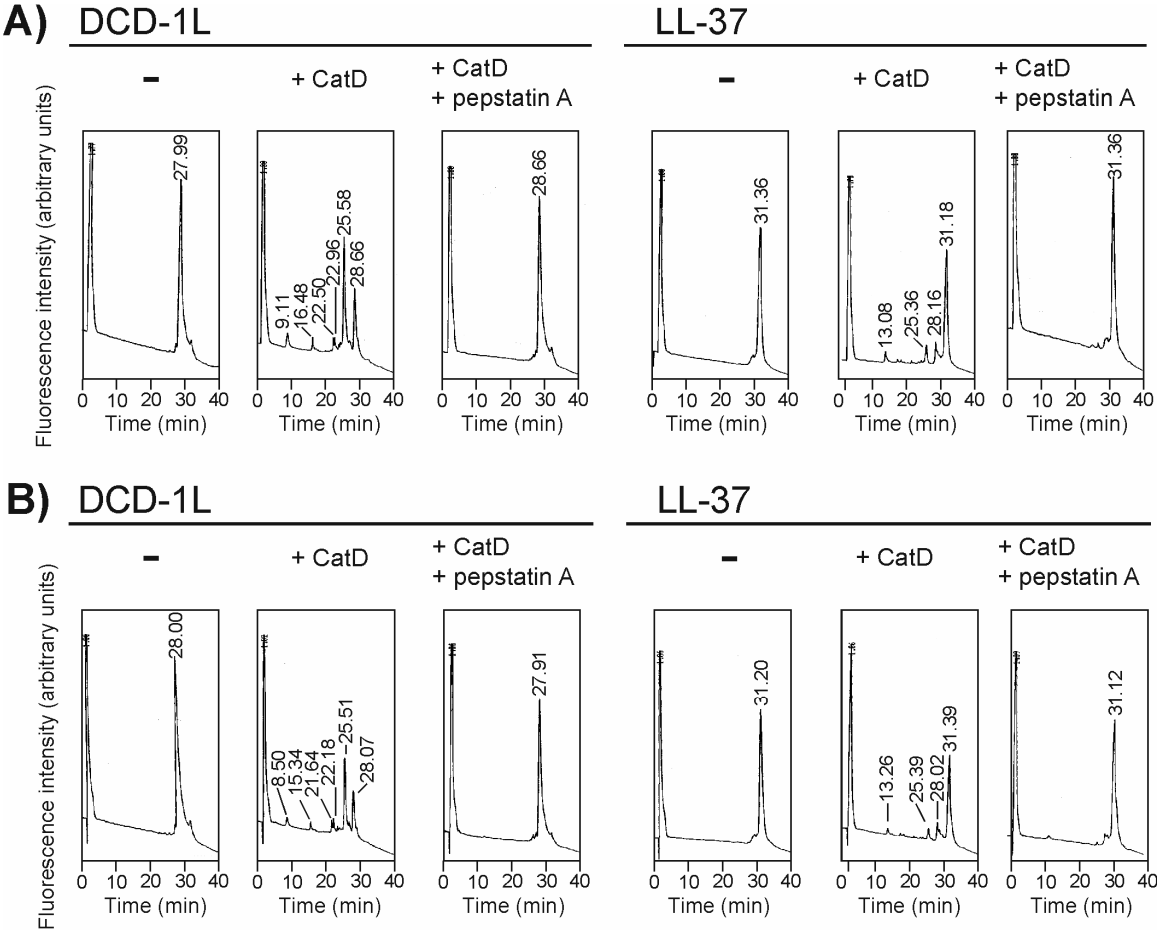

Figure 13 *In vitro* digestion of synthetic DCD-1L and LL-37 with CatD in 50 mM Gly/HCl buffer pH 3.5 (A) and in sweat buffer pH 5.5 (B). Digestion products were separated using RP-HPLC with UV-detection at 214 nm. Peaks then were collected and peptides were analyzed using MALDI-MS and Edman microsequencing (see Table 5).

DCD-1L (28.66 min) was cleaved by CatD dominantly between ^{44}L and ^{45}D yielding SSL-44 (25.58 min) and the tetrapeptide DSVL (9.11 min) and to a lower amount between ^{29}L and ^{30}E leading to the peptides SSL-29 (22.96 min) and the corresponding peptides ESV-19 (22.50 min) and ESV-15 (16.48 min), respectively. These cleavage sites agree well with the specificity of CatD, which preferably cleaves proteins and peptides with leucine or an aromatic amino acid residue in P1 position [van Noort & van der Drift 1989].

LL-37 (31.18 min) was also digested with purified CatD but only weak cleavage was observed between ^{5}F and ^{6}F yielding FRK-32 (28.16 min) and between ^{27}F and ^{28}L yielding LRN-10 (13.08 min) and LLG-27 (25.36 min). Taken together, DCD-1L proved to be a good substrate for CatD (more than 60 % degradation) whereas LL-37 is barely digested by CatD (less than 20 % degradation) under the same experimental conditions. These results agree well with recently published data, stating that LL-37 is processed by a serine protease and not by an aspartate protease like CatD [Murakami et al. 2004].

Table 5 Identified peptides after *in vitro* digestion of DCD-1L and LL-37 with cathepsin D as determined by MALDI-MS and Edman microsequencing. Retention times allude to those in figure 14.

name	DCD-1L	expected $[M+H]^+$	found $[M+H]^+$	Edman sequencing	retention time (min)
	1 11 21 31 41				
DCD-1L	SSLLEKGLDG AKKAVGGLGK LGKDAVEDLE SVGKGAVHDV KDVLDSVL	4819.5	4819.3		28.66
SSL-29	SSLLEKGLDG AKKAVGGLGK LGKDAVEDL	2870.3	2870.5	SSLLEKG	22.96
ESV-19	E SVGKGAVHDV KDVLDSVL	1968.2	1966.8	ESVGKGA	22.50
SSL-44	SSLLEKGLDG AKKAVGGLGK LGKDAVEDLE SVGKGAVHDV KDVL	4405.0	4403.6	SSLLEKG	25.58
DSVL	DSVL	433.5	n.f.	DSVL	9.11
ESV-15	E SVGKGAVHDV KDVL	1553.8	1553.6	ESVGKGA	16.48
name	**LL-37**				
	1 11 21 31				
LL-37	LLGDFFRKSK EKIGKEFKRI VQRIKDFLRN LVPRTES	4494.3	4485.2		31.39
LRN-10	LRN LVPRTES	1185.4	1185.3	LRNLVPR	13.26
LLG-27	LLGDFFRKSK EKIGKEFKRI VQRIKDF	3328.0	3327.0	LLGDFFK	25.39
LLG-5	LLGDF	564.7	n.f.	n.f.	n.f.
FRK-32	FRKSK EKIGKEFKRI VQRIKDFLRN LVPRTES	3948.7	3948.3	FRKSKEK	28.02

n.f. = not found

Since CatD shows almost no reaction with LL-37 further studies concerning the function of CatD in human eccrine sweat focused on DCD-1L. The CatD generated DCD-1L derived peptides as well as intact DCD-1L are further processed by the above described 1,10-phenanthroline sensitive carboxypeptidase causing a successive release of C-terminal amino acids. As a consequence of these *in vitro* results, *in vivo* investigations were made to find out if one or more of these predicted

peptides upon cleavage with CatD and/or the carboxypeptidase are present in human eccrine sweat.

4.2.5 In vivo detection of DCD-1L derived peptides in human eccrine sweat

The following DCD-1L derived peptides were found after *in vitro* digestion of DCD-1L with CatD: SSL-29, SSL-44, ESV-19, ESV 15 and DSVL (Table 5). These DCD-1L derived peptides could be further processed by the carboxypeptidase and lack one or more C-terminal amino acids leading to a bigger set of predicted DCD-1L derived peptides. Now we investigated if one or more of these DCD-1L peptides are present in human eccrine sweat. For their detection, sweat samples of 18 healthy individuals were applied to SELDI Protein Chip® Technology using reversed-phase (H4) chips. Figure 14 shows a representative SELDI-spectrum of sweat in the mass range between 2000 Da and 5000 Da. The expected and found molecular masses are assigned to the different processed DCD-1L derived peptides seen in the SELDI-spectrum and are listed in Table 6.

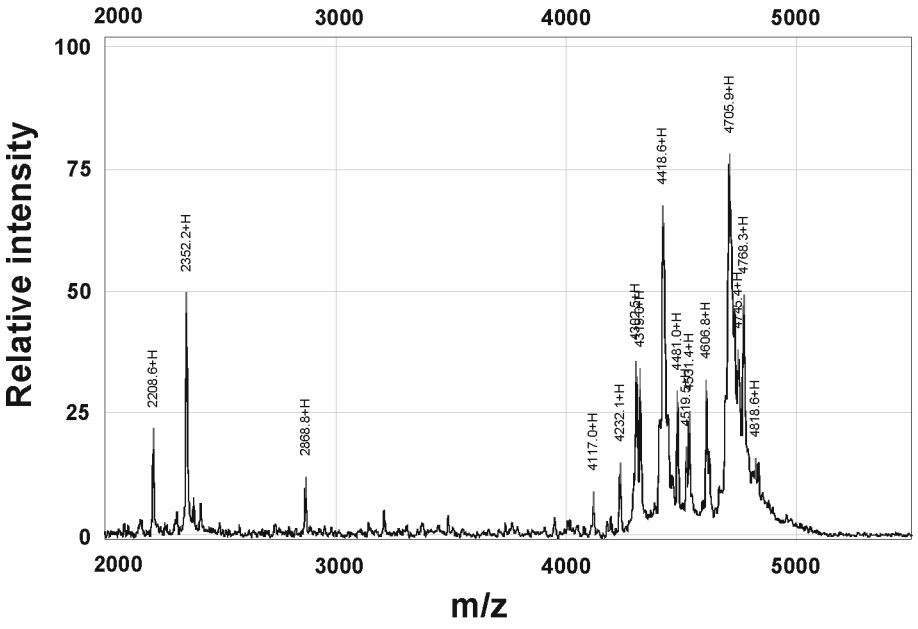

Figure 14 *In vivo* detection of DCD-1L derived peptides in human eccrine sweat using SELDI protein chip® technology. 1 µl sweat was diluted into 2 µl binding buffer (50 mM sodium phosphate pH 6.5) and applied to a reversed phase (H4) chip surface for 30 min in a humid chamber. After washing three times with binding buffer and a final water wash, peptide masses then were read directly from the array surface using a ProteinChip reader.

Altogether we identified 12 DCD-1L derived peptides in sweat in agreement with recently published data [Rieg et al. 2005]. The DCD-1L peptides in sweat agree well with our *in vitro* prediction for the processing of DCD-1L. In addition, peptides lacking of the N-terminal tripeptide SSL have been identified. Further enzymatically specification of postsecretory processing was achieved by kinetic measurements.

Table 6 DCD-1L derived peptides present in human eccrine sweat and their theoretical isoelectric points (pI's). Asterisks (*) indicate the DCD-1L derived peptides generated upon cleavage with cathepsin D.

name	DCD-1L derived peptides	expected mass (Da)	found mass (Da)	theoretical pI
	1 11 21 31 41			
DCD-1L	SSLLEKGLDG AKKAVGGLGK LGKDAVEDLE SVGKGAVHDV KDVLDSVL	4818.5	4818.6	5.07
DCD-1	SSLLEKGLDG AKKAVGGLGK LGKDAVEDLE SVGKGAVHDV KDVLDSV	4705.3	4705.9	5.07
SSL-46	SSLLEKGLDG AKKAVGGLGK LGKDAVEDLE SVGKGAVHDV KDVLDS	4606.2	4606.8	5.07
SSL-45	SSLLEKGLDG AKKAVGGLGK LGKDAVEDLE SVGKGAVHDV KDVLD	4519.1	4519.5	5.15
LEK-45	LEKGLDG AKKAVGGLGK LGKDAVEDLE SVGKGAVHDV KDVLDSVL	4531.2	4531.4	5.08
LEK-44	LEKGLDG AKKAVGGLGK LGKDAVEDLE SVGKGAVHDV KDVLDSV	4418.0	4418.6	5.08
LEK-43	LEKGLDG AKKAVGGLGK LGKDAVEDLE SVGKGAVHDV KDVLDS	4318.9	4319.0	5.08
LEK-42	LEKGLDG AKKAVGGLGK LGKDAVEDLE SVGKGAVHDV KDVLD	4231.8	4232.1	5.15
LEK-41	LEKGLDG AKKAVGGLGK LGKDAVEDLE SVGKGAVHDV KDVL	4116.7	4117.0	5.62
SSL-29*	SSLLEKGLDG AKKAVGGLGK LGKDAVEDL	2869.3	2868.8	5.97
LEK-24*	LEKGLDG AKKAVGGLGK LGKDAVE	2353.7	2352.2	8.38
SSL-25*	SSLLEKGLDG AKKAVGGLGK LGKDA	2412.8	2412.8	9.40
LEK-26*	LEKGLDG AKKAVGGLGK LGKDAVEDL	2582.0	2582.5	6.24

4.2.6 Temporal order of the postsecretory processing

Sweat was analyzed at various time points after secretion using SELDI-MS to elucidate the temporal order of the postsecretory processing steps. Initially the 48 amino acid peptide DCD-1L is processed from its C-terminus into the peptide DCD-1 agreeing with our *in vitro* results that a carboxypeptidase is active in human sweat. This initial processing step starts immediately after secretion of DCD-1L into sweat and therefore is experimental difficult to detect. Since harvesting measurable amounts of sweat takes time the initial processing steps are barely detectable. To solve this problem synthetic DCD-1L was spiked to sweat so that the initial cleavage steps could be analyzed in detail. The resulting enzyme-substrate ratio decelerated the reaction so that longer incubation was needed. After cleavage of C-terminal leucine the peptide DCD-1 (4705.3 Da) is further C-terminally processed into SSL-46 (4606.2 Da). This processing step occurs simultaneously to the N-terminal cleavage of SSL since the peptide LEK-44 (4418.0 Da) arises at about the same time (Fig. 15).

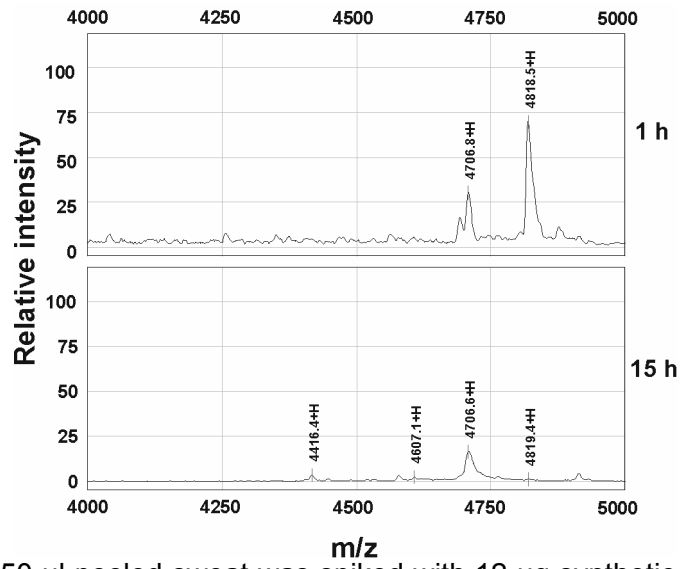

Figure 15 50 µl pooled sweat was spiked with 12 µg synthetic DCD-1L and analyzed by SELDI protein chip® technology after 1 h (upper lane) and 15 h (lower lane) at 37 °C.

Figure 16 shows an example for the temporal order of one particular sweat sample whereas the initial processing step into DCD-1 is not apparent for the above-described reason so the time point “0 min” indicates the time point when the sweat sample was thawed and set at 37 °C to start the kinetic measurement.

After the carboxypeptidase has processed DCD-1L into DCD-1 the next processing step is further C-terminal trimming in parallel with N-terminal cleavage of the tripeptide SSL by an endoprotease. This processing step generates the peptides LEK-45, LEK-44, LEK-43, LEK-42 and LEK-41 (Fig. 16, first 4 spectra).

Cleavage between ^{44}L and ^{45}D can be performed by CatD as well as by subsequent cleavage of four C-terminal amino acids by the carboxypeptidase. We wanted to find out which of the two proteases is mainly responsible for this processing step. Therefore we synthesized the peptide ESV-17 which represents the C-terminus of DCD-1L lacking the last C-terminal amino acids leucine and valine. ESV-17 showed no reaction with purified CatD *in vitro* (data not shown) indicating that the two amino acids are essential for the cleavage by CatD. This finding shows that the C-terminus of DCD-1L is dominantly processed by the carboxypeptidase.

In a third processing step the previously generated peptides are cleaved between ^{29}L and ^{30}E by CatD obtaining the peptides LEK-26 and SSL-29 (Figure 16, last 2 spectra). The two peptides can be generated from all present DCD-1L derived peptides in sweat differing only in their N-terminal sequence.

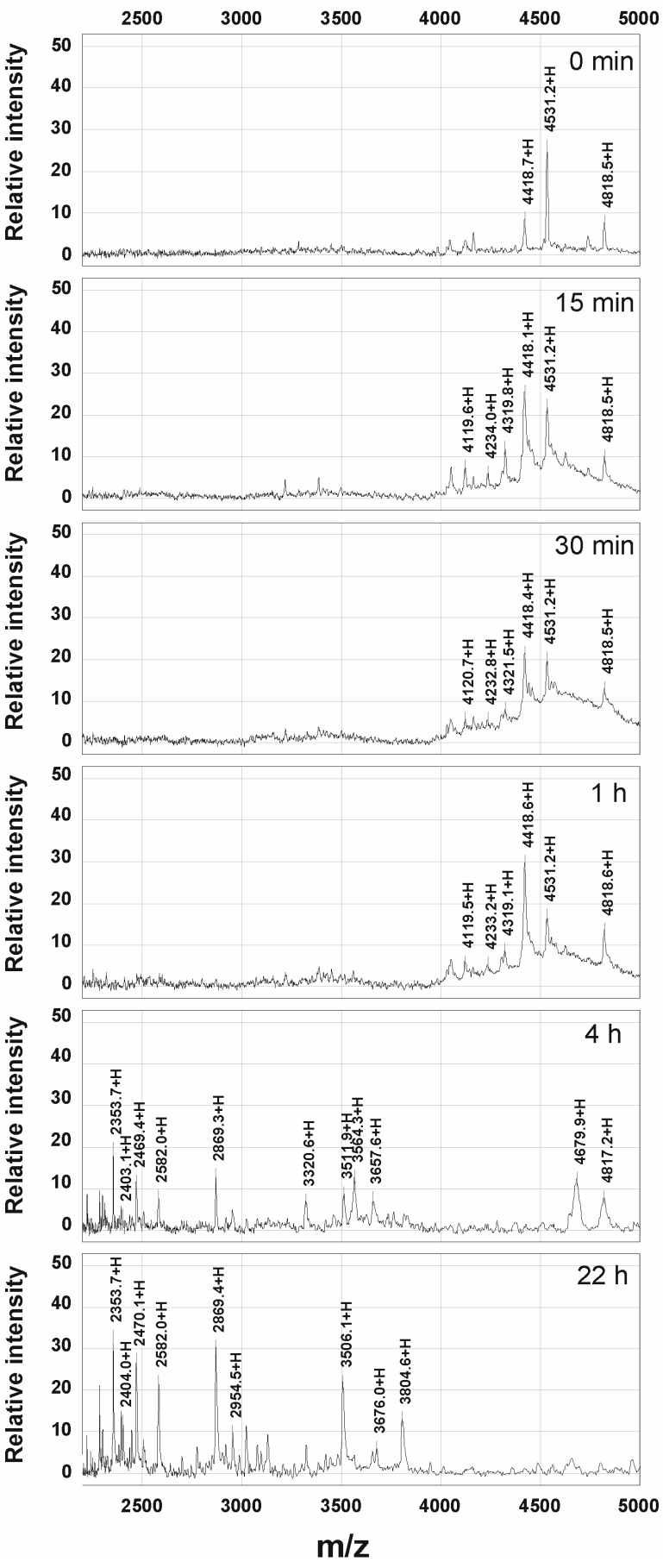

Figure 16 SELDI spectra of sweat after the indicated incubation times at 37 °C.

The final processing step consists of two reactions which occur in parallel. One reaction is the successive cleavage of the C-terminal amino acids leucine and aspartic acid of LEK-26 yielding LEK-24 which is stable against further proteolytic breakdown. The other reaction is the conversion of SSL-29 into SSL-25. Since the intermediate peptides SSL-28, SSL-27 and SSL-26 could not be detected it remains unclear whether this proteolytic degradation is also caused by the 1,10-phenanthroline sensitive carboxypeptidase or by another endoprotease. The peptide SSL-25 undergoes no further enzymatic degradation.

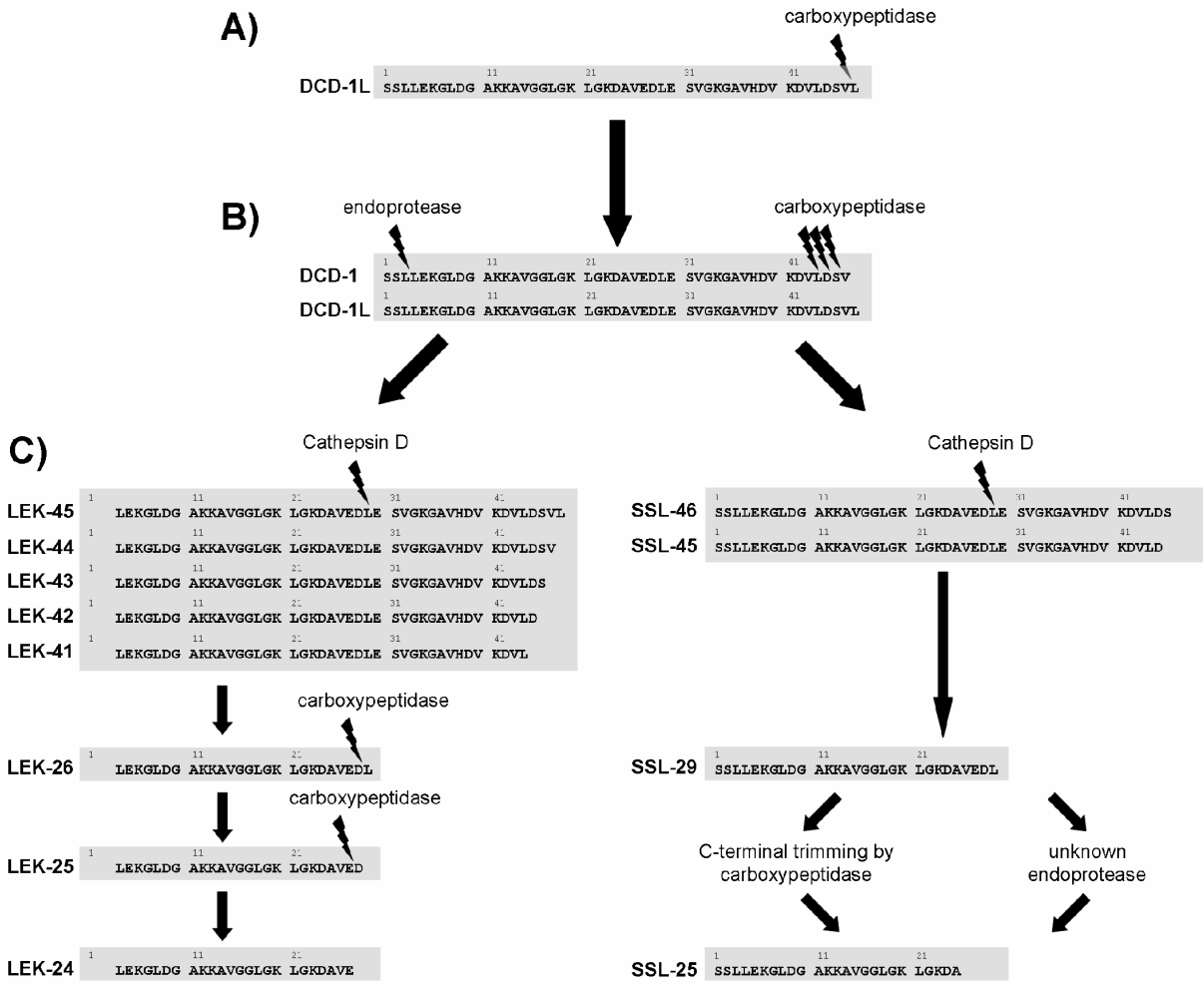

Figure 17 Temporal order of the postsecretory processing of DCD-1L in sweat. The initial processing step is the cleavage of the C-terminal amino acid leucine by a 1,10-phenanthroline sensitive carboxypeptidase (A). The second processing step is the cleavage between ^{3}L and ^{4}L by an unidentified endoprotease simultaneously to further C-terminal trimming steps (B). The generated DCD-1L derived peptides are finally digested by CatD yielding LEK-26 and SSL-29 which are processed to LEK-24 and SSL-25, respectively (C).

Single processing steps are summarized in Figure 17 considering data of various sweat samples and not only those representatively shown in Figure 15 and Figure 16, respectively. First DCD-1L is converted to DCD-1 by the 1,10-phenanthroline sensitive carboxypeptidase (Fig. 17A). In a next step DCD-1 undergoes further C-terminal trimming simultaneously to the cleavage of the N-terminal tripeptide SSL by an endoprotease (Fig. 17B). Since no aminopeptidase activity was detectable using the specific substrate H-Leu-AMC (data not shown) this processing step is caused by an endoprotease and not by an aminopeptidase. The third processing step is the cleavage between ^{29}L and ^{30}E by CatD obtaining the peptides LEK-26 and SSL-29 which are further processed to the proteolytical stable peptides LEK-24 and SSL-25 (Fig. 17C).

4.2.7 Antimicrobial activity of the DCD-1L derived peptides

Antimicrobial peptides such as LL-37 and DCD-1L play an important part in establishing a skin defense barrier against microbes and should be considered as an integral part of the innate immune system [Murakami et al. 2002, Schittek et al. 2001, Murakami et al. 2004]. Therefore the effect of the postsecretory processing on the antimicrobial activity of DCD-1L and DCD-1L derived peptides was investigated.

The above-described postsecretory processing leads to the proteolytic stable peptides LEK-24 and SSL-25 which differ from all other DCD-1L derived peptides since they are cationic (for pI values see Table 6, last column). Therefore further studies focused on these peptides. In addition, the peptide SSL-29 was chosen since recently published data showed that SSL-29 is contained in 89% of sweat samples analyzed [Rieg et al. 2005]. This indicates that SSL-29 is a quite stable intermediate in postsecretory processing.

In order to elucidate the biological function of the postsecretory processing by CatD, the peptides SSL-29, SSL-25 and LEK-24 were tested for their antimicrobial activity against *E. coli* (Fig. 18A) and *Staph. aureus* (Fig. 18B) and compared to the activity of DCD-1L.

DCD-1L is highly active against *E. coli* (LC_{50} = 30 µg/ml) and *Staph. aureus* (LC_{50} = 10 µg/ml). The peptides LEK-24 and SSL-29 were found to have lost the antimicrobial activity against these microorganisms. The peptide SSL-25, the most

cationic peptide (pI = 9.4) among the DCD-1L derived peptides shows higher activity against *E. coli* and *Staph. aureus* (LC_{50} = 7 µg/ml) compared to DCD-1L.

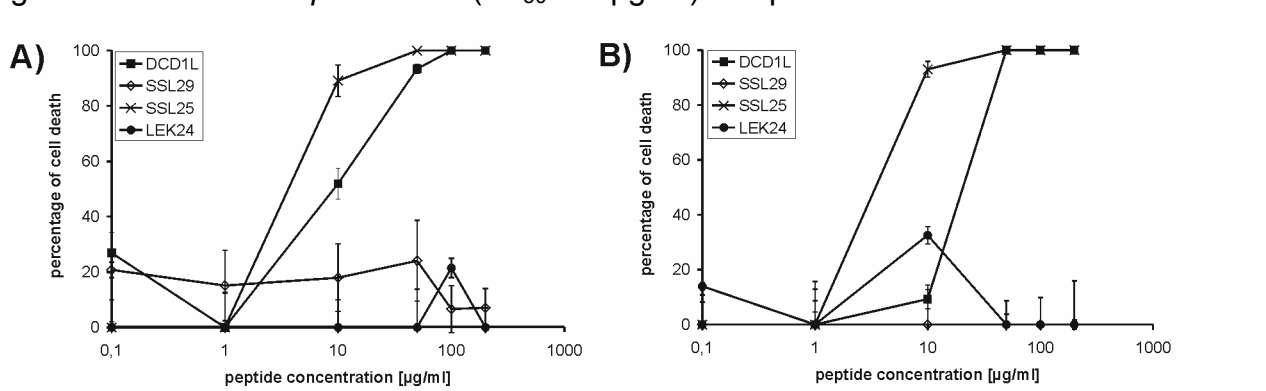

Figure 18 The antimicrobial activity of DCD-1L and DCD-1L derived peptides SSL-29, LEK-24 and SSL-25 evaluated by colony-forming units assay against *E. coli* (A) and *Staph. aureus* (B).

4.3 Discussion

Altogether we identified 10 dominant proteins in human eccrine sweat from which 6 proteins (human serum albumin, cytokeratin I, Zn-α-2-glycoprotein, prolactin-inducible protein, cystatin A, DCD-1L) have already been described in sweat or in sweat glands. Psoriasin was recently identified in keratinocytes as a secretory antimicrobial protein [Glaser et al. 2005] indicating, that sweat also contains proteins secreted by keratinocytes. The proteins apolipoprotein D, lipophilin B and CatD were identified for the first time in human eccrine sweat. Their origin, from sweat glands or keratinocytes still remains to be determined. The presented sweat protein pattern summarizes the dominant proteins in human eccrine sweat and thus provides useful information for further investigations concerning skin diseases such as atopic dermatitis or psoriasis in which some of the proteins are involved e.g. cytokeratin I [Algermissen et al. 1996].

The presence of proteases in sweat and their function is barely understood. There are only a few proteases described until now, such as the serine proteases tissue kallikrein and kininase II Hibino et al. 1994] and the human stratum corneum chymotryptic enzyme [Kishi et al. 2004]. Beside these serine proteases Yokozeki *et al*. [Yokozeki et al. 1987] described cysteine proteases in general to be present in sweat but without further specifications. Screening studies revealed that sweat also contains several gelatinolytic and caseinolytic proteases [Horie et al. 1986].

However, the functional significance of these proteases in sweat is almost completely unknown.

Recently published data show, that a yet unidentified serine protease is responsible for the postsecretory processing of LL-37 in sweat [Murakami et al. 2004] revealing one possible physiological function of sweat proteases. In consideration of these results we show that DCD-1L is postsecretory processed into 12 DCD-1L derived peptides. Additionally the temporal order of the postsecretory processing was investigated in more detail. The initial step is the cleavage of the C-terminal amino acid leucine by a 1,10-phenanthroline sensitive carboxypeptidase which has not been described in sweat until know. The data show, that the 1,10-phenanthroline sensitive carboxypeptidase resembles carboxypeptidase A (EC 3.4.17.1) concerning their specificity to release C-terminal amino acids such as Leu, Val, Phe, Ile, and Ser but little or no action with Arg, Lys, Glu, Asp or Pro [Peterson et al. 1976]. Furthermore the sweat carboxypeptidase is inhibited with 1,10-phenanthroline but not with EDTA indicating that it is presumably a Zn^{2+}-metalloprotease. The second processing step is the cleavage between ^{3}L and ^{4}L by an unidentified endoprotease which occurs simultaneously to further C-terminal trimming steps. Afterwards DCD-1L derived peptides are cleaved by CatD between ^{29}L and ^{30}E leading to the peptides SSL-29 and LEK-26 which are further processed yielding the proteolytic stable peptides LEK-24 and SSL-25. These peptides and the peptide SSL-29 were tested for their antimicrobial activity to show the physiological significance of the postsecretory processing. The peptide SSL-25 is highly active against *E. coli* and *Staph. aureus* whereas the cleavage products LEK-24 and SSL-29 loose their antimicrobial activity.

The biological role of the postsecretory processing of the antimicrobial peptide DCD-1L is to modulate the innate immune response of human skin by the generation of a set of shortened peptides which differ in their antibacterial activity. CatD, a 1,10-phenanthroline sensitive carboxypeptidase and at least one endoprotease are involved in the postsecretory processing of DCD-1L and therefore modulate the immune defense on the skin surface. The described postsecretory immune modulation on the skin surface may smoothen the way for new clinical approaches in treatment of skin diseases such as psoriasis since CatD is involved in the etiopathology of this inflammatory disease [Chen et al. 2000].

5 A cell permeable CatD substrate

5.1 Intention

Proteases play central roles in many physiological and pathological processes such as cell death, cancer and infectious diseases. Posttranslational modifications and interactions with other cellular components may affect the proteolytic activity. To obtain maximum information about the pathological relevance of a given protease, it is therefore required to measure not only the amount and distribution of the enzyme, but also its specific activity in living cells. For this purpose activity-based probes need to be developed that specifically probe for protease activities in living cells.

Here, we present a cell-penetrating protease substrate developed to specifically probe the activity of the endolysomal protease cathepsin D (CatD) in living cells. The R9-CatD-substrate consists of the highly cationic sequence (RRRRRRRRR, R9) which has been described as a cell-penetrating peptide [Futaki et al. 2001] and the cathepsin D specific peptide substrate EEKPISFFRLGK which is specifically cleaved by cathepsin D between the aromatic phenylalanine residues [Baechle et al. 2005] (Fig. 19).

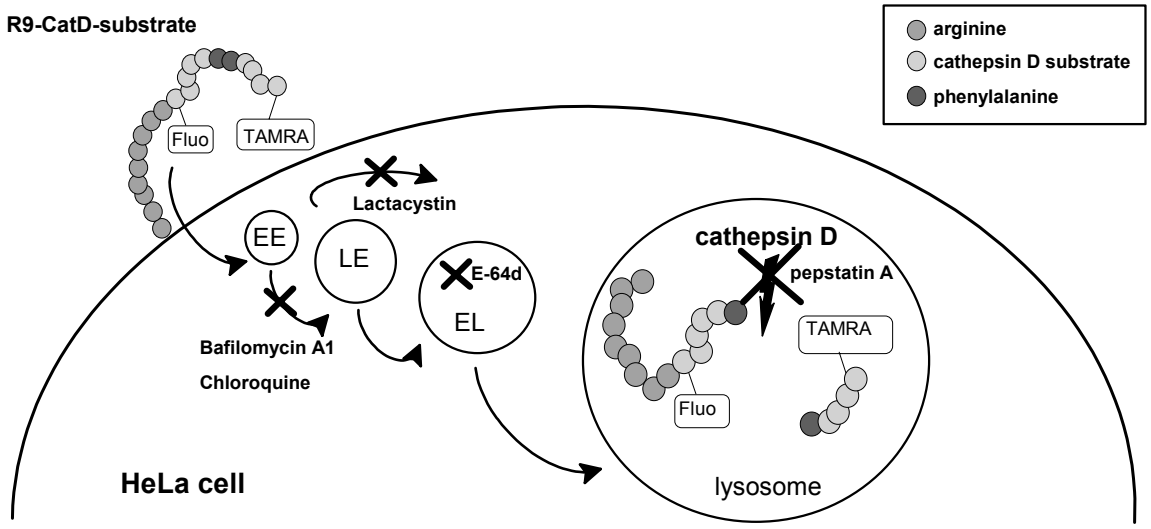

Figure 19 Principle of the R9-CatD-substrate

The cell-penetrating R9-CatD-substrate was synthesized by a robust and straight-forward procedure (Fig. 20) which will be generally applicable to a large variety of different protease substrates. Efficient endolysosomal targeting was achieved by N-

terminal elongation of the probe with the cell-penetrating peptide (CPP) nona-arginine. So far, in spite of several reports on the import of CPPs by endocytosis, the application of CPPs as low molecular weight endosomal targeting sequences has received only marginal attention. The protease substrate was flanked by two different fluorophores – cleavage of the substrate was detected by changes in the efficiency of fluorescence resonance energy transfer (FRET). By incubation of cells with different protease inhibitors the contribution of individual proteolytic activities and especially of CatD to the break-down of the probe in living cells could be determined quantitatively (Fig. 19).

5.2 Results and discussion

DNA microarray analysis and two-dimensional gel electrophoresis have revolutionized the analysis of changes in the levels of transcription and translation of proteins. However, for enzymes, the levels of transcription and translation, in many cases, do not correlate with their activities [Gygi et al. 1999]. Therefore, in order to arrive at a functional understanding of molecular networks, the large scale approaches for expression analysis have to be complemented by functional analyses. Proteases play essential roles in all live cycles of organisms. Given this importance, different strategies have been developed for measuring enzyme activities. Activity-based probes (ABPs) have been widely used for the analysis of cysteine, serine and threonine proteases [Speers & Cravatt 2004]. Especially for caspases, proteases essential in the initiation and execution of programmed cell death, numerous small and large molecule probes have been presented [Chahroudi et al. 2003, Bullok & Piwnica-Worms 2005]. However, many of these protease-directed ABPs lack specificity. Therefore, especially quantitative information on the activity of a particular enzyme is difficult to obtain. Until now lengthy biochemical analyses such as SDS-PAGE of cell lysates and identification of proteases bound by the ABP are required.

Ideally, (i) an activity-based probe should provide quantitative information on a specific enzymatic activity in living cells, and (ii) the manipulations required for processing of samples be minimized enabling such functional analyses in high through-put. For a general application in tissue culture, tumor samples and *in vivo* synthetic low molecular weight probes are highly preferable as transfection of cells

with genetically encoded enzyme probes imposes severe constraints on the experimental design [Harpur et al. 2001]. Finally, the design of these probes should be based on a principle that can easily be adapted to different proteases.

Here, we present a synthetic low molecular probe that efficiently targets the endolysosomal compartment for probing the activity of the aspartic protease cathepsin D (CatD, EC 3.4.23.5). The aspartic protease CatD possesses major physiological and pathophysiological implications. In the control of the immune response, CatD is involved in the degradation of proteins and generation of peptides presented by MHC class II molecules [Rodriguez & Diment 1992]. Moreover, CatD is necessary for the processing of the β-amyloid precursor protein playing a major role in Alzheimer's disease [Ladror et al. 1994]. Finally, overexpression of CatD in breast cancer cells is associated with an increased risk of metastasis, caused by the CatD-induced cancer cell proliferation [Glondu et al. 2001].

A short doubly-labeled substrate for a fluorescence-based read-out was combined with a cell-penetrating peptide (CPP), serving as an endolysosomal targeting peptide. Cell-penetrating peptides represent widely used vectors for the import of molecules into mammalian cells in basic and applied biomedical research [Fischer et al. 2005]. However, to this point, the application of these peptides nearly exlusively intended to target molecules into the cytoplasm or nucleus. Recent findings demonstrated a role of endocytosis in the uptake of CPPs [Richard et al. 2003]. We therefore intended to explore whether these synthetic low molecular weight vectors could be used to efficiently target a substrate to lysosome-resident CatD. Because of its efficient cellular uptake, nona-arginine was selected as a CPP [Wender et al. 2000].

As a substrate we selected a peptide recently developed in our laboratory [Baechle et al. 2005]. This substrate is cleaved efficiently by CatD between the two phenylalanine residues. This peptide was N-terminally elongated with nona-arginine. Fluorescence resonance energy transfer (FRET) was selected for detecting the degradation of the targeted substrate. Site-specific attachment of carboxyfluorescein and carboxytetramethylrhodamine to either terminus of the substrate, instead of attachment to the termini of the entire peptide, was intended to maximize the specificity of this probe for CatD. The design and the synthesis of this targeted protease substrate are depicted in Figure 20.

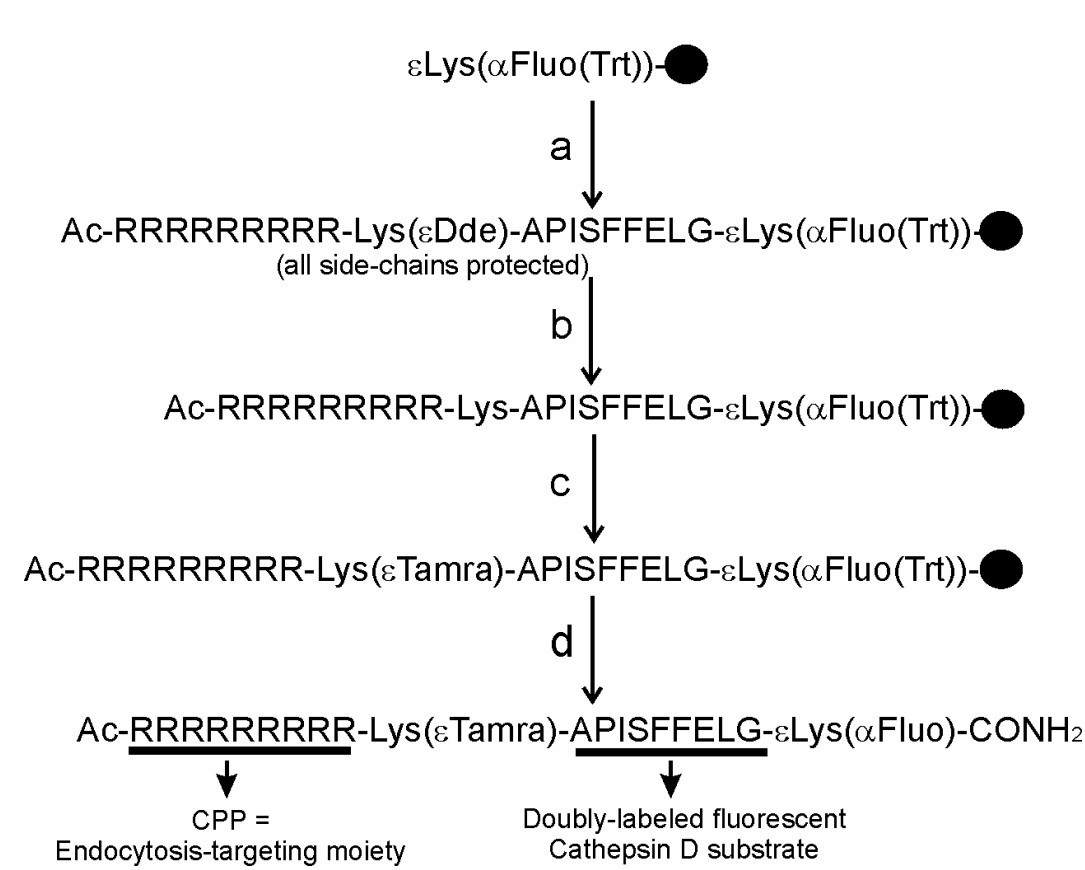

Figure 20 Synthesis of the doubly-labeled R9-CatD-substrate (Ac-RRRRRRRRR-Lys(εTamra)-APISFFELG-εLys(αFluo)-$CONH_2$). The peptide was assembled by automated solid-phase peptide synthesis on the free ε-amino group of the N^{α}-carboxyfluorescein(Trt)lysine-preloaded Rink amide resin [Fischer et al. 2003]. a) Repeated cycles of SPPS, the N-terminal amino group was blocked post-synthesis by acetylation b) Removal of the Dde-protecting group c) Introduction of the second fluorophore using carboxytetramethylrhodamine-N-succinimidyl ester d) Cleavage of the peptide amide off the resin and side-chain deprotection

The synthesis of this molecule was based on a Rink amide-based resin preloaded with a lysyl-residue carrying a tritylated carboxyfluorescein (Fluo) at its α-amino group that enables the highly efficient synthesis of peptide collections labeled with fluorescein at the C-terminus [Fischer et al. 2003]. Following automated synthesis of the conjugate, the orthogonal Dde (1-(4,4-dimethyl-2,6-dioxocyclohexylidene)ethyl)-protecting group was removed smoothly [Bycroft et al. 1993]. The free ε-amino group of the lysine was derivatized with carboxytetramethylrhodamine (Tamra) using the succinimidylester-preactivated fluorophore. The resulting peptide (= R9-CatD-substrate) was cleaved off the resin and side-chain deprotected.

The crude peptide amide was obtained at 65% purity (Fig. 21) and was purified for further investigations.

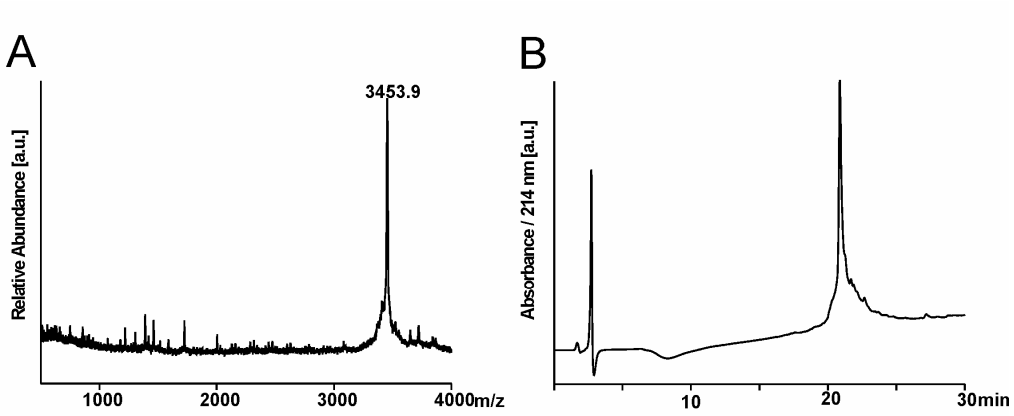

Figure 21 **(A)** MALDI-TOF mass spectrum of the crude R9-CatD-substrate, calc. $[M+H]^+$ = 3455.0 Da). **(B)** HPLC elution profile of the crude peptide (purity 70 % (RP-HPLC, 214 nm)).

Digestion of the peptide with purified human CatD and analysis of the digestion products by RP-HPLC and MALDI-MS revealed that the R9-CatD-substrate is specifically cleaved between the two phenylalanine residues (Fig. 22). Therefore purified R9-CatD-substrate (30 µM) was incubated for 1 h in 50 mM Gly/HCl buffer pH 3.5 with 0.65 µM bovine CatD in a volume of 50 µl. The reaction was stopped by adding 50 µl of a H_2O/ACN/TFA (94:5:1, v/v/v). Digestion products were then separated by analytical RP-HPLC with detection at 214 nm. The column was eluted at a flow rate of 0.2 ml/min with the following solvent system: (A) 0.055% (v/v) TFA in H_2O and (B) 0.047% (v/v) TFA in ACN/water (4:1, v/v) using a linear gradient from 5% B to 80% B within 30 min. The chromatograms are shown in Figure 22A. Identified peptides are listed in Figure 22B.

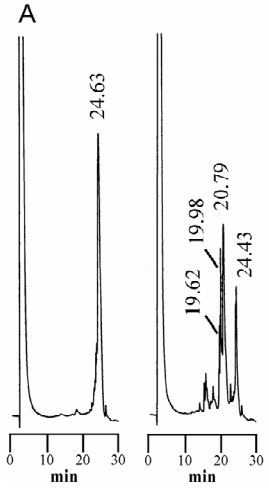

B

peptide	retention time [min]	calc. $[M + H]^+$	exper. $[M + H]^+$
FELGK(Fluo)	19.62	951.0	950.1
FELGK(Fluo)	19.98	951.0	950.1
Ac-RRRRRRRRRK(Tamra)APISF	20.79	2523.0	2519.6
intact R9-substrate	24.43	3455.0	3453.6

Figure 22 **(A)** HPLC elution profile of the purified R9-CatD-substrate (left) and of the CatD digested R9-CatD-substrate (right). **(B)** Identification of the CatD digestion products. The two FELGK(Fluo) fragments result from the positional isomers of carboxyfluorescein used for the preparation of the N^{α}-carboxyfluorescein-labeled lysyl-Rink amide resin [Fischer et al. 2003].

In order to confirm that the R9-CatD-substrate was targeted to endocytic compartments we performed live cell confocal fluorescence microscopy (CLSM) of HeLa cells incubated with the peptide. The R9-CatD-substrate was taken up efficiently (Fig. 23). A high degree of co-localization for the fluorescence of both fluorophores attached to the R9-CatD-substrate could be observed within vesicular structures. Moreover the vesicular staining of both peptide-derived fluorescence signals co-localized with AlexaFluor 633-labeled transferrin, which is internalized by clathrin-mediated endocytosis. These microscopy data demonstrate that the R9-CatD-substrate is internalized by endocytosis and subsequently found in endocytic compartments.

Inside intact cells, the reduction of fluorescein fluorescence by the acidic conditions within lysosomes and concentration quenching set a limit to a quantitative assessment of the proteolytic break-down using microscopy [Sjöback et al. 1995, Chen & Knutson 1988]. For this reason, we complemented the cellular analyses by spectral analyses in cell lysates prepared from HeLa cells pulsed with the R9-CatD-substrate.

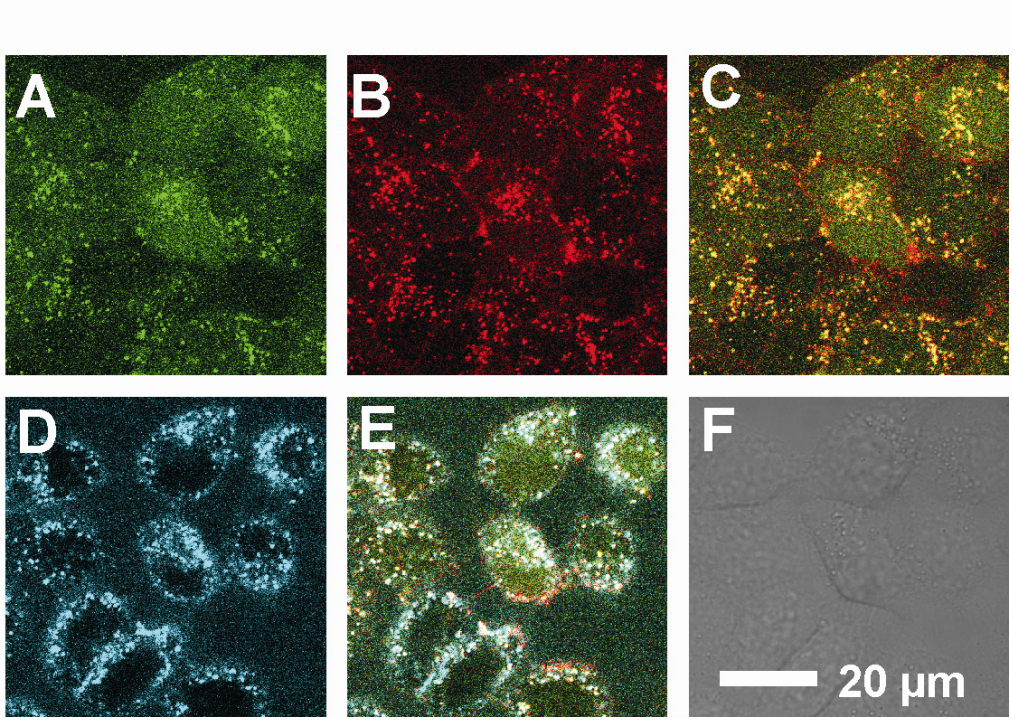

Figure 23 Endocytic uptake and intracellular localization of the R9-CatD-substrate in HeLa cells. HeLa cells were incubated with serum-free medium containing the R9-CatD-substrate (2 µM) and AlexaFluor 633-transferrin (25 µg/ml) for 30 min and were then analyzed by multi-channel CLSM: **(A)** Fluorescein fluorescence, **(B)** Tamra fluorescence of the substrate, **(C)** overlay of these two channels, **(D)** AlexaFluor 633-transferrin fluorescence, **(E)** overlay of all three fluorescence channels, **(F)** transmission.

HeLa cells were selected since this cell line has served as a model for investigating the internalization of CPPs [Richard et al. 2003, Fittipaldi et al. 2003, Console et al. 2003, Potocky et al. 2003, Saalik et al. 2004] and more importantly these cells express CatD (Fig. 24) [Deiss et al. 1996, Cirman et al. 2004].

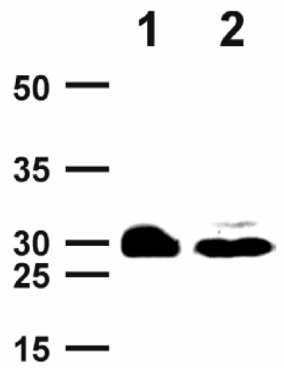

Figure 24 Western Blot analysis for the validation of the CatD expression in HeLa cells (lane 1: 30 ng of purified human CatD, lane 2: 100 µg total protein of HeLa cell lysate).

In order to validate this technique for a quantitative determination of break-down we recorded fluorescence emission spectra upon excitation at 492 nm after mixing different amounts of completely digested and intact R9-CatD-substrate (Fig. 25A).

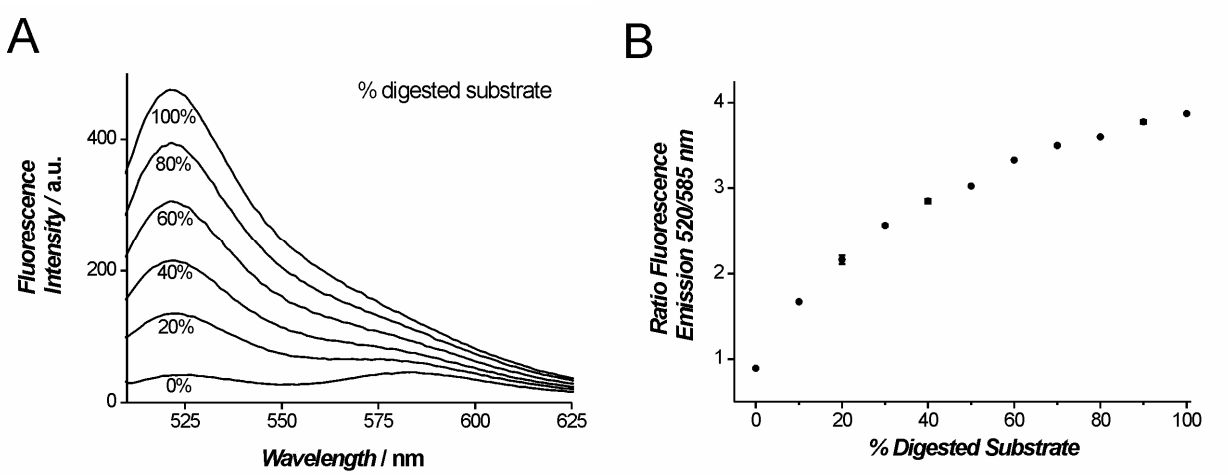

Figure 25 **(A)** A solution containing 100 nM of the R9-CatD-substrate was digested with proteinase K. After blocking protease activity by addition of PMSF different amounts of this solution and a 100 nM R9-CatD-substrate solution were mixed to yield the indicated fractions of digested peptide. The fluorescence emission spectra were recorded upon excitation at 492 nm. **(B)** Ratios of fluorescence at 520 nm and 585 nm were calculated from the fluorescence emission spectra. All digests and measurements were performed as duplicates; error bars represent the absolute deviations from the mean value (*a.u.*, arbitraty units).

Calculation of ratios of fluorescence at 520 and 585 nm rendered the detection of peptide break-down independent of concentration [Takakusa et al. 2002]. Ratios of fluorescence emissions ranged from 1.0 to 3.8 and correlated positively with the fraction of degraded peptide (Figure 25B). This experiment clearly indicates that for the R9-CatD-substrate ratiometric measurements can be used to determine quantitatively the degree of proteolytic breakdown.

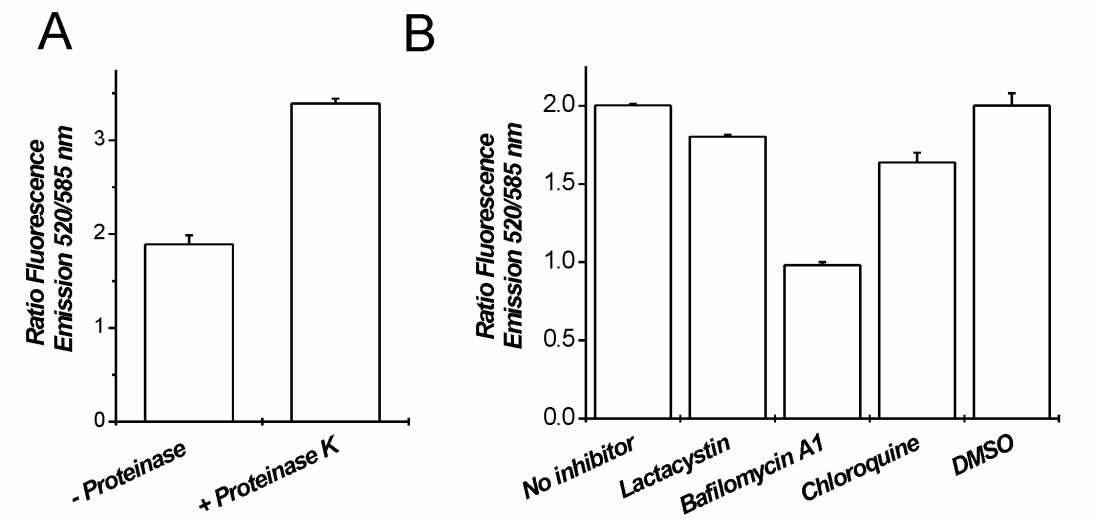

Figure 26 Fluorescence emission ratios for the determination of proteolytic degradation in the endolysosomal pathway. **(A)** HeLa cells were incubated with the R9-CatD-substrate (1 µM) for 1 h. **(B)** HeLa cells were incubated with the R9-CatD-substrate (1 µM) for 1 h in the absence or presence of different inhibitors (300 nM bafilomycin A1, 100 µM chloroquine, 50 µM lactacystin). The inhibitors were added 1 h prior to the probe. Each condition was tested in duplicate; error bars represent the absolute deviations from the mean value.

For HeLa cell lysates, after a 1 h peptide pulse, a ratio of about 2.0 was measured (Fig. 26A). Further treatment of this cell lysate with proteinase K yielded a ratiometric value of about 3.6, indicating that in the lysate about 50% of the substrate moiety had still been intact.

We suspected that a significant part of the degradation inside the cell had resulted from the activity of other enzymes. As a first step towards a quantitative determination of the fraction of probe digested by CatD we therefore investigated whether intracellular peptide stability was affected in the presence of inhibitors that perturb the activity of proteases inside living cells. A set of three inhibitors was selected. Bafilomycin A1 and chloroquine represent widely used inhibitors of endosomal acidification and exert an indirect inhibitory effect on endolysosomal proteolysis. The bacterial metabolite lactacystin selectively inhibits the 20S

proteasome and was selected to block the major protease activity in the cytoplasm. For cells pulsed with peptide in the absence of inhibitor, the emission ratio was 2.0. Both bafilomycin A1 and chloroquine had a significant effect on the intracellular stability of the R9-CatD-substrate. The emission ratios decreased to about 1.0 (bafilomycin A1) and 1.6 (chloroquine). Lactacystin had a little, albeit reproducible effect on the emission ratio (Fig. 26B). These results clearly demonstrate that inhibitors can be used to dissect the contributions of proteolytic activities in subcellular compartment on the degradation of the R9-CatD-substrate in living cells. The proteasome cleaves only a small amount of the internalized peptide whereas the endosomal passage and endosome-resident proteases have a major impact on the integrity of the probe inside HeLa cells.

After having determined the contribution of proteases inside the endolysosomal compartment on the digestion of the R9-CatD-substrate we next sought to quantify the role of individual proteases in this compartment and especially of CatD. Instead of inhibitors that exert a general effect on endolysosomal proteases, in this case, protease-specific compounds were employed. Pepstatin A was selected as a specific inhibitor of CatD and aspartic proteases. In addition the influence of E-64d acting as a broad-band irreversible cysteine protease inhibitor was investigated. This chemical is commonly used for the inhibition of cysteine proteases involved in endosomal degradation. Members of the cysteine protease family make up most of the proteases that are present in the endolysosomal compartment. In this case, a calibration curve (Fig. 25B) obtained from cell lysates that contained different amounts of digested and intact peptide was used to convert the ratiometric values into absolute values for the fraction of digested peptide (for detailed description see material and methods section). In HeLa cells pepstatin A decreased the amount of digested peptide from 30% to 25%, E-64d from 30% to about 15% (Fig. 27).

Since pepstatin A inhibits CatD as an aspartic protease and E-64d endolysosomal cysteine proteases, the inhibitory effect of both drugs should be additive. Indeed the amount of digested peptide was diminished to less than 5 % indicating almost complete inhibition of intracellular proteolysis by a combination of E-64d and pepstatin A.

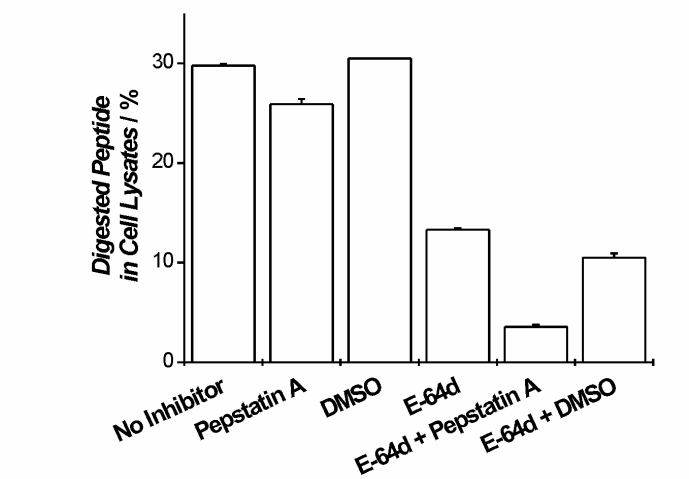

Figure 27 Fraction of the R9-CatD-substrate digested by CatD. HeLa cells were incubated with the R9-CatD-substrate (1 µM) for 1 h in serum-free medium in the absence or presence of protease inhibitors (100 µM pepstatin A, 40 µM E-64d or both inhibitors). The inhibitors were added 1 h prior to the substrate. Then cells were washed, harvested with EDTA/PBS and lysed. Afterwards fluorescence emission spectra were recorded in cell lysates. The percentage of digested peptide in cell lysates was calculated based on internal standard lysis buffer solutions containing definite amounts of digested and intact peptide. Each condition was tested in duplicate and error bars represent the absolute deviations from the mean value.

In summary our data clearly show that conjugation of a protease substrate to nona-arginine results in a highly efficient targeting of this enzyme probe to the endolysosomal compartment. In combination with protease inhibitors, the small molecule smart protease probe yielded detailed quantitative information on proteolytic activities inside a cell. The concept is highly relevant for pharmaceutical applications since it the probe design and assay format are compatible with quantitative cellular screening formats.

6 A new method for the detection of fluorescein-labeled substances using RP-HPLC

6.1 Intention

A vast number of applications in bioanalytical chemistry depend on fluorescently labeled molecules [Brand & Johnson 1997]. Fluorescein derivatives have evolved to widely used reagents for the preparation of hydrolytically stable fluorescent peptide and protein conjugates [Weber et al. 1998]. Fluorescein-labeled peptide derivatives have been employed as fluorescent markers in bioanalytical applications such as confocal laser scanning microscopy [Schmidt et al. 1998] and intracellular fluorescence correlation spectroscopy [Waizenegger et al. 2002]. One major drawback of this fluorophore apart from the moderate photostability [Song et al. 1995] is the strong pH-dependence of the fluorescence properties [Sjöback et al. 1995]. Carboxyfluorescein exhibits bright fluorescence emission in neutral and basic buffers. However, under acidic conditions, protonation lowers the fluorescence quantum yield, decreases the molar extinction coefficient and shifts the maximum of the excitation spectrum towards shorter wavelengths.

Exploiting either pre- or post-column derivatization procedures, fluorescein has been employed for the highly sensitive detection of molecules after chromatographic separation [Krull et al. 1997]. However, standard reversed-phase high-performance liquid chromatography (RP-HPLC) solvents commonly contain trifluoroacetic acid (TFA) as ion-pairing agent. When standard RP-HPLC analysis of fluorescein-labeled compounds is combined with fluorescence detection, the acidic pH of TFA drastically reduces the sensitivity of the analytical system. Our aim was to develop a method that would enable the highly sensitive detection of fluorescein-labeled peptides by RP-HPLC, however, would not require a modification of established optimized gradient systems. Here we demonstrate that post-column alkalinization of RP-HPLC eluates before detection enabled the highly sensitive detection of fluorescein-labeled peptides.

6.2 Results and discussion

A commercially available fluorescence-based HPLC-system (Shimadzu, Duisburg, Germany) consisting of a system controller (SCL-10A VP), an auto injector (SIL-10AD VP), two micro-plunger piston pumps (LC-10 AD VP), a UV detector (SPD-10AV VP) and a fluorescence detector (RF-10A XL) was modified (Fig. 31). Peptides were separated on a RP-column (Nucleosil 100, C18, 125×2 mm, 5 µm particle diameter) using a binary solvent gradient (solvent (A) 0.055% (v/v) TFA in H_2O, solvent (B) 0.047% TFA (v/v) in acetonitrile/water (4:1, v/v) with a flow rate of 0.2 ml/min and a linear gradient from 5% B to 80% B within 40 min. The pH value of both solvents approximated 2.5. Post column, the eluate was mixed on-line with an aqueous ammonia solution (NH_4OH/water, 2.5:100, v/v, pH 11.5) which was delivered by another micro-plunger piston pump (L-6200 A, Merck/Hitachi (Darmstadt, Germany) with a flow rate of 0.15 ml/min resulting in a pH value of the eluate of 10. The flow rate and the concentration of the aqueous ammonia solution was optimized so that no mixing chamber was required. Under these conditions no loss of reproducibility and peak resolution was observed. Detection was carried out using both the UV detector (214 nm) and the fluorescence detector (λ_{ex} = 490 nm and λ_{em} = 520 nm).

To demonstrate the bioanalytical applicability of the post-column alkalinization method we selected the cell-penetrating peptide (CPP) penetratin [Derossi et al. 1994] as a model peptide. Fluorescein represents the most-widely used fluorophore for the investigation of the cellular uptake and intracellular routing of CPPs [Fischer et al. 2004]. Penetratin (RQIKIWFQNRRMKWKK-COOH) and the non cell-penetrating control peptide ANDREASDANIEL-COOH were synthesized using standard solid-phase peptide synthesis and labeled at their N-termini with the fluorophore 5-carboxyfluorescein (Fluo) as described previously [Baechle et al. 2005]. The crude peptides were purified by preparative RP-HPLC (purities > 95%) and the identity of both peptides was confirmed using matrix-assisted laser desorption/ionization mass spectrometry (MALDI-MS).

Twenty fmol Fluo-penetratin (52.1 pg) were separated according to the above described procedure and elution profiles were recorded. Using the settings routinely used for the detection of fluorescein (λ_{ex} = 490 nm and λ_{em} = 520 nm) [Oefner et al. 1994], only little signal intensity could be detected in the TFA-containing eluents (Fig.

28, chromatogram a). Adjustment of the excitation wavelength to 435 nm, the maximum of the absorption spectrum of fluorescein at pH 2.5 [Sjöback et al. 1995], yielded a 2.7-fold signal increase compared to chromatogram a). For the same sample the above described post-column alkalinization procedure (chromatogram c) yielded a 42-fold signal amplification compared to chromatogram a) and a 15-fold signal amplification compared to chromatogram b).

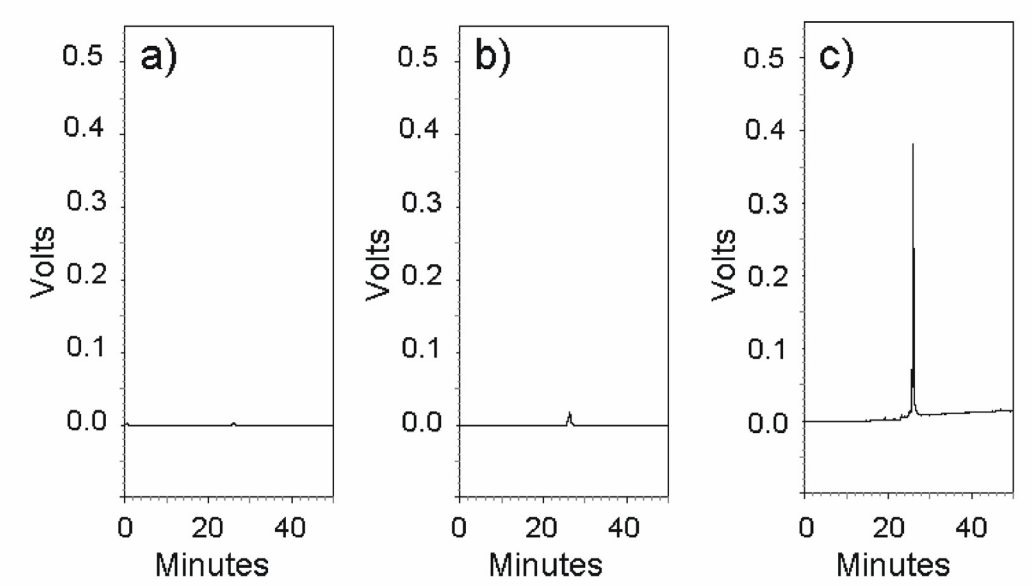

Figure 28 Dependence of peak intensities on detection conditions. Detection without sample alkalinization with excitation at 490 nm (a) and 435 nm (b) and with sample alkalinization and excitation at 490 nm (c). In all cases 20 fmol Fluo-penetratin (52.1 pg, 2 nM) were loaded onto the column and fluorescence detection was carried out at 520 nm.

In order to validate the method for quantification of fluorescein-labeled peptides, the response function was recorded for 7 different amounts of Fluo-penetratin ranging from 0.2 fmol (0.52 pg) to 40 fmol (104.2 pg). A linear concentration dependence (R^2=0.99) was obtained for the entire concentration range. The detection limit was approximately 0.2 fmol with a signal-to-noise ratio of 5. Fluo-penetratin eluted at 26.10 min and retention times exhibited an excellent reproducibility (relative standard deviation for the retention time: 0.13%). Previously published detection limits for post-column derivatization including fluorescein isothiocyanate (detection limit: 50 fmol, S/N = 2)[Muramoto et al. 1984], N-hydroxysuccinimidyl fluorescein-O-acetate (detection limit: 3.2 fmol, S/N = 3) [Wang et al. 2000], and 6-oxy-(N-succinimidyl acetate)-9-(2'-methoxycarbonyl)fluorescein (detection limit: 2.0 fmol, S/N = 3) [Cao et al. 2005] were 10 to 100 fold higher than

the detection limit of our post-column alkalinization method which is 0.2 fmol with a signal-to-noise ratio of 5.

In addition to a strong benefit in sensitivity, fluorescence-based detection is highly attractive for the analysis of peptide uptake and break-down in complex biological samples. Fluorescence enables the highly specific discrimination of exogeneously added CPP's from endogenous molecules. To demonstrate the applicability of the post-column alkalinization RP-HPLC method for biological samples, the two above mentioned peptides were compared with respect to their ability to interact with cells. Human EBV-transformed B cells (Boleth, IMGT/HLA sequence database number: HC10329) were incubated with Fluo-penetratin and Fluo-ANDREASDANIEL. Fluo-penetratin is described to efficiently associates with the plasma membrane and to be internalized into different cell types [Derossi et al. 1994]. For the control peptide Fluo-ANDREASDANIEL no such association and internalization were expected.

B cells were diluted in serum-free RPMI 1640 medium (Gibco, Invitrogen-Gibco, Karlsruhe, Germany) and transferred into a 96-well plate (Nunc, Wiesbaden, Germany) with 200 µl cell suspension per well (10^5 cells/well). The two peptides were added to a final concentration of 5 µM to the cell suspensions. After 2 h incubation at 37 °C cells were washed 5 times with PBS (pH 7.4, Gibco-Invitrogen, Karlsruhe, Germany), lysed in 200 µl detergent-containing buffer (0.5% (w/v) Zwittergent 3-12 in 50 mM Tris(hydroxymethyl)aminomethane, pH 8.0) and boiled for 5 min. After removal of cell debris by centrifugation (13000 rpm, 5 min, Heraeus Biofuge pico), 50 µl of the supernatants (total volume: 200 µl) were applied to the post-column alkalinization RP-HPLC system (Fig. 29). All chromatographic measurements were performed as triplicates. The amount of Fluo-penetratin (chromatogram a) was more than 10 times greater than that of the control peptide Fluo-ANDREASDANIEL (chromatogram b).

Absolute amounts of cell-associated fluorescence were calculated based on the calibration curve ($y = 242.91 \times x$, where y is the peak area and x stands for the absolute amount of fluorescein-labeled peptide in fmol) and yielded 117.3 fmol (0.3 ng, 2.3 nM in 50 µl cell lysate) of Fluo-penetratin and 9.7 fmol (17.2 pg, 0.2 nM in 50 µl cell lysate) of Fluo-ANDREASDANIEL per 2.5×10^4 B cells. The total amount of Fluo-penetratin eluting at 26.17 min compared to the one of all other fragments indicated that only 10% of the internalized CPP had remained intact. These data

show that the post-column alkalinization RP-HPLC method can be used for the quantification of the cellular internalization of fluorescent cell-penetrating peptides and the identification of proteolytic break-down. In addition this approach may be combined with off-line MALDI-MS for the identification of degradation products [Elmquist & Langel 2003].

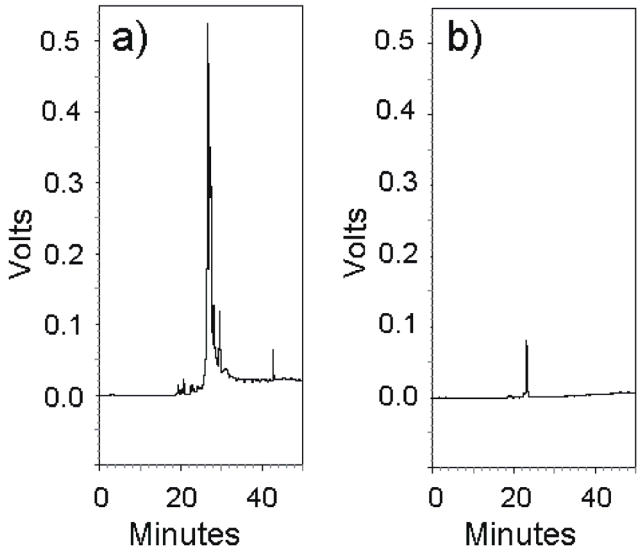

Figure 29 Detection of Fluo-penetratin (a) and Fluo-ANDREASDANIEL (b) in cell lysates. B cells (2.5×10^4 B cells) were incubated with the indicated amount of the corresponding peptide (5 µM), washed and lysed in 200 µl lysis buffer. Subsequently 50 µl of each lysate were subjected to the described separation procedure (including post-column alkalinization and fluorescence detection (λ_{ex} = 490 nm and λ_{em} = 520 nm).

The presented data clearly demonstrate that our post-column alkalinization RP-HPLC method strongly enhances the sensitivity of fluorescence detection of fluorescein-labeled compounds by more than 40-fold compared to previously published protocols. Moreover the method is highly reproducible and suitable for the determination of fluorescent peptides in complex cell lysates. The method represents a valuable complementation to the analysis of peptide uptake and distribution by flow cytometry and fluorescence microscopy [Fischer et al. 2004] as it provides absolute quantities and allows the differentiation between degraded and intact fluorescent peptides.

6.3 Supplemental data

The following figure illustrates the configuration of the RP-HPLC system for the postcolumn alkalinization method. Only an additional pump for the delivery of the ammonium hydroxide solution is necessary without a mixing chamber. Optimization of the flow rates of the solvents is sufficient for the optimal separation and detection of fluorescein-labeled peptides.

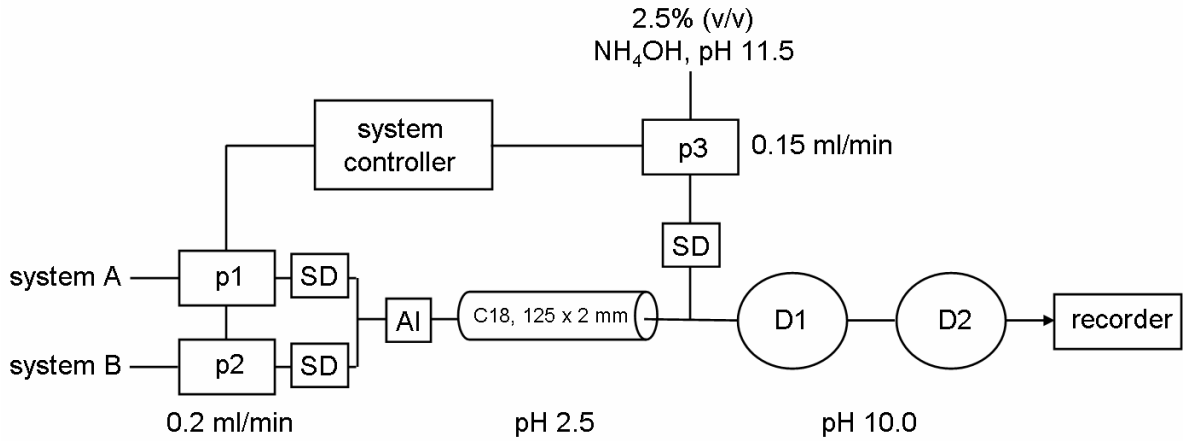

Figure 30 Configuration of the RP-HPLC system for post-column sample alkalinization including system controller, auto injector (AI), peristaltic pumps (p), solvent degasser (SD), UV detector (D1, 214 nm) and fluorescence detector (D2, λ_{ex} = 490 nm and λ_{em} = 520 nm). The samples are separated at pH 2.5, alkalinized and detected at pH 10.

The calibration curve stated below points out, that the post-column alkalinization method is highly reproducible indicated by the small standard deviation. Furthermore the method is suitable for the determination of fluorescein-labeled substances within a wide concentration range since the signals (i.e. peak areas) are linear from 0.2 fmol to 40 fmol (R^2 = 0.99) (Fig. 31).

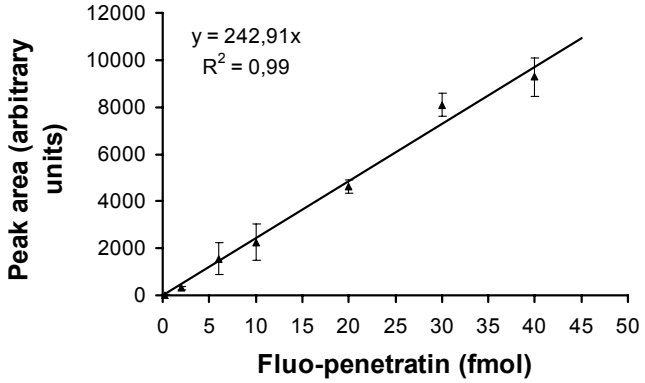

Figure 31 Calibration curve for the total amount of Fluo-penetratin (fmol) determined using the postcolumn alkalinization procedures followed by peak integration.

Recently the uptake of different CPPs (penetratin [Derossi et al. 1994], pVEC (LLIILRRRIRKQAHAHSK) [Säälik et al. 2004] and $(KFF)_3K$ [Petersen et al. 2004]) in two yeast species, Saccharomyces cerevisiae and Candida albicans, was studied using fluorescence HPLC-analyses of cell content whereas the intracellular degradation of the CPPs varies from complete stability to complete degradation according to our results [Holm et al. 2005].

Moreover the described postcolumn alkalinization procedure was applied for the detection of the peptide inhibitor D-JNKI-1 for the c-Jun N-terminal Kinase (EC 2.7.1.37) in cooperation with the Hearing Research Center Tübingen. Results were part of the final report within a research project financially supported by the University Hospital Tübingen (*fortüne project* 1309-0-0). The peptide was conjugated to Tat and labelled with FITC. Continuous local application of the peptide to the guinea pig cochlea yielded only low signal intensities due to the different membrane structure of the cochlea compared to, for example, HeLa cells or EBV-transformed B cells.

7 Conclusion

7.1 Abstract

The specific and sensitive detection of protease activities within aqueous biological fluids such as blood, urine, sweat or cell lysates is important since proteases are widely used biomarkers for the discrimination between diseased and healthy samples. Recently, great efforts have been made to develop new proteomic approaches implying screening studies for the parallel determination of various parameters. Therefore specific and high-throughput compatible methods are required. The present work describes a new method for the determination of CatD activity which is generally applicable on peptide substrates and represents a useful tool and complements established enzyme assays. The applicability of the digest & pull down assay was applied to biological samples such as cell lysates and sweat. As a result thereof, CatD was detected in human eccrine sweat. Furthermore, we could show that CatD, in combination with at least two other proteases, is involved in the postsecretory processing of the antimicrobial peptide DCD-1L into 12 DCD-1L derived peptides from which at least one (SSL-25) shows an higher activity than DCD-1L. Thus postsecretory processing by CatD modulates the innate immune defense of human skin by generating a bigger set of DCD-1L derived peptides with different antimicrobial activities.

Recently, fluorescence based visualization techniques such as confocal laser scanning microscopy (CLSM) and fluorescence associated cell sorting (FACS) more and more became the methods of choice for cellular investigations. So it is highly desirable to develop innovative fluorescent probes which are compatible to these bioanalytical methods. Since protease activities commonly can only be detected in cell lysates a new cell permeable peptide substrate was designed for the visualization of protease activity within living cells. The developed R9-CatD-substrate consists of the cell-penetrating peptide R_9 and the specific CatD-substrate. The scissile bond is flanked by TAMRA and carboxyfluorescein respectively. Upon cleavage with CatD the quenching of the fluorophores is abolished and both the TAMRA and the carboxyfluorescein fluorescence can be measured. Once in the endolysosomal pathway the R_9-substrate is cleaved and the fluorescence increases as can be determined by CLSM and FACS analysis. The presented design of cell-

penetrating, doubly-labeled peptide substrates and their application for cellular investigations is an innovative and promising approach which reasonably endorses other common techniques such as *in vitro* digestion experiments or western blot analysis.

As already mentionend above, a vast number of applications in bioanalytical chemistry depend on fluorescein labeled molecules. Fluorescein derivatives have evolved to widely used reagents for the preparation of hydrolytically stable fluorescent peptide and protein conjugates. However, the strong pH dependence of the fluorophore narrows its applicability especially in acidic buffer systems such as it is the case for commonly used RP-HPLC systems. Therefore a new RP-HPLC method was developed yielding a 40-fold signal increase without loss of reproducibility or peak resolution. This method has been used for the quantification of cellular uptake of the fluorescent labeled cell-penetrating peptide penetratin by human EBV-transformed B cells.

Taken together, a new method for the determination of CatD activity based on biotinylated and fluorescent peptide substrates was developed and applied to various biological samples particularly to human eccrine sweat, where CatD could be detected for the first time. In this context the physiological function of CatD in human eccrine sweat was investigated stating its involvement in the postsecretory processing of the antimicrobial peptide DCD-1L and therefore its role in the modulation of the immune defense of human skin. Moreover the designed CatD substrate was modified by making it cell permeable and by the introduction of two fluorophores so that it can be used as an activity-based probe for the intracellular localisation and quantification of CatD activity within living cells. In general, the cellular uptake of fluorescein-labelled cell-penetrating peptides by human EBV-transformed B cells was quantified by a new RP-HPLC based method.

7.2 Zusammenfassung

Der spezifische und empfindliche Nachweis von Proteaseaktivitäten in wässrigen biologischen Proben wie Blut, Urin, Schweiß oder Zelllysaten ist wichtig, da Proteasen häufig als Biomarker verwendet werden um zwischen Proben von Kranken und Gesunden zu unterscheiden. In den letzten Jahren wurden neue Proteomics-Anwendungen entwickelt um in einem Ansatz parallel mehrere

Parameter zu detektieren. Aufgrund dieser Tatsache werden spezifische Methoden, die sich zur Automatisierung eignen benötigt. In der vorliegenden Arbeit wird eine neue Methode zum Nachweis der CatD Aktivität vorgestellt, die sich prinzipiell auch auf beliebige andere Peptidsubstrate übertragen lässt und deshalb eine sinnvolle Ergänzung zu den bisher bekannten Enzymaktivitätstests darstellt. Der entwickelte *Digest & Pull Down Assay* wurde zur Bestimmung der CatD-Aktivität in biologischen Proben wie Zelllysaten und Schweiß verwendet. CatD konnte so in menschlichem Schweiß nachgewiesen werden. Des weiteren konnte gezeigt werden, dass CatD in Verbindung mit noch mindestens zwei weiteren Proteasen für die postsekretorische Prozessierung des antimikrobiellen Peptids DCD-1L in 12 DCD-1L abgeleitete Peptide verantwortlich ist, von denen mindestens ein Peptid (SSL-25) eine höhere antimikrobielle Aktivität besitzt als DCD-1L. Die angeborene Immunabwehr der Haut wird durch postsekretorische Prozessierung mittels CatD moduliert, indem 12 DCD-1L abgeleitete Peptide generiert werden, die unterschiedliche antimikrobielle Aktivitäten besitzen.

Die fluoreszenzbasierenden Visualisierungstechniken konfokale Laser-Raster-Mikroskopie (CLSM) und Durchflusszytometrie (FACS) entwickelten sich in den letzten Jahren immer mehr zur bevorzugten Methode für zelluläre Untersuchungen. Die Entwicklung innovativer fluoreszierender Substanzen für diese Anwendungen ist deshalb von größter Bedeutung. Da Proteaseaktivitäten üblicherweise nur in Zelllysaten detektierbar sind, wurde ein neues zellgängiges Peptidsubstrat konstruiert, um Proteaseaktivitäten auch in lebende Zellen nachweisbar und sichtbar zu machen. Das R_9-Substrat setzt sich aus dem zellgängigen Peptid R9 und dem spezifischen CatD-Substrat zusammen. An die zu spaltende Bindung grenzen die Fluorophore TAMRA und Carboxyfluorescein. Nach der Spaltung durch CatD ist der Quenching-Effekt der beiden Fluorophore aufgehoben und sowohl die TAMRA- als auch die Fluorescein-Fluoreszenz kann detektiert werden. In endolysosomalen Kompartimenten wird das R9-Substrat unter Zunahme des Fluoreszenzsignales gespalten und kann durch konfokale Laser-Raster-Mikroskopie oder durchflußzytometrisch nachgewiesen werden. Das vorgestellte Prinzip der zellpermeablen, doppelt markierten Peptidsubstrate und ihre Anwendung für zelluläre Untersuchungen ist ein innovativer und viel versprechender Ansatz, der eine sinnvolle Ergänzung zu herkömmlichen Techniken wie *in vitro* Verdauexperimente oder Western Blot Analysen bietet.

Wie bereits oben erwähnt, basieren viele bioanalytische Anwendungen auf Fluoreszenz-markierten Substanzen. Besonders die hydrolytisch stabilen, mit Fluorescein gekoppelten Peptide und Proteine finden eine breite Anwendung. Jedoch verringert die starke pH-Abhängigkeit von Fluorescein dessen Anwendung vor allem in sauren Puffersystemen, wie sie zum Beispiel bei gängigen RP-HPLC-Systemen verwendet werden. Dieses Problem wurde durch die Entwicklung einer neuen RP-HPLC-Methode gelöst, die um den Faktor 40 sensitiver ist als herkömmliche Systeme und mit der gleichen Reproduzierbarkeit und Peak-Auflösung arbeitet. Mit dieser Methode wurde die Aufnahme des zellgängigen Peptids Penetratin von humanen EBV-transformierten B-Zellen quantifiziert.

Eine neue Methode zum Nachweis von CatD Aktivität basierend auf biotinylierten und fluoreszierenden Peptidsubstraten wurde entwickelt und auf verschiedene biologische Proben angewendet, insbesondere auf Schweiß, wo CatD zum ersten Mal nachgewiesen wurde. In diesem Zusammenhang wurde die physiologische Funktion von CatD im Schweiß gezeigt. CatD ist an der postsekretorischen Prozessierung des antimikrobiellen Peptids DCD-1L beteiligt und dadurch an der Modulation der Immunabwehr der Haut. Des weiteren wurde das konstruierte CatD-Substrat zellgängig und durch die Kopplung mit zwei Fluorophoren nachweisbar gemacht und kann so zur intrazellulären Lokalisation von CatD-Aktivität verwendet werden. Die Internalisierung von fluoreszenzmarkierten, zellgängigen Peptiden von humanen EBV-transformierten B-Zellen im allgemeinen wurde durch eine neu entwickelte RP-HPLC-Methode quantifiziert.

8 References

Adachi,W. *et al.* Isolation and characterization of human cathepsin V: a major proteinase in corneal epithelium. *Invest Ophthalmol. Vis. Sci.* **39**, 1789-1796 (1998).

Algermissen,B., Sitzmann,J., LeMotte,P. & Czarnetzki,B. Differential expression of CRABP II, psoriasin and cytokeratin 1 mRNA in human skin diseases. *Arch. Dermatol. Res.* **288**, 426-430 (1996).

Ali,R.S. *et al.* Expression of the peptide antibiotics human beta defensin-1 and human beta defensin-2 in normal human skin. *J. Invest Dermatol.* **117**, 106-111 (2001).

Ali,S.Y. The degradation of cartilage matrix by an intracellular protease. *Biochem. J.* **93**, 611-618 (1964).

Alnemri,E.S. *et al.* Human ICE/CED-3 protease nomenclature. *Cell* **87**, 171 (1996).

Anson, M.L. The estimation of pepsin, trypsin, papain, and cathepsin with haemoglobin. *J. Gen. Physiol* **22**, 79-89 (1938).

Anson,M.L. & Mirsky,A.E. The estimation of pepsin with haemoglobin. *J. Gen. Physiol* **16**, 59-63 (1932).

Anson,M.L. The estimation of cathepsin with haemoglobin and the partial purification of cathepsin. *J. Gen. Physiol* **20**, 561-563 (1937).

Anson,M.L. The estimation of papain with haemoglobin, *J. Gen. Physiol* **20**, 565-574 (1937).

Anson,M.L. The purification of cathepsin. *J. Gen. Physiol* **23**, 695-704 (1940).

Arnold,D. *et al.* Substrate specificity of cathepsins D and E determined by N-terminal and C-terminal sequencing of peptide pools. *Eur. J. Biochem.* **249**, 171-179 (1997).

Authier,F., Metioui,M., Fabrega,S., Kouach,M. & Briand,G. Endosomal proteolysis of internalized insulin at the C-terminal region of the B chain by cathepsin D. *J. Biol. Chem.* **277**, 9437-9446 (2002).

Azuma,T., Pals,G., Mohandas,T.K., Couvreur,J.M. & Taggart,R.T. Human gastric cathepsin E. Predicted sequence, localization to chromosome 1, and sequence homology with other aspartic proteinases. *J. Biol. Chem.* **264**, 16748-16753 (1989).

Baechle,D. *et al.* Biotinylated fluorescent peptide substrates for the sensitive and specific determination of cathepsin D activity. *J. Pept. Sci.* **11**, 166-174 (2005).

Baldwin,E.T. *et al.* Crystal structures of native and inhibited forms of human cathepsin D: implications for lysosomal targeting and drug design. *Proc. Natl. Acad. Sci. U. S. A* **90**, 6796-6800 (1993).

Barrett,A.J. & Kirschke,H. Cathepsin B, Cathepsin H, and cathepsin L. *Methods Enzymol.* **80 Pt C**, 535-561 (1981).

Barrett,A.J. Cathepsin D. Purification of isoenzymes from human and chicken liver. *Biochem. J.* **117**, 601-607 (1970).

Barrett,A.J. Lysosomal acid proteinase of rabbit liver. *Biochem. J.* **104**, 601-608 (1967).

Bergmann,M. & Fruton,J.S. On proteolytic enzymes. XIII. Synthetic substrates for chymotrypsin. *J. Biol. Chem.* **118**, 405-415 (1939).

Bergmann,M., Fruton,J.S. & Fraenkel-Conrat,H. On proteolytic enzymes. XV. Regarding the general nature of intracellular proteolytic enzymes. *J. Biol. Chem.* **119**, 35-46 (1937).

Bergmann,M., Fruton,J.S. & Pollok,H. The specificity of trypsin, *J. Biol. Chem.* **127**, 643-648 (1939).

Bergmann,M., Zervas,L. & Fruton,J.S. On proteolytic enzymes. VI. On the specificity of papain. *J. Biol. Chem.* **111**, 225-244 (1935).

Bergmann,M., Zervas,L. & Fruton,J.S. On proteolytic enzymes. XI. The specificity of the enzyme papain peptidase I. *J. Biol. Chem.* **115**, 593-611 (1936).

Beyer,B.M. & Dunn,B.M. Prime region subsite specificity characterization of human cathepsin D: the dominant role of position 128. *Protein Sci.* **7**, 88-95 (1998).

Beyer,B.M. & Dunn,B.M. Self-activation of recombinant human lysosomal procathepsin D at a newly engineered cleavage junction, "short" pseudocathepsin D. *J. Biol. Chem.* **271**, 15590-15596 (1996).

Bidere,N. *et al.* Cathepsin D triggers Bax activation, resulting in selective apoptosis-inducing factor (AIF) relocation in T lymphocytes entering the early commitment phase to apoptosis. *J. Biol. Chem.* **278**, 31401-31411 (2003).

Bond,J.S. & Barrett,A.J. Degradation of fructose-1,6-bisphosphate aldolase by cathepsin B. *Biochem. J.* **189**, 17-25 (1980).

Bowman,E.J., Siebers,A. & Altendorf,K. Bafilomycins: a class of inhibitors of membrane ATPases from microorganisms, animal cells, and plant cells. *Proc. Natl. Acad. Sci. U. S. A* **85**, 7972-7976 (1988).

Boya,P., Roques,B. & Kroemer,G. New EMBO members' review: viral and bacterial proteins regulating apoptosis at the mitochondrial level. *EMBO J.* **20**, 4325-4331 (2001).

Bradford,M.M. A rapid and sensitive method for the quantitation of microgram quantities of protein utilizing the principle of protein-dye binding. *Anal. Biochem.* **72**, 248-254 (1976).

Brand,L. & Johnson,M.L. (Eds.). Fluorescence spectroscopy: *Methody in Enzymology*. **278**, Academic Press, San Diego (1997).

Bromme,D. *et al.* The specificity of bovine spleen cathepsin S. A comparison with rat liver cathepsins L and B. *Biochem. J.* **264**, 475-481 (1989).

Bromme,D., Bescherer,K., Kirschke,H. & Fittkau,S. Enzyme-substrate interactions in the hydrolysis of peptides by cathepsins B and H from rat liver. *Biochem. J.* **245**, 381-385 (1987).

Bromme,D., Klaus,J.L., Okamoto,K., Rasnick,D. & Palmer,J.T. Peptidyl vinyl sulphones: a new class of potent and selective cysteine protease inhibitors: S2P2 specificity of human cathepsin O2 in comparison with cathepsins S and L. *Biochem. J.* **315 (Pt 1)**, 85-89 (1996).

Bromme,D., Li,Z., Barnes,M. & Mehler,E. Human cathepsin V functional expression, tissue distribution, electrostatic surface potential, enzymatic characterization, and chromosomal localization. *Biochemistry* **38**, 2377-2385 (1999).

Bullok,K. & Piwnica-Worms,D. Synthesis and characterization of a small, membrane-permeant, caspase-activatable far-red fluorescent peptide for imaging apoptosis. *J. Med. Chem.* **48**, 5404-5407 (2005).

Bursch,W. The autophagosomal-lysosomal compartment in programmed cell death. *Cell Death. Differ.* **8**, 569-581 (2001).

Bycroft,B.W., Chan,W.C., Chhabra,S.R. & Hone,N.D. A novel lysine-protecting procedure for continous flow solid phase synthesis of branched peptides. *J. Chem. Soc. , Chem. Commun.* 778-779 (1993).

Campbell,P.N. & Blobel,G. The role of organelles in the chemical modification of the primary translation products of secretory proteins. *FEBS Letters* **72**, 215-226 (1976).

Cao,L.W., Wang,H., Li,J.S. & Zhang,H.S. 6-Oxy-(N-succinimidyl acetate)-9-(2'-methoxycarbonyl)fluorescein as a new fluorescent labeling reagent for aliphatic amines in environmental and food samples using high-performance liquid chromatography. *J. Chromatogr. A* **1063**, 143-151 (2005).

Chahroudi,A., Silvestri,G. & Feinberg,M.B. Measuring T cell-mediated cytotoxicity using fluorogenic caspase substrates. *Methods* **31**, 120-126 (2003).

Chain,B.M. *et al.* The expression and function of cathepsin E in dendritic cells. *J. Immunol.* **174**, 1791-1800 (2005).

Chandran,K., Sullivan,N.J., Felbor,U., Whelan,S.P. & Cunningham,J.M. Endosomal proteolysis of the Ebola virus glycoprotein is necessary for infection. *Science* **308**, 1643-1645 (2005).

Chen,J.M. *et al.* Cloning, isolation, and characterization of mammalian legumain, an asparaginyl endopeptidase. *J. Biol. Chem.* **272**, 8090-8098 (1997).

Chen,J.M., Rawlings,N.D., Stevens,R.A. & Barrett,A.J. Identification of the active site of legumain links it to caspases, clostripain and gingipains in a new clan of cysteine endopeptidases. *FEBS Lett.* **441**, 361-365 (1998).

Chen,R.F. & Knutson,J.R. Mechanism of fluorescence concentration quenching of carboxyfluorescein in liposomes: energy transfer to nonfluorescent dimers. *Anal. Biochem.* **172**, 61-77 (1988).

Chen,S.H. *et al.* Response of keratinocytes from normal and psoriatic epidermis to interferon-gamma differs in the expression of zinc-alpha(2)-glycoprotein and cathepsin D. *FASEB J.* **14**, 565-571 (2000).

Chou,K.C. Modeling the tertiary structure of human cathepsin-E. *Biochem. Biophys. Res. Commun.* **331**, 56-60 (2005).

Cirman,T. *et al.* Selective disruption of lysosomes in HeLa cells triggers apoptosis mediated by cleavage of Bid by multiple papain-like lysosomal cathepsins. *J. Biol Chem.* **279**, 3578-3587 (2004).

Clague,M.J., Urbe,S., Aniento,F. & Gruenberg,J. Vacuolar ATPase activity is required for endosomal carrier vesicle formation. *J. Biol. Chem.* **269**, 21-24 (1994).

Conner,G.E. Isolation of procathepsin D from mature cathepsin D by pepstatin affinity chromatography. Autocatalytic proteolysis of the zymogen form of the enzyme. *Biochem. J.* **263**, 601-604 (1989).

Conner,G.E. The role of the cathepsin D propeptide in sorting to the lysosome. *J. Biol. Chem.* **267**, 21738-21745 (1992).

Console,S., Marty,C., Garcia-Echeverria,C., Schwendener,R. & Ballmer-Hofer,K. Antennapedia and HIV transactivator of transcription (TAT) "protein transduction domains" promote endocytosis of high molecular weight cargo upon binding to cell surface glycosaminoglycans. *J. Biol. Chem.* **278**, 35109-35114 (2003).

Cote,C., Solioz,M. & Schatz,G. Biogenesis of the cytochrome bc1 complex of yeast mitochondria. A precursor form of the cytoplasmically made subunit V. *J. Biol. Chem.* **254**, 1437-1439 (1979).

Daher,K.A., Lehrer,R.I., Ganz,T. & Kronenberg,M. Isolation and characterization of human defensin cDNA clones. *Proc. Natl. Acad. Sci. U. S. A* **85**, 7327-7331 (1988).

Dalton,J.P. & Brindley,P.J. Cathepsin W. In *Handbook of Proteolytic Enzymes*, 2 edn (Barrett,A.J., Rawlings,N.D. & Woessner,J.F. eds), Elsevier, London, 1109-1112, (2004).

Davies,D.R. The structure and function of the aspartic proteinases. *Annu. Rev. Biophys. Biophys. Chem.* **19**, 189-215 (1990).

de Duve,C. *et al.* Commentary. Lysosomotropic agents. *Biochem. Pharmacol.* **23**, 2495-2531 (1974).

Deiss,L.P., Galinka,H., Berissi,H., Cohen,O. & Kimchi,A. Cathepsin D protease mediates programmed cell death induced by interferon-gamma, Fas/APO-1 and TNF-alpha. *EMBO J.* **15**, 3861-3870 (1996).

Demoz,M. *et al.* Endosomal-lysosomal proteolysis mediates death signalling by TNFalpha, not by etoposide, in L929 fibrosarcoma cells: evidence for an active role of cathepsin D. *Biol. Chem.* **383**, 1237-1248 (2002).

Derossi,D. *et al.* Cell internalization of the third helix of the Antennapedia homeodomain is receptor-independent. *J. Biol. Chem.* **271**, 18188-18193 (1996).

Derossi,D., Joliot,A.H., Chassaing,G. & Prochiantz,A. The third helix of the Antennapedia homeodomain translocates through biological membranes. *J. Biol. Chem.* **269**, 10444-10450 (1994).

Deussing,J. *et al.* Cathepsins B and D are dispensable for major histocompatibility complex class II-mediated antigen presentation. *Proc. Natl. Acad. Sci. U. S. A* **95**, 4516-4521 (1998).

Dick,L.R. *et al.* Mechanistic studies on the inactivation of the proteasome by lactacystin: a central role for clasto-lactacystin beta-lactone. *J. Biol. Chem.* **271**, 7273-7276 (1996).

Dreyer,R.N. *et al.* Processing of the pre-beta-amyloid protein by cathepsin D is enhanced by a familial Alzheimer's disease mutation. *Eur. J. Biochem.* **224**, 265-271 (1994).

Dunn,B.M. *et al.* A systematic series of synthetic chromophoric substrates for aspartic proteinases. *Biochem. J.* **237**, 899-906 (1986).

Elmquist,A. & Langel,U. In vitro uptake and stability study of pVEC and its all-D analog. *Biol. Chem.* **384**, 387-393 (2003).

Erdal,H. *et al.* Induction of lysosomal membrane permeabilization by compounds that activate p53-independent apoptosis. *Proc. Natl. Acad. Sci. U. S. A* **102**, 192-197 (2005).

Erickson,A.H. & Blobel,G. Carboxyl-terminal proteolytic processing during biosynthesis of the lysosomal enzymes beta-glucuronidase and cathepsin D. *Biochemistry* **22**, 5201-5205 (1983).

Erickson,A.H. & Blobel,G. Early events in the biosynthesis of the lysosomal enzyme cathepsin D. *J. Biol. Chem.* **254**, 11771-11774 (1979).

Erickson,A.H., Conner,G.E. & Blobel,G. Biosynthesis of a lysosomal enzyme. Partial structure of two transient and functionally distinct NH2-terminal sequences in cathepsin D. *J. Biol. Chem.* **256**, 11224-11231 (1981).

Evan,G.I. *et al.* Induction of apoptosis in fibroblasts by c-myc protein. *Cell* **69**, 119-128 (1992).

Faust,P.L., Kornfeld,S. & Chirgwin,J.M. Cloning and sequence analysis of cDNA for human cathepsin D. *Proc. Natl. Acad. Sci. U. S. A* **82**, 4910-4914 (1985).

Fawell,S. *et al.* Tat-mediated delivery of heterologous proteins into cells. *Proc. Natl. Acad. Sci. U. S. A* **91**, 664-668 (1994).

Fell,H.B. & Dingle,J.T. Studies on the mode of action of excess of vitamin A. 6. Lysosomal protease and the degradation of cartilage matrix. *Biochem. J.* **87**, 403-408 (1963).

Fenteany,G. *et al.* Inhibition of proteasome activities and subunit-specific amino-terminal threonine modification by lactacystin. *Science* **268**, 726-731 (1995).

Fiebiger,E. *et al.* Cytokines regulate proteolysis in major histocompatibility complex class II-dependent antigen presentation by dendritic cells. *J. Exp. Med.* **193**, 881-892 (2001).

Fields,C.G., Lloyd,D.H., Macdonald,R.L., Otteson,K.M. & Noble,R.L. HBTU activation for automated Fmoc solid-phase peptide synthesis. *Pept. Res.* **4**, 95-101 (1991).

Filippova,I.Y. *et al.* Fluorogenic peptide substrates for assay of aspartyl proteinases. *Anal. Biochem.* **234**, 113-118 (1996).

Fischer,R., Fotin-Mleczek,M. & Brock,R. Break on through to the other side - Biophysics and cell biology shed light on cell-penetrating peptides. *ChemBioChem* **in print**, (2005).

Fischer,R., Kohler,K., Fotin-Mleczek,M. & Brock,R. A stepwise dissection of the intracellular fate of cationic cell-penetrating peptides. *J. Biol. Chem.* **279**, 12625-12635 (2004).

Fischer,R., Mader,O., Jung,G. & Brock,R. Extending the applicability of carboxyfluorescein in solid-phase synthesis. *Bioconjug. Chem.* **14**, 653-660 (2003).

Fittipaldi,A. *et al.* Cell membrane lipid rafts mediate caveolar endocytosis of HIV-1 Tat fusion proteins. *J. Biol. Chem.* **278**, 34141-34149 (2003).

Flad,T. *et al.* Detection of dermcidin-derived peptides in sweat by ProteinChip technology. *J. Immunol. Methods* **270**, 53-62 (2002).

Foekens,J.A. *et al.* Cathepsin-D in primary breast cancer: prognostic evaluation involving 2810 patients. *Br. J. Cancer* **79**, 300-307 (1999).

Folin,O. & Ciocalteu,V. On tyrosine and tryptophane determinations in proteins. *J. Biol. Chem.* **73**, 627-650 (1927).

Folin,O. & Looney,J.M. Colorimetric methods for the separate determination of tyrosine, tryptophane, and cystine in proteins. *J. Biol. Chem.* **51**, 421-434 (1922).

Frankel,A.D. & Pabo,C.O. Cellular uptake of the tat protein from human immunodeficiency virus. *Cell* **55**, 1189-1193 (1988).

Frohm,M. *et al.* The expression of the gene coding for the antibacterial peptide LL-37 is induced in human keratinocytes during inflammatory disorders. *J. Biol. Chem.* **272**, 15258-15263 (1997).

Fruton,J.S. & Bergmann,M. The specificity of pepsin. *J. Biol. Chem.* **127**, 627-641 (1939).

Fruton,J.S., Irving,G.W. & Bergmann,M. On the proteolytic enzymes of animal tissues. II. The composite nature of beef spleen cathepsin. *J. Biol. Cchem.* **138**, 249-262 (1941).

Funeriu,D.P., Eppinger,J., Denizot,L., Miyake,M. & Miyake,J. Enzyme family-specific and activity-based screening of chemical libraries using enzyme microarrays. *Nat. Biotechnol.* **23**, 622-627 (2005).

Fusek,M. & Vetvicka,V. Dual role of cathepsin D: ligand and protease. *Biomed. Pap. Med. Fac. Univ Palacky. Olomouc. Czech. Repub.* **149**, 43-50 (2005).

Futaki,S. *et al.* Arginine-rich peptides. An abundant source of membrane-permeable peptides having potential as carriers for intracellular protein delivery. *J. Biol. Chem.* **276**, 5836-5840 (2001).

Glaser,R. *et al.* Antimicrobial psoriasin (S100A7) protects human skin from Escherichia coli infection. *Nat. Immunol.* **6**, 57-64 (2005).

Glondu,M. *et al.* A mutated cathepsin-D devoid of its catalytic activity stimulates the growth of cancer cells. *Oncogene* **20**, 6920-6929 (2001).

Graslund,A. & Eriksson,L.E. Properties and applications of cell-penetrating peptides. *Genet. Eng (N. Y.)* **26**, 19-31 (2004).

Greenbaum,L.M. & Fruton,J.S. Purification and properties of beef spleen cathepsin B, *J. Biol. Chem.* **226**, 173-180 (1957).

Greiner,A., Lautwein,A., Overkleeft,H.S., Weber,E. & Driessen,C. Activity and subcellular distribution of cathepsins in primary human monocytes. *J. Leukoc. Biol.* **73**, 235-242 (2003).

Guagliardi,L.E. *et al.* Co-localization of molecules involved in antigen processing and presentation in an early endocytic compartment. *Nature* **343** , 133-139 (1990).

Guicciardi,M.E., Leist,M. & Gores,G.J. Lysosomes in cell death. *Oncogene* **23**, 2881-2890 (2004).

Gulnik,S.V. *et al.* Design of sensitive fluorogenic substrates for human cathepsin D. *FEBS Lett.* **413**, 379-384 (1997).

Gupta,B., Levchenko,T.S. & Torchilin,V.P. Intracellular delivery of large molecules and small particles by cell-penetrating proteins and peptides. *Adv. Drug Deliv. Rev.* **57**, 637-651 (2005).

Gygi,S.P., Rochon,Y., Franza,B.R. & Aebersold,R. Correlation between protein and mRNA abundance in yeast. *Mol. Cell Biol* **19**, 1720-1730 (1999).

Harder,J., Bartels,J., Christophers,E. & Schroder,J.M. A peptide antibiotic from human skin. *Nature* **387**, 861 (1997).

Harpur,A.G., Wouters,F.S. & Bastiaens,P.I. Imaging FRET between spectrally similar GFP molecules in single cells. *Nat. Biotechnol.* **19**, 167-169 (2001).

Hasilik,A. & Neufeld,E.F. Biosynthesis of lysosomal enzymes in fibroblasts. Phosphorylation of mannose residues. *J. Biol. Chem.* **255**, 4946-4950 (1980).

Hasilik,A., von Figura,K., Conzelmann,E., Nehrkorn,H. & Sandhoff,K. Lysosomal enzyme precursors in human fibroblasts. Activation of cathepsin D precursor in vitro and activity of beta-hexosaminidase A precursor towards ganglioside GM2. *Eur. J. Biochem.* **125**, 317-321 (1982).

Hengartner,M.O. The biochemistry of apoptosis. *Nature* **407**, 770-776 (2000).

Hershko,A. & Fry,M. Post-translational cleavage of polypeptide chains: role in assembly. *Annu. Rev. Biochem.* **44**, 775-797 (1975).

Hewitt,E.W. *et al.* Natural processing sites for human cathepsin E and cathepsin D in tetanus toxin: implications for T cell epitope generation. *J. Immunol.* **159**, 4693-4699 (1997).

Hibino,T., Takemura,T. & Sato,K. Human eccrine sweat contains tissue kallikrein and kininase II. *J. Invest Dermatol.* **102**, 214-220 (1994).

Holm,T. Netzereab,S., Hansen,M. Langel,U. & Hallbrink,M. Uptake of cell-penetrating peptides in yeasts. *FEBS Lett.* in press (2005)

Hoogerhout,P. *et al.* Solid-phase synthesis and application of double-fluorescent-labeled lipopeptides, containing a CTL-epitope from the measles fusion protein. *J. Pept. Res.* **54**, 436-443 (1999).

Horie,N., Yokozeki,H. & Sato,K. Proteolytic enzymes in human eccrine sweat: a screening study. *Am. J. Physiol* **250**, R691-R698 (1986).

Huang,J.S., Huang,S.S. & Tang,J. Cathepsin D isozymes from porcine spleens. Large scale purification and polypeptide chain arrangements. *J. Biol. Chem.* **254**, 11405-11417 (1979).

Inaoka,T. *et al.* Molecular cloning of human cDNA for cathepsin K: novel cysteine proteinase predominantly expressed in bone. *Biochem. Biophys. Res. Commun.* **206**, 89-96 (1995).

Iodice,A.A. & Weinstock,I.M. Cathepsin A in nutritional and hereditary muscular dystrophy. *Nature* **207**, 1102 (1965).

Iodice,A.A., Leong, V. & Weinstock,I.M. Separation of cathepsin A and D of skeletal muscle. *Arch. Biochem. Biophys.* **117**, 477-486 (1966b).

Iodice,A.A., Leong,V. & Weinstock,I.M. Proteolytic activity of skeletal muscle of normal and dystrophic chickens and rabbits. *Enzymol. Biol. Clin. (Basel)* **6**, 269-278 (1966a).

Jedeszko,C. & Sloane,B.F. Cysteine cathepsins in human cancer. *Biol. Chem.* **385**, 1017-1027 (2004).

Johansson,A.C., Steen,H., Ollinger,K. & Roberg,K. Cathepsin D mediates cytochrome c release and caspase activation in human fibroblast apoptosis induced by staurosporine. *Cell Death. Differ.* **10**, 1253-1259 (2003).

Jones,L.J. *et al.* Quenched BODIPY dye-labeled casein substrates for the assay of protease activity by direct fluorescence measurement. *Anal. Biochem.* **251**, 144-152 (1997).

Kagedal,K., Johansson,U. & Ollinger,K. The lysosomal protease cathepsin D mediates apoptosis induced by oxidative stress. *FASEB J.* **15**, 1592-1594 (2001).

Kaufmann,S.H. & Gores,G.J. Apoptosis in cancer: cause and cure. *Bioessays* **22**, 1007-1017 (2000).

Kazakova,O.V. & Orekhovich,V.N. Crystallization of cathepsin D. *Biochem. Biophys. Res. Commun.* **72**, 747-752 (1976).

Kerr,J.F., Wyllie,A.H. & Currie,A.R. Apoptosis: a basic biological phenomenon with wide-ranging implications in tissue kinetics. *Br. J. Cancer* **26**, 239-257 (1972).

Kirschke,H., Wiederanders,B., Bromme,D. & Rinne,A. Cathepsin S from bovine spleen. Purification, distribution, intracellular localization and action on proteins. *Biochem. J.* **264**, 467-473 (1989).

Kirschke,H., Wikstrom,P. & Shaw,E. Active center differences between cathepsins L and B: the S1 binding region. *FEBS Lett.* **228**, 128-130 (1988).

Kishi,T. *et al.* Development of an immunofluorometric assay and quantification of human kallikrein 7 in tissue extracts and biological fluids. *Clin. Chem.* **50**, 709-716 (2004).

Knight,C.G. & Barrett,A.J. Interaction of human cathepsin D with the inhibitor pepstatin. *Biochem. J.* **155**, 117-125 (1976).

Kokkonen,N. *et al.* Defective acidification of intracellular organelles results in aberrant secretion of cathepsin D in cancer cells. *J. Biol. Chem.* **279**, 39982-39988 (2004).

Kornfeld,S. & Mellman,I. The biogenesis of lysosomes. *Annu. Rev. Cell Biol.* **5**, 483-525 (1989).

Kozak,S.L., Kuhmann,S.E., Platt,E.J. & Kabat,D. Roles of CD4 and coreceptors in binding, endocytosis, and proteolysis of gp120 envelope glycoproteins derived from human immunodeficiency virus type 1. *J. Biol. Chem.* **274**, 23499-23507 (1999).

Krull,I.S. *et al.* Labeling reactions applicable to chromatography and electrophoresis of minute amounts of proteins. *J. Chromatogr. B Biomed. Sci. Appl.* **699**, 173-208 (1997).

Ladror,U.S., Snyder,S.W., Wang,G.T., Holzman,T.F. & Krafft,G.A. Cleavage at the amino and carboxyl termini of Alzheimer's amyloid-beta by cathepsin D. *J. Biol. Chem.* **269** , 18422-18428 (1994).

Ladror,U.S., Snyder,S.W., Wang,G.T., Holzman,T.F. & Krafft,G.A. Cleavage at the amino and carboxyl termini of Alzheimer's amyloid-beta by cathepsin D. *J. Biol Chem.* **269**, 18422-18428 (1994).

Langbein,L. *et al.* Characterization of a novel human type II epithelial keratin K1b, specifically expressed in eccrine sweat glands. *J. Invest Dermatol.* **125**, 428-444 (2005).

Lapresle,C. & WebbB,T. The purification and properties of a proteolytic enzyme, rabbit cathepsin E, and further studies on rabbit cathepsin D. *Biochem. J.* **84**, 455-462 (1962).

Lapresle,C., Puizdar,V., Porchon-Bertolotto,C., Joukoff,E. & Turk,V. Structural differences between rabbit cathepsin E and cathepsin D. *Biol. Chem. Hoppe Seyler* **367**, 523-526 (1986).

Lee,A.Y., Gulnik,S.V. & Erickson,J.W. Conformational switching in an aspartic proteinase. *Nat. Struct. Biol.* **5**, 866-871 (1998).

Leist,M. & Jaattela,M. Triggering of apoptosis by cathepsins. *Cell Death. Differ.* **8**, 324-326 (2001).

Li,W. *et al.* Induction of cell death by the lysosomotropic detergent MSDH. *FEBS Lett.* **470**, 35-39 (2000).

Lin,T.Y. & Williams,H.R. Inhibition of cathepsin D by synthetic oligopeptides. *J. Biol. Chem.* **254**, 11875-11883 (1979).

Lindgren,M., Hallbrink,M., Prochiantz,A. & Langel,U. Cell-penetrating peptides. *Trends Pharmacol. Sci.* **21**, 99-103 (2000).

Liu,J. & Shapiro,J.I. Endocytosis and signal transduction: basic science update. *Biol. Res. Nurs.* **5**, 117-128 (2003).

Looney,J.M. The colorimetric estimation of tyrosine, tryptophane, and cystine in proteins. *J. Biol. Chem.* **69**, 519-538 (1926).

Lopez-Garcia,B., Lee,P.H., Yamasaki,K. & Gallo,R.L. Anti-fungal activity of cathelicidins and their potential role in Candida albicans skin infection. *J. Invest Dermatol.* **125**, 108-115 (2005).

Lopez-Otin,C. & Overall,C.M. Protease degradomics: a new challenge for proteomics. *Nat. Rev. Mol. Cell Biol.* **3**, 509-519 (2002).

Luedtke,N.W., Carmichael,P. & Tor,Y. Cellular uptake of aminoglycosides, guanidinoglycosides, and poly-arginine. *J. Am. Chem. Soc.* **125**, 12374-12375 (2003).

Maccecchini,M.L., Rudin,Y., Blobel,G. & Schatz,G. Import of proteins into mitochondria: precursor forms of the extramitochondrially made F1-ATPase subunits in yeast. *Proc. Natl. Acad. Sci. U. S. A* **76**, 343-347 (1979).

Mackay,E.A. *et al.* A possible role for cathepsins D, E, and B in the processing of beta-amyloid precursor protein in Alzheimer's disease. *Eur. J. Biochem.* **244**, 414-425 (1997).

Majer,P., Collins,J.R., Gulnik,S.V. & Erickson,J.W. Structure-based subsite specificity mapping of human cathepsin D using statine-based inhibitors. *Protein Sci.* **6**, 1458-1466 (1997).

Mason,R.W. Lysosomal metabolism of proteins. *Subcell. Biochem.* **27**, 159-190 (1996).

Mason,R.W., Bergman,C.A., Lu,G., Frenck,H.J. & Sol-Church,K. Expression and characterization of cathepsin P. *Biochem. J.* **378**, 657-663 (2004).

Matayoshi,E.D., Wang,G.T., Krafft,G.A. & Erickson,J. Novel fluorogenic substrates for assaying retroviral proteases by resonance energy transfer. *Science* **247**, 954-958 (1990).

Merrifield,R.B. Solid phase peptide synthesis. I. The synthesis of a tetrapeptide. *J. Am. Cchem. Soc.* **85**, 2149-2154 (1963).

Metcalf,P. & Fusek,M. Two crystal structures for cathepsin D: the lysosomal targeting signal and active site. *EMBO J.* **12**, 1293-1302 (1993).

Metroione,R.M., Neves,A.G. & FRUTON,J.S. Purification and properties of dipeptidyl transferase (Cathepsin C). *Biochemistry* **5**, 1597-1604 (1966).

Miller,J.J., Changaris,D.G. & Levy,R.S. Purification, subunit structure and inhibitor profile of cathepsin A. *J. Chromatogr.* **627**, 153-162 (1992).

Mizuochi,T. *et al.* Both cathepsin B and cathepsin D are necessary for processing of ovalbumin as well as for degradation of class II MHC invariant chain. *Immunol. Lett.* **43**, 189-193 (1994).

Morishima,H., Takita,T., Aoyagi,T., Takeuchi,T. & Umezawa,H. The structure of pepstatin. *J. Antibiot. (Tokyo)* **23**, 263-265 (1970).

Mousavi,S.A. *et al.* Uptake of denatured collagen into hepatic stellate cells: evidence for the involvement of urokinase plasminogen activator receptor-associated protein/Endo180. *Biochem. J.* **387**, 39-46 (2005).

Murakami,M. *et al.* Cathelicidin anti-microbial peptide expression in sweat, an innate defense system for the skin. *J. Invest Dermatol.* **119**, 1090-1095 (2002).

Murakami,M., Lopez-Garcia,B., Braff,M., Dorschner,R.A. & Gallo,R.L. Postsecretory processing generates multiple cathelicidins for enhanced topical antimicrobial defense. *J. Immunol.* **172**, 3070-3077 (2004).

Muramoto,K., Kamiya,H. & Kawauchi,H. The application of fluorescein isothiocyanate and high-performance liquid chromatography for the microsequencing of proteins and peptides. *Anal. Biochem.* **141**, 446-450 (1984).

Myal,Y. *et al.* The prolactin-inducible protein (PIP/GCDFP-15) gene: cloning, structure and regulation. *Mol. Cell Endocrinol.* **80**, 165-175 (1991).

Nagahara,H. *et al.* Transduction of full-length TAT fusion proteins into mammalian cells: TAT-p27Kip1 induces cell migration. *Nat. Med.* **4**, 1449-1452 (1998).

Nagler,D.K. *et al.* Human cathepsin X: A cysteine protease with unique carboxypeptidase activity. *Biochemistry* **38**, 12648-12654 (1999).

Nakayashiki,N. Sweat protein components tested by SDS-polyacrylamide gel electrophoresis followed by immunoblotting. *Tohoku J. Exp. Med.* **161**, 25-31 (1990).

Nizet,V. *et al.* Innate antimicrobial peptide protects the skin from invasive bacterial infection. *Nature* **414**, 454-457 (2001).

Nomura,T. & Katunuma,N. Involvement of cathepsins in the invasion, metastasis and proliferation of cancer cells. *J. Med. Invest* **52**, 1-9 (2005).

Oefner,P.J. *et al.* High-resolution liquid chromatography of fluorescent dye-labeled nucleic acids. *Anal. Biochem.* **223**, 39-46 (1994).

Ong,P.Y. *et al.* Endogenous antimicrobial peptides and skin infections in atopic dermatitis. *N. Engl. J. Med.* **347**, 1151-1160 (2002).

Ostermann,N., Gerhartz,B., Worpenberg,S., Trappe,J. & Eder,J. Crystal structure of an activation intermediate of cathepsin E. *J. Mol. Biol.* **342**, 889-899 (2004).

Perkins,D.N., Pappin,D.J., Creasy,D.M. & Cottrell,J.S. Probability-based protein identification by searching sequence databases using mass spectrometry data. *Electrophoresis* **20**, 3551-3567 (1999).

Petersen,L. *et al.* Synthesis and in vitro evaluation of PNA-peptide-DETA conjugates as potential cell penetrating artificial ribonucleases. *Bioconjug. Chem.* **15**, 576-582 (2004).

Peterson,L.M., Sokolovsky,M. & Vallee,B.L. Purification and crystallization of human carboxypeptidase A. *Biochemistry* **15**, 2501-2508 (1976).

Pitot,H.C. & Gohda,E. Cathepsin T. *Methods Enzymol.* **142**, 279-289 (1987).

Planta,R.J., Gorter,J. & Gruber,M. The Catalytic Properties of Cathepsin C. *Biochim. Biophys. Acta* **89**, 511-519 (1964).

Pooga,M. *et al.* Cell penetrating PNA constructs regulate galanin receptor levels and modify pain transmission in vivo. *Nat. Biotechnol.* **16**, 857-861 (1998).

Pooga,M. *et al.* Cellular translocation of proteins by transportan. *FASEB J.* **15**, 1451-1453 (2001).

Pooga,M., Hallbrink,M., Zorko,M. & Langel,U. Cell penetration by transportan. *FASEB J.* **12** , 67-77 (1998).

Potocky,T.B., Menon,A.K. & Gellman,S.H. Cytoplasmic and nuclear delivery of a TAT-derived peptide and a beta-peptide after endocytic uptake into HeLa cells. *J. Biol. Chem.* **278**, 50188-50194 (2003).

Press,E.M., Porter,R.R. & Cebra,J. The isolation and properties of a proteolytic enzyme, cathepsin D from bovine spleen. *Biochem. J.* **74**, 501-514 (1960).

Puizdar,V. & Turk,V. Cathepsinogen D: characterization and activation to cathepsin D and inhibitory peptides. *FEBS Lett.* **132**, 299-304 (1981).

Puzer,L. *et al.* Defining the substrate specificity of mouse cathepsin P. *Arch. Biochem. Biophys.* **435**, 190-196 (2005).

Rao,C.M. *et al.* Specificity in the binding of inhibitors to the active site of human/primate aspartic proteinases: analysis of P2-P1-P1'-P2' variation. *J. Med. Chem.* **36**, 2614-2620 (1993).

Richard,J.P. *et al.* Cell-penetrating peptides-A reevaluation of the mechanism of cellular uptake. *J. Biol. Chem.* **278**, 585-590 (2003).

Richard,J.P. *et al.* Cellular uptake of unconjugated TAT peptide involves clathrin-dependent endocytosis and heparan sulfate receptors. *J. Biol. Chem.* **280**, 15300-15306 (2005).

Rieg,S. *et al.* Deficiency of dermcidin-derived antimicrobial peptides in sweat of patients with atopic dermatitis correlates with an impaired innate defense of human skin in vivo. *J. Immunol.* **174**, 8003-8010 (2005).

Rieg,S., Garbe,C., Sauer,B., Kalbacher,H. & Schittek,B. Dermcidin is constitutively produced by eccrine sweat glands and is not induced in epidermal cells under inflammatory skin conditions. *Br. J. Dermatol.* **151**, 534-539 (2004).

Rijnboutt,S., Aerts,H.M., Geuze,H.J., Tager,J.M. & Strous,G.J. Mannose 6-phosphate-independent membrane association of cathepsin D, glucocerebrosidase, and sphingolipid-activating protein in HepG2 cells. *J. Biol. Chem.* **266**, 4862-4868 (1991a).

Rijnboutt,S., Kal,A.J., Geuze,H.J., Aerts,H. & Strous,G.J. Mannose 6-phosphate-independent targeting of cathepsin D to lysosomes in HepG2 cells. *J. Biol. Chem.* **266**, 23586-23592 (1991b).

Rijnboutt,S., Stoorvogel,W., Geuze,H.J. & Strous,G.J. Identification of subcellular compartments involved in biosynthetic processing of cathepsin D. *J. Biol. Chem.* **267**, 15665-15672 (1992).

Roberg,K., Johansson,U. & Ollinger,K. Lysosomal release of cathepsin D precedes relocation of cytochrome c and loss of mitochondrial transmembrane potential during apoptosis induced by oxidative stress. *Free Radic. Biol. Med.* **27**, 1228-1237 (1999).

Rochefort,H. & Liaudet-Coopman,E. Cathepsin D in cancer metastasis: a protease and a ligand. *APMIS* **107**, 86-95 (1999).

Rodriguez,G.M. & Diment,S. Role of cathepsin D in antigen presentation of ovalbumin. *J. Immunol.* **149**, 2894-2898 (1992).

Rothman,J.H., Yamashiro,C.T., Raymond,C.K., Kane,P.M. & Stevens,T.H. Acidification of the lysosome-like vacuole and the vacuolar H+-ATPase are deficient in two yeast mutants that fail to sort vacuolar proteins. *J. Cell Biol.* **109**, 93-100 (1989).

Ryser,H.J. & Shen,W.C. Conjugation of methotrexate to poly(L-lysine) increases drug transport and overcomes drug resistance in cultured cells. *Proc. Natl. Acad. Sci. U. S. A* **75**, 3867-3870 (1978).

Saalik,P. *et al.* Protein cargo delivery properties of cell-penetrating peptides. A comparative study. *Bioconjug. Chem.* **15**, 1246-1253 (2004).

Saar,K. *et al.* Cell-penetrating peptides: A comparative membrane toxicity study. *Anal. Biochem.* **345**, 55-65 (2005).

Sakai,H., Saku,T., Kato,Y. & Yamamoto,K. Quantitation and immunohistochemical localization of cathepsins E and D in rat tissues and blood cells. *Biochim. Biophys. Acta* **991**, 367-375 (1989).

Saku,T., Sakai,H., Shibata,Y., Kato,Y. & Yamamoto,K. An immunocytochemical study on distinct intracellular localization of cathepsin E and cathepsin D in human gastric cells and various rat cells. *J. Biochem. (Tokyo)* **110**, 956-964 (1991).

Salvesen,G.S. A lysosomal protease enters the death scene. *J. Clin. Invest* **107**, 21-22 (2001).

Sanger,F. The terminal peptides of insulin. *Biochem. J.* **45**, 563-574 (1949).

Sapolsky,A.I. & Woessner,J.F., Jr. Multiple forms of cathepsin D from bovine uterus. *J. Biol. Chem.* **247** , 2069-2076 (1972).

Scarborough,P.E. *et al.* Exploration of subsite binding specificity of human cathepsin D through kinetics and rule-based molecular modeling. *Protein Sci.* **2**, 264-276 (1993).

Schittek,B. *et al.* Dermcidin: a novel human antibiotic peptide secreted by sweat glands. *Nat. Immunol.* **2**, 1133-1137 (2001).

Schmidt,M.C. *et al.* Translocation of human calcitonin in respiratory nasal epithelium is associated with self-assembly in lipid membrane. *Biochemistry* **37**, 16582-16590 (1998).

Schröter,C.J. *et al.* A rapid method to separate endosomes from lysosomal contents using differential centrifugation and hypotonic lysis of lysosomes. *J. Immunol. Methods* **227**, 161-168 (1999).

Schwarz,G. *et al.* Characterization of legumain. *Biol. Chem.* **383**, 1813-1816 (2002).

Schwarze,S.R., Ho,A., Vocero-Akbani,A. & Dowdy,S.F. In vivo protein transduction: delivery of a biologically active protein into the mouse. *Science* **285**, 1569-1572 (1999).

Shewale,J.G. & Tang,J. Amino acid sequence of porcine spleen cathepsin D. *Proc. Natl. Acad. Sci. U. S. A* **81**, 3703-3707 (1984).

Shibagaki,N. & Udey,M.C. Dendritic cells transduced with protein antigens induce cytotoxic lymphocytes and elicit antitumor immunity. *J. Immunol.* **168**, 2393-2401 (2002).

Shibata,M. *et al.* Cathepsin D is specifically inhibited by deoxyribonucleic acids. *FEBS Lett.* **517**, 281-284 (2002).

Silhol,M., Tyagi,M., Giacca,M., Lebleu,B. & Vives,E. Different mechanisms for cellular internalization of the HIV-1 Tat-derived cell penetrating peptide and recombinant proteins fused to Tat. *Eur. J. Biochem.* **269**, 494-501 (2002).

Sjöback,R., Nygren,J. & Kubista,M.. Absorption and fluorescence properties of fluorescein. *Spectrochim. Acta A* **51**, L7-L21 (1995).

Skrzydlewska,E., Sulkowska,M., Wincewicz,A., Koda,M. & Sulkowski,S. Evaluation of serum cathepsin B and D in relation to clinicopathological staging of colorectal cancer. *World J. Gastroenterol.* **11**, 4225-4229 (2005).

Skudlarek,M.D. & Swank,R.T. Biosynthesis of two lysosomal enzymes in macrophages. Evidence for a precursor of beta-galactosidase. *J. Biol. Chem.* **254**, 9939-9942 (1979).

Snyder,D.S., Simonis,S., Uzman,B.G. & Whitaker,J.N. Rat neural tissue cathepsin D: ultrastructural immunocytochemistry. *J. Neurocytol.* **14**, 579-596 (1985).

Song,L., Hennink,E.J., Young,I.T. & Tanke,H.J. Photobleaching kinetics of fluorescein in quantitative fluorescence microscopy. *Biophys. J.* **68**, 2588-2600 (1995).

Sorensen,O.E. *et al.* Human cathelicidin, hCAP-18, is processed to the antimicrobial peptide LL-37 by extracellular cleavage with proteinase 3. *Blood* **97**, 3951-3959 (2001).

Speers,A.E. & Cravatt,B.F. Chemical strategies for activity-based proteomics. *ChemBioChem* **5**, 41-47 (2004).

Stoka,V. *et al.* Lysosomal protease pathways to apoptosis. Cleavage of bid, not pro-caspases, is the most likely route. *J. Biol. Chem.* **276**, 3149-3157 (2001).

Suzuki,T. *et al.* Possible existence of common internalization mechanisms among arginine-rich peptides. *J. Biol. Chem.* **277**, 2437-2443 (2002).

Tada,T. *et al.* Immunohistochemical localization of Zn-alpha 2-glycoprotein in normal human tissues. *J. Histochem. Cytochem.* **39**, 1221-1226 (1991).

Takahashi,T. & Tang,J. Amino acid sequence of porcine spleen cathepsin D light chain. *J. Biol. Chem.* **258**, 6435-6443 (1983a).

Takahashi,T. & Tang,J. Cathepsin D from porcine and bovine spleen. *Methods Enzymol.* **80 Pt C**, 565-581 (1981).

Takahashi,T., Schmidt,P.G. & Tang,J. Oligosaccharide units of lysosomal cathepsin D from porcine spleen. Amino acid sequence and carbohydrate structure of the glycopeptides. *J. Biol. Chem.* **258**, 2819-2830 (1983b).

Takakusa,H. *et al.* Design and synthesis of an enzyme-cleavable sensor molecule for phosphodiesterase activity based on fluorescence resonance energy transfer. *J Am Chem Soc.* **124**, 1653-1657 (2002).

Tallan,H.H., Jones,M.E. & Fruton,J.S. On the proteolytic enzymes if animal tissues. X. Beef spleen cathepsin C. *J. Biol. Chem.* **194**, 793-805 (1952).

Tamai,M. *et al.* In vitro and in vivo inhibition of cysteine proteinases by EST, a new analog of E-64. *J. Pharmacobiodyn.* **9**, 672-677 (1986).

Tanaka,T., Minematsu,Y., Reilly,C.F., Travis,J. & Powers,J.C. Human leukocyte cathepsin G. Subsite mapping with 4-nitroanilides, chemical modification, and effect of possible cofactors. *Biochemistry* **24**, 2040-2047 (1985).

Tang,J. & Wong,R.N. Evolution in the structure and function of aspartic proteases. *J. Cell Biochem.* **33**, 53-63 (1987).

Tappel,A.L., Zalkin,H., Caldwell,K.A., Desai,I.D. & Shibko,S. Increased lysosomal enzymes in genetic muscular dystrophy. *Arch. Biochem. Biophys.* **96**, 340-346 (1962).

Tardy,C., Tyynela,J., Hasilik,A., Levade,T. & Andrieu-Abadie,N. Stress-induced apoptosis is impaired in cells with a lysosomal targeting defect but is not affected in cells synthesizing a catalytically inactive cathepsin D. *Cell Death. Differ.* **10**, 1090-1100 (2003).

Toneguzzo,F. & Ghosh,H.P. In vitro synthesis of vesicular stomatitis virus membrane glycoprotein and insertion into membranes. *Proc. Natl. Acad. Sci. U. S. A* **75**, 715-719 (1978).

Trehin,R. & Merkle,H.P. Chances and pitfalls of cell penetrating peptides for cellular drug delivery. *Eur. J. Pharm. Biopharm.* **58**, 209-223 (2004).

Trombetta,E.S., Ebersold,M., Garrett,W., Pypaert,M. & Mellman,I. Activation of lysosomal function during dendritic cell maturation. *Science* **299**, 1400-1403 (2003).

Turk,B. *et al.* Apoptotic pathways: involvement of lysosomal proteases. *Biol. Chem.* **383**, 1035-1044 (2002).

Turk,B., Turk,D. & Turk,V. Lysosomal cysteine proteases: more than scavengers. *Biochim. Biophys. Acta* **1477**, 98-111 (2000).

Turk,D. & Guncar,G. Lysosomal cysteine proteases (cathepsins): promising drug targets. *Acta Crystallogr. D. Biol. Crystallogr.* **59**, 203-213 (2003).

Turk,V., Turk,B. & Turk,D. Lysosomal cysteine proteases: facts and opportunities. *EMBO J.* **20**, 4629-4633 (2001).

Turner,J.J., Arzumanov,A.A. & Gait,M.J. Synthesis, cellular uptake and HIV-1 Tat-dependent trans-activation inhibition activity of oligonucleotide analogues disulphide-conjugated to cell-penetrating peptides. *Nucleic Acids Res.* **33**, 27-42 (2005).

Valore,E.V. & Ganz,T. Posttranslational processing of defensins in immature human myeloid cells. *Blood* **79**, 1538-1544 (1992).

Valore,E.V. *et al.* Human beta-defensin-1: an antimicrobial peptide of urogenital tissues. *J. Clin. Invest* **101**, 1633-1642 (1998).

van Noort,J.M. & Jacobs,M.J. Cathepsin D, but not cathepsin B, releases T cell stimulatory fragments from lysozyme that are functional in the context of multiple murine class II MHC molecules. *Eur. J. Immunol.* **24**, 2175-2180 (1994).

van Noort,J.M. & van der Drift,A.C. The selectivity of cathepsin D suggests an involvement of the enzyme in the generation of T-cell epitopes. *J. Biol. Chem.* **264**, 14159-14164 (1989).

Van Noort,J.M. *et al.* Antigen processing by endosomal proteases determines which sites of sperm-whale myoglobin are eventually recognized by T cells. *Eur. J. Immunol.* **21**, 1989-1996 (1991).

Vaux,D.L., Cory,S. & Adams,J.M. Bcl-2 gene promotes haemopoietic cell survival and cooperates with c-myc to immortalize pre-B cells. *Nature* **335**, 440-442 (1988).

Velasco,G., Ferrando,A.A., Puente,X.S., Sanchez,L.M. & Lopez-Otin,C. Human cathepsin O. Molecular cloning from a breast carcinoma, production of the active enzyme in Escherichia coli, and expression analysis in human tissues. *J. Biol. Chem.* **269**, 27136-27142 (1994).

Vergelli,M. *et al.* T cell response to myelin basic protein in the context of the multiple sclerosis-associated HLA-DR15 haplotype: peptide binding, immunodominance and effector functions of T cells. *J. Neuroimmunol.* **77**, 195-203 (1997).

Vetvicka,V., Benes,P. & Fusek,M. Procathepsin D in breast cancer: what do we know? Effects of ribozymes and other inhibitors. *Cancer Gene Ther.* **9**, 854-863 (2002).

Vetvicka,V., Vetvickova,J. & Benes,P. Role of enzymatically inactive procathepsin D in lung cancer. *Anticancer Res.* **24**, 2739-2743 (2004).

Villadangos,J.A. *et al.* Proteases involved in MHC class II antigen presentation. *Immunol. Rev.* **172**, 109-120 (1999).

Vives,E., Brodin,P. & Lebleu,B. A truncated HIV-1 Tat protein basic domain rapidly translocates through the plasma membrane and accumulates in the cell nucleus. *J. Biol. Chem.* **272**, 16010-16017 (1997).

von Figura,K. & Hasilik,A. Lysosomal enzymes and their receptors. *Annu. Rev. Biochem.* **55**, 167-193 (1986).

Waizenegger,T., Fischer,R. & Brock,R. Intracellular concentration measurements in adherent cells: a comparison of import efficiencies of cell-permeable peptides. *Biol. Chem.* **383**, 291-299 (2002).

Wang,B. *et al.* Human cathepsin F. Molecular cloning, functional expression, tissue localization, and enzymatic characterization. *J. Biol. Chem.* **273**, 32000-32008 (1998).

Wang,H., Li,J., Liu,X., Yang,T.X. & Zhang,H.S. N-hydroxysuccinimidyl fluorescein-O-acetate as a fluorescent derivatizing reagent for catecholamines in liquid chromatography. *Anal. Biochem.* **281**, 15-20 (2000).

Wasi,S., Uriuhara,T., Taichman,N.S., Murray,R.K. & Movat,H.Z. Proteolytic activity in the serum of rabbits during anaphylaxis. *Experientia* **22**, 196-198 (1966).

Weber,P.J., Bader,J.E., Folkers,G. & Beck-Sickinger,A.G. A fast and inexpensive method for N-terminal fluorescein-labeling of peptides. *Bioorg. Med. Chem. Lett.* **8**, 597-600 (1998).

Wei,A.P., Blumenthal,D.K. & Herron,J.N. Antibody-mediated fluorescence enhancement based on shifting the intramolecular dimer<-->monomer equilibrium of fluorescent dyes. *Anal. Chem.* **66**, 1500-1506 (1994).

Wender,P.A. *et al.* The design, synthesis, and evaluation of molecules that enable or enhance cellular uptake: peptoid molecular transporters. *Proc. Natl. Acad. Sci. U. S. A* **97**, 13003-13008 (2000).

Weston,P.D., Barrett,A.J. & Dingle,J.T. Specific inhibition of cartilage breakdown. *Nature* **222**, 285-286 (1969).

Wex,T., Levy,B., Wex,H. & Bromme,D. Human cathepsins F and W: A new subgroup of cathepsins. *Biochem. Biophys. Res. Commun.* **259**, 401-407 (1999).

Wille,A. *et al.* Cathepsin L is involved in cathepsin D processing and regulation of apoptosis in A549 human lung epithelial cells. *Biol. Chem.* **385**, 665-670 (2004).

Williamson,A.L. *et al.* Cleavage of hemoglobin by hookworm cathepsin D aspartic proteases and its potential contribution to host specificity. *FASEB J.* **16**, 1458-1460 (2002).

Willstätter,R. & Bamann,E. Über die Proteasen der Magenschleimhaut. Erste Abhandlung über die Enzyme der Leukozyten. *Hoppe-Seylers Z. Physiol. Chemie* **180**, 127-143 (1929).

Woessner,J.F., Jr. Acid hydrolases of the rat uterus in relation to pregnancy, post-partum involution and collagen breakdown. *Biochem. J.* **97**, 855-866 (1965).

Wright,G.L., Jr. SELDI proteinchip MS: a platform for biomarker discovery and cancer diagnosis. *Expert. Rev. Mol. Diagn.* **2**, 549-563 (2002).

Xie,D. *et al.* Dissection of the pH dependence of inhibitor binding energetics for an aspartic protease: direct measurement of the protonation states of the catalytic aspartic acid residues. *Biochemistry* **36**, 16166-16172 (1997).

Yamamoto,K., Katsuda,N. & Kato,K. Affinity purification and properties of cathepsin-E-like acid proteinase from rat spleen. *Eur. J. Biochem.* **92**, 499-508 (1978).

Yaron,A., Carmel,A. & Katchalski-Katzir,E. Intramolecularly quenched fluorogenic substrates for hydrolytic enzymes. *Anal. Biochem.* **95**, 228-235 (1979).

Yasuda,Y., Kageyama,T., Akamine,A., Shibata,M., Kominami,E., Uchiyama,Y. & Yamamoto,K. Characterisation of new fluorogenic substrates for the rapid and sensitive assay of cathepsin E and D. *J. Biochem. (Tokyo)* **125**, 1139-1143 (1999).

Yasuda,Y., Kohmura,K., Kadowaki,T., Tsukuba,T. & Yamamoto,K. A new selective substrate for cathepsin E based on the cleavage site sequence of alpha2-macroglobulin. *Biol. Chem.* **386**, 299-305 (2005).

Yokota,S. & Atsumi,S. Immunoelectron microscopic localization of cathepsin D in lysosomes of rat nerve cells. *Histochemistry* **79**, 345-352 (1983).

Yokozeki,H., Hibino,T. & Sato,K. Partial purification and characterization of cysteine proteinases in eccrine sweat. *Am. J. Physiol* **252**, R1119-R1129 (1987).

Yonezawa,S. *et al.* Structures at the proteolytic processing region of cathepsin D. *J. Biol. Chem.* **263**, 16504-16511 (1988).

Zanetti,M., Gennaro,R. & Romeo,D. Cathelicidins: a novel protein family with a common proregion and a variable C-terminal antimicrobial domain. *FEBS Lett.* **374**, 1-5 (1995).

Zeeuwen,P.L. *et al.* Cystatin M/E expression is restricted to differentiated epidermal keratinocytes and sweat glands: a new skin-specific proteinase inhibitor that is a target for cross-linking by transglutaminase. *J. Invest Dermatol.* **116**, 693-701 (2001).

Zeeuwen,P.L., Vlijmen-Willems,I.M., Egami,H. & Schalkwijk,J. Cystatin M / E expression in inflammatory and neoplastic skin disorders. *Br. J. Dermatol.* **147**, 87-94 (2002).

Zhang,H., Li,X.J., Martin,D.B. & Aebersold,R. Identification and quantification of N-linked glycoproteins using hydrazide chemistry, stable isotope labeling and mass spectrometry. *Nat. Biotechnol.* **21**, 660-666 (2003).

9 Abbreviations

For amino acids the suggestions of the IUPAC-IUB-commission for biological nomenclature [*Eur. J. Biochem.* **138**, 9-37 (1984)] were applied.

#	fraction
ACN	acetonitrile
Amca	7-Amino-4-methylcoumarin-3-acetic acid
Cat	cathepsin
CatD	cathepsin D
CCE	crude cell extract
CLSM	confocal laser scanning microscopy
CPP	cell-penetrating peptide
DABCYL	4'-dimethylaminoazobenzene-4-carboxylic acid
DC	dendritic cell
DG	digestion product
E	endosomal fraction
EC number	enzyme commission number
EDANS	5-(2-aminoethyl) aminonaphthalene-1-sulfonic acid
EDTA	ethylenediaminetetraacetic acid
ESI	electrospray ionisation
eq	equivalent
FACS	fluorescence activated cell sorting
Fluo	5-carboxyfluorescein
IFN-γ	interferon γ
L	lysosomal fraction
LPS	lipopolysacharid
MALDI	matrix-assisted laser desorption/ionization
MS	mass spectrometry
MW	molecular weight
m/z	mass/charge ratio
Pbf	2, 2, 5, 7, 8-pentamethyl-dihydrobenzofuran-5-sulfonyl
RP-HPLC	reversed-phase high-performance liquid chromatography
RT	room temperature

SPPS	solid-phase peptide synthesis
t	time
TAMRA	5(6)-carboxytetramethylrhodamine
TBST	Tris-buffered saline with Tween
TBTU	2-(1H-benzotriazol-1-yl)-1, 1, 3, 3-tetramethyluronium
tBu	tert.-butyl
TCA	trichloroacetic acid
TFA	trifluoroacetic acid
TNF-α	tumor necrosis factor α
Tris	tris(hydroxymethyl)aminomethane
UV	ultraviolet
V	volume

10 Verzeichnis der akademischen Lehrer

H. Bisswanger, R. Brock, W. Dammertz, A. Donges, M. Duszenko, K. Grillenberger, H. Guth, B. Hamprecht, H. Höchstetter, W. Ilg, G. Jung, A. Nordheim, H. Probst, H.-G. Rammensee, S. Stevanović, R. Thalacker, U. Weser

11 Publications

11.1 Papers

Daniel Baechle, Rainer Fischer, Jens Brandenburg, Roland Brock, and Hubert Kalbacher, *Synthesis and applications of a new cell-penetrating cathepsin D substrate*, M. Flegel, M. Fridkin, C. Gilon, M. Lebl, J. Slaninovia (Eds.) in Peptides 2004: Proceedings of the 3rd International and 28th European Peptide Symposium, Prague (2004)

Daniel Baechle, Alexander Cansier, Rainer Fischer, Jens Brandenburg, Timo Burster, Christoph Driessen and Hubert Kalbacher, *Biotinylated fluorescent peptide substrates for the sensitive and specific determination of cathepsin D activity*, J. Peptide Sci., 11: 166-175 (2005)

Daniel Baechle[*], Rainer Fischer[*], Alexander Cansier, Roland Brock, and Hubert Kalbacher, *A postcolumn alkalinization procedure enhances the sensitivity of fluorescence detection of fuorescein-labeled substances in RP–HPLC*, Anal. Biochem., 345(1): 161-163 (2005), [*]These authors equally contributed to this work

Daniel Baechle, Thomas Flad, Alexander Cansier, Heiko Steffen, Birgit Schittek, Jonathan Tolson, Timo Herrmann, Hassan Dihazi, Alexander Beck, Gerhard Anton Mueller, Margret Mueller, Stefan Stevanović S, Claus Garbe, Mueller and Hubert Kalbacher, *Cathepsin D is present in human eccrine sweat and involved in the postsecretory processing of DCD-1L*, J. Biol. Chem., in press (2005)

Timo Burster, Alexander Beck, Anita Oeren, Simone Poeschel, Daniel Baechle, Michael Reich, Olaf Rötzschke, Kirsten Falk, Hubert Kalbacher, Eva Tolosa, Herman Overkleeft and Christoph Driessen, *Interferon gamma controls the lysosomal processing of myelin basic protein in microglia cells by regulating cathepsin G activity*, J. Immunol., in revision (2005)

Rainer Fischer[*], Daniel Baechle[*], Mariola Fotin-Mleczek, Günther Jung, Hubert Kalbacher, and Roland Brock, *Smart protease substrates*, submitted (2005), [*]These authors equally contributed to this work

Rainer Fischer, Hans-Jörg Hufnagel, Daniel Baechle, Oda Stoevesandt, Günther Jung and Roland Brock, *A doubly labeled Penetratin analogue as ratiometric sensor for intracellular proteolytic stability*, submitted (2005)

11.2 Posters and abstracts

Daniel Baechle and Hubert Kalbacher, *Peptide based proteome analysis: Generation of fluorescence labelled protein specific peptide epitopes for anti-peptide-antibody-arrays*, poster presentation at the 1st BMBF-Statusseminar des Förderschwerpunktes „Neue effiziente Verfahren für die funktionelle Proteomanalyse“ (2003), Bad Honnef

Timo Burster, Alexander Beck, Anita Øren, Viviana Marin-Esteban, Eva Tolosa, Olaf Rötzschke, Kirsten Falk, Michael Reich, Marianne Kraus, Daniel Baechle, Jens Brandenburg, Hubert Kalbacher and Christoph Driessen, *IFN-γ downregulates Cathepsin G activity in microglia and results in increased stability of the major immunodominant region of myelin basic protein in lysosomal compartments*, Poster presentation at 34th Annual Meeting of the German Society of Immunology and the 3rd Meeting of the European Mucosal Immunology Group (2003), Berlin

Daniel Baechle, Rainer Fischer, Jens Brandenburg, Roland Brock, and Hubert Kalbacher, *Synthesis and applications of a new cell-penetrating cathepsin D substrate*, Poster presentation at the 3rd International and 28th European Peptide Symposium (2004), Prague

Rainer Fischer, Hansjörg Hufnagel, Oda Stoevesandt, Daniel Baechle, Hubert Kalbacher, Günther Jung and Roland Brock, *A doubly-labelled fluorescent Penetratin analogue as ratiometric sensor for intracellular peptide stability*, at the 7th German Peptide Symposium (2005), Braunschweig

Daniel Baechle, Thomas Flad, Alexander Cansier, Timo Herrmann, Heiko Steffen, Claus Garbe, Birgit Schittek and Hubert Kalbacher, Postsecretory Processing of DCD-1L by Cathepsin D in Human Eccrine Sweat, at the Annual Meeting of the European Society for Dermatological Research (2005), Tübingen

12 Curriculum vitae

Name:	Daniel Bächle
Geburtsdatum:	23.4.1978
Geburtsort:	Münsingen
Staatsangehörigkeit:	deutsch
Heimanschrift:	Lichtensteinstraße 9 72587 Römerstein-Böhringen

1984 - 1988	Grundschule, Zainingen
1988 – 1997	Gymnasium, Bad Urach Fremdsprachen: Englisch, Latein, Französisch Abschluss: Allgemeine Hochschulreife
1997 - 1998	Zivildienst bei der katholischen Sozialstation der Caritas, Freiburg im Breisgau
1998 - 1999	Grundstudium „Chemie“ an der Naturwissenschaftlich-technischen Akademie (NTA) Prof. Dr. Grübler (Fachhochschule), Isny im Allgäu Abschluss: Vordiplom
1999 – 2000	Hauptstudium „Pharmazeutische Chemie“ Zusatzqualifikationen: Toxikologie, spezielles Recht für Chemiker
2000 – 2001	Praxissemester am Medizinisch – naturwissenschaftlichem Forschungsinstitut (MNF) der Universität Tübingen in der Arbeitsgruppe von Dr. Kalbacher Abschlussbericht: *Synthese biologisch aktiver Somatostatin-Derivate und Identifizierung von Nebenprodukten bei der Peptidsynthese*
2001 – 2002	Hauptstudium mit Abschluss der Diplomprüfung im Fach pharmazeutische Chemie
2002	Diplomarbeit am MNF der Universität Tübingen in der Arbeitsgruppe von Dr. Kalbacher Diplomarbeit: *Entwicklung eines neuartigen Tests zur Bestimmung der Aktivität von Cathepsin D in biologischen Proben mittels fluoreszenzmarkierter und biotinylierter Substrate*
2003 – 2004	Erlangung der Promotionsberechtigung der Fakultät für Chemie und Pharmazie an der Universität Tübingen in den Arbeitsgruppen von Dr. Kalbacher, Prof. Dr. Brock und Prof. Dr. Jung Berichte: 1) *Generierung, Isolierung und Charakterisierung von polyklonalen Antikörpern gegen Hydrolyseprodukte von MBP nach Umsetzung mit der Endoprotease LysC* 2) *Synthese und Charakterisierung zellgängiger Substrate zum Nachweis intrazellulärer Cathepsin D Aktivität* Kenntnisstandsprüfung im Fach Biochemie und Organische Chemie bei Prof. Dr. Probst und Prof. Dr. Jung
2004 – 2005	Dissertation am MNF der Universität Tübingen unter Leitung von Dr. Kalbacher Dissertation: *Cathepsin D - Entwicklung und Charakterisierung von neuen in vitro und in vivo Substraten und deren Anwendung in biologischen Proben*